University of Twente

Faculty of Electrical Engineering,
Mathematics & Computer Science

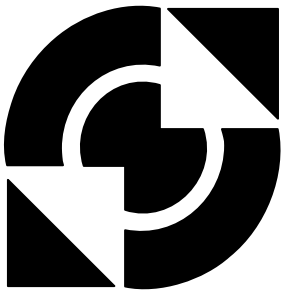

Higher Order Feedback Loop for a Pulse Width Modulator

Willem Stapelbroek
MSc. Thesis
June 2006

Supervisors:
prof. ir. A.J.M. van Tuijl
dr. ir. R.A.R. van der Zee
dr. ir. M. Berkhout
ir. D. Schinkel

Report number: 067.3157
Chair of Integrated Circuit Design
Faculty of Electrical Engineering,
Mathematics & Computer Science
University of Twente
P. O. Box 217
7500 AE Enschede
The Netherlands

Abstract

This report is about the research of a feedback loop for a Pulse Width Modulator. Different loop filters are investigated. The optimal type of loop filter depends on the types of noise in the system. In general a higher filter order of the loop-filter leads to a better noise suppression, but there are limits. Out of this study it emerged that a 3rd order Butterworth type filter with at 700 kHz carrier signal inserted in the last integrator is a good option for implementation. A SINAD of 112 dB in the audio band is possible in case of 50% modulation depth. This is 29 dB better than for a 2nd order Butterworth filter with a 350 kHz carrier signal. This last filter is used the Philips' design which was the motive for this project. In the simulations the noise/distortion sources are jitter noise from the carrier signal, supply voltage distortion and intrinsic modulation errors. Distortion in the output stage is neglected.

Also a start is made for the implementation of the actual loop-filter. A chain of integrators with distributed feedforward is chosen as loop-filter topology, because it is considered as the best choice in perspective of the power consumption and internal component requirements. All integrators in the loop filter are of the Miller type, due to their linearity, low power consumption and because of simplicity reasons. Although some components inside the loop filter are still idealized, a lot of parasitic effects are visible. Parasitic zeros and poles from the integrators are analyzed. The simulations results of this implementation show that a dynamic range of 122 dB in the audio band would be possible if only the internal thermal noise is considered as noise source. The component values for this implementation are calculated so that the internal thermal noise is not too large, the voltage swings of the integrators are within limits, the parasitics do no harm and that the component values are realistic.

Preface

In the course of the last 8 months the author of this report was engaged in his graduation (master) project. This report is a result of this project. Early October the author started his research on higher order feedback loops for Pulse Width Modulators.
The project was done in cooperation with Philips Semiconductors Nijmegen. Philips developed a good working second order feedback loop for a pulse width modulator. The initial assignment was to research if a higher order feedback loop would result in a significant better performance of the pulse width modulator. For this purpose a model was created and simulated. From the results of these simulations a loop-filter was chosen which was considered as feasible for implementation and with an optimal performance.
Next a start was made for the implementation of the loop filter. In this implementation some components were still considered as ideal or semi-ideal to simplify the analysis and to achieve a first implementation design within the time which was left for this project. The developed implementation design already gives the most important bottlenecks in order to develop an actual device.
In the monthly meetings between the author, his supervisors from the University of Twente and supervisors from Philips Semiconductors Nijmegen, many interesting discussion provided much insight in the world of pulse width modulation and feedback systems.
The author of this report likes to thank his supervisors at the University of Twente: Ronan van der Zee, Daniël Schinkel and Ed van Tuijl for their excellent guidance during this project and time for discussion which provided much insight in the field of pulse width modulation and analog designing. The author also likes tot thank his supervisors from Philips Semiconductors Nijmegen: Marco Berkhout and Arnold Freeke (at the first part of the project), who provided the project and who provide numerous of good ideas and interesting discussions.

Willem Stapelbroek
June, 2006

Table of content

1 Introduction

Pulse Width Modulators are widely used at the present day. When Pulse Width Modulators (PWM) are used as amplifier they are also called Class-D amplifiers.

Class-D amplifiers have a much higher efficiency than conventional AB-amplifiers. This is the big advantage of a Class-D amplifier over a conventional AB-amplifier. This efficiency is advantageous in many ways:

- From the power consumption point of view: Because less power is lost a device could run longer on a battery. In other words it has a longer battery life. This is very preferable in case of portable devices. Think about the various assortment of portable MP3 players, portable DVD players and of course the mobile phones nowadays.
- The amplifier will produce less heat when it has a high efficiency. Dissipated energy in an amplifier will be converted to heat. High efficiency means less energy is dissipated and therefore less heat is produced. When less heat is produced, it is not necessary to equip the amplifier with large and bulky heat sinks. This is very attractive for car-audio. The amplifiers can be made smaller so it is easier to build in a car. Small amplifiers are also very attractive for consumer Hi-Fi.

The concept of pulse width modulation is already known for a long time, but in the early years the manufactures were not able to produce a reliable Class-D amplifier. At the present day the technology is advanced enough and today's Class-D amplifiers equals or even exceeds the performance of conventional AB-amplifiers.

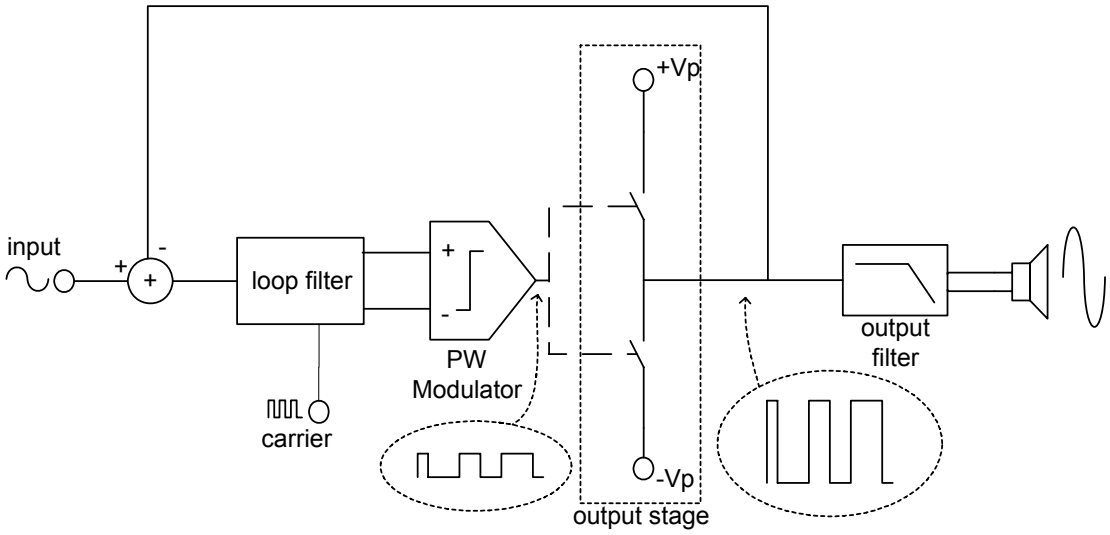

Figure 1: Class-D amplifier with feedback

A way to improve the performance of the Pulse Width Modulator is to equip the PWM with a feedback loop and a loop filter. This feedback loop is the main subject of this project.

Philips has already designed a good working 2nd order feedback loop for a PWM. This is a good starting point for this project. It provides some good design ideas and good reference material.

First, in chapter 2 it is explained how a PWM operates, what its drawbacks are and why a feedback loop improves the PWM. The 2nd order feedback loop developed by Philips is quickly analyzed to develop some first ideas for design choices and to produce some reference material.

In chapter 3 the loop-filter and its effect on the performance of the PWM is analyzed in a mathematical way. Different types of loop-filters and filters with different filter orders are calculated and analyzed.

In chapter 4 the most important noise and distortion sources in a PWM are analyzed and modeled. A model for the PWM is created which includes these noise/distortion sources and the feedback loop. The different loop-filters from chapter 3 are simulated and from the results the optimal loop-filter for implementation is chosen.

Chapter 5 and 6 show the way how such a loop-filter could be implemented. The pros and cons of different implementation topologies are investigated and the best solution for implementation is determined.

In chapter 7 some actual parameter values for the implementation are calculated and the implementation is simulated. The simulation results will be compared with the analysis from the previous chapters to verify them.

2 Problem Description

The assignment is to research and design a higher order feedback loop for a Pulse Width Modulator (PWM). Philips developed a good-working 2nd order feedback loop for a Class-D audio amplifier (= PWM) ([2]). It is interesting to research if a higher order feedback loop improves the PWM significantly. First let's take a look at how a PWM actually works and what the advantage is of a feedback loop. Next the 2nd order feedback loop developed by Philips is discussed. This is a nice starting point and a good comparison for the simulation results of the higher order feedback system which is designed in this report. Finally the specifications and goals of the project are discussed before discussing the actual project.

2.1 The Pulse Width Modulator

The amplifier used in this project is a Class-D amplifier. The Class-D amplifiers have some advantages over the conventional AB-amplifiers. First of all they are much more efficient than AB-amplifiers. The idea behind the efficiency of a Class-D type amplifier is that, ideally, the switches and the output filter do not dissipate energy (Figure 1). Therefore the high power output stage doesn't dissipate much energy.

To start, first one should know how a Class-D amplifier or Pulse Width Modulator (PWM) works. §2.1.1 first explains the operation of the basic feed-forward PWM and gives its drawbacks. Some of those drawbacks could be eliminated by using a feedback loop. While a feedback PWM eliminates some drawbacks of the feed-forward PWM, it also has its own drawbacks. The operation and drawbacks of the feedback PWM is discussed in §2.1.2.

2.1.1 The Feed-forward Pulse Width Modulator

The basic idea behind the feed-forward Pulse Width Modulation is to compare the input signal with a triangle carrier-signal, this method is known as double-sided natural sampling [1]. This method is shown in Figure 2. If the comparator and the carrier signal are ideal and the modulation depth (ratio between input signal and carrier signal) is not more than 100%, the only distortion components are the harmonics of the input signal modulated around the carrier signal (Figure 3). When choosing a carrier signal with frequency (f_{car}) high enough, the output can be filtered by simple low pass filter (2nd order) to retrieve only the desired input signal.

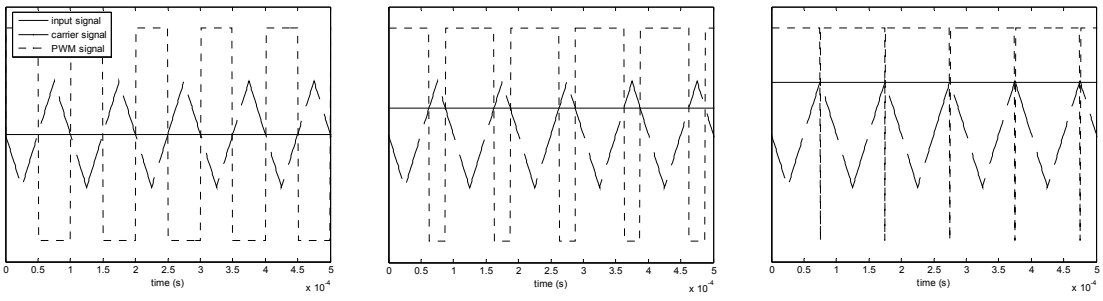

a) b) c)

Figure 2: Feedforward Pulse Width Modulation for different input values

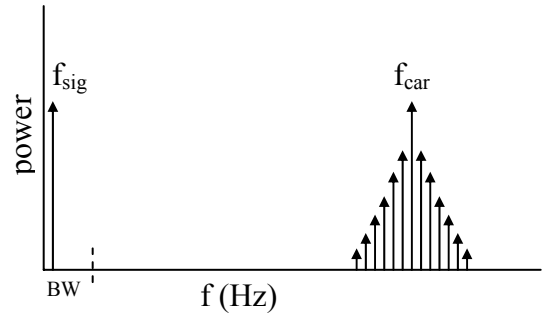

Figure 3: Modulation errors in a PWM

As long as the input signal has a much lower frequency as the carrier frequency, it can be considered as quasi-static. As long the input signal can be considered as quasi-static, the PWM output signal represents a time reference signal of the input signal. This is clearly visible in Figure 2, where 3 timeframes are given of situations with 3 different modulation depths. This figure is merely a raw example of how PWM works.

A model of this system is given in Figure 4.

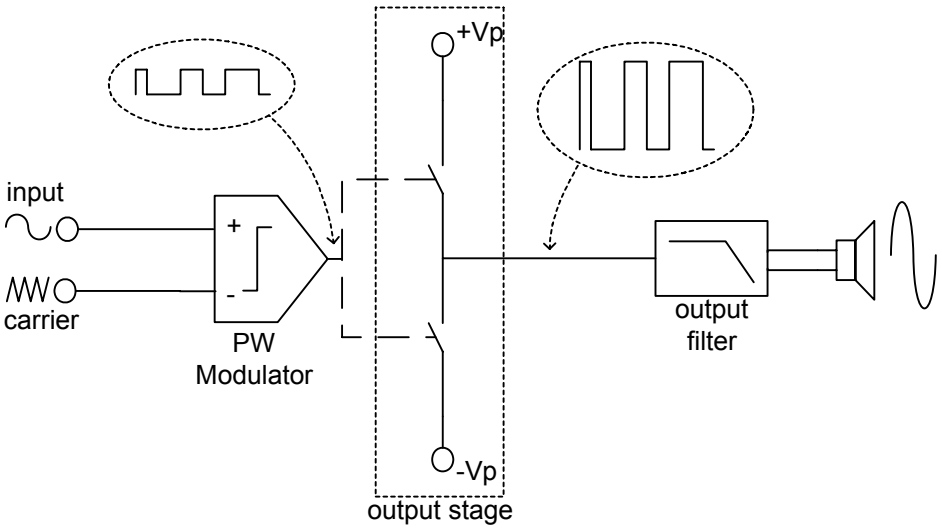

Figure 4: Basic feedforward Class-D Model

Unfortunately in practice a PWM is not ideal. For example the supply-voltage (V_p) will not be constant but will contain a ripple which translates into a tone at the ripple frequency harmonics due to the modulation. Due to modulation, the ripple frequency and its harmonics also folds around the input signal. Another non-ideality is clock jitter in the carrier generator. This clock jitter will corrupt the triangular carrier signal and so the comparator decision will be slightly wrong. Also dead-time used to be a source of distortion. Dead-time is the small time during the switching of the output stage, when the pull-up and pull-down transistors in the output stage are both off in order not to short-circuit the supply voltage ([2]). Due to new techniques, dead-time is not considered as a big source of distortion anymore ([3]).

Most of these distortions can be effectively suppressed by applying feedback to the system. But feedback has to be designed with care, due to the chance of instability. In

the next paragraph a feedback PWM is described in more detail. But before continuing some definitions are given to ease the explanation.

- *Modulation depth* ($\Delta = V_{in}/V_t$): the ratio between the amplitude of the input signal (V_{in}) and the amplitude of the carrier signal at the input of the comparator (V_t)
- *Feedforward gain* ($G_{PWM} \approx V_{PWM}/V_t$): considering only the low frequency (the audio frequency rang in this case), the ratio between the amplitude of the output and the amplitude of the carrier signal at the input of the comparator.

2.1.2 The Feedback Pulse Width Modulator

In a feedback PWM, the output is compared with the input of the system. This way the error of the system is estimated and thus can be compensated. A loop filter needs to be inserted with the denominator at least one order higher than the nominator to avoid instability and to achieve the desired noise suppression ([5]). In chapter 3 we will see that a well designed loop filter will have low-pass characteristics for the input signal, while every signal introduced inside the feedback loop has high-pass characteristics. If the input bandwidth is low frequency, the noise and distortion introduced by for example the output stage is very low at the input frequencies (Figure 5). The noise and distortion at high frequencies are not suppressed, but these can be filtered out by a low-pass output filter. This way the noise and distortion in the filtered output signal is very low.

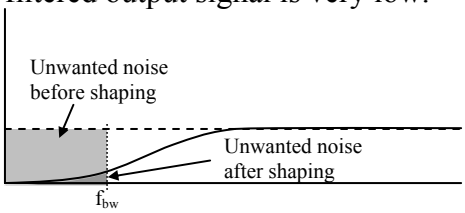

Figure 5: Principle of feedback noise suppression

An example of a feedback PWM is given in Figure 6. In this example the output filter is not part of the feedback system.

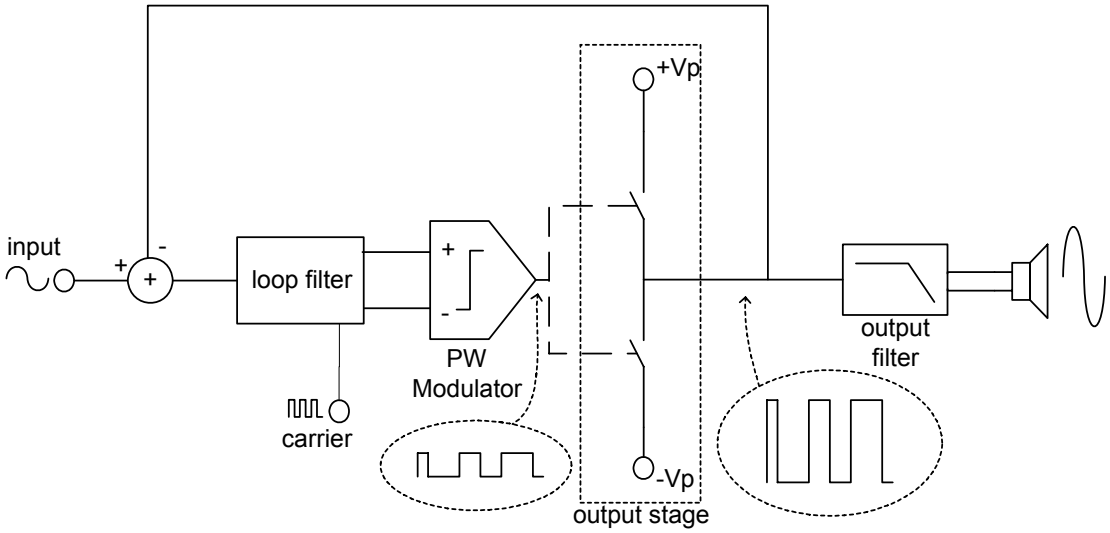

Figure 6: Basic feedback Pulse Width Modulator Model

When feedback is applied this way, every source introduced inside the feedback loop will be suppressed due to the feedback loop. So as mentioned in the previous paragraph, adding feedback to a PWM will effectively decrease the non-ideality effects like the supply voltage modulation and clock jitter (in most cases).

But feedback also introduces its own distortions:

- Due to PWM modulation the input frequency and its higher harmonics are present around multiples of the carrier frequency. For a feedforward system this is not an issue, because they are filtered out by the output filter. In case of feedback the higher harmonics fold back to the baseband creating noise/distortion components in the baseband (Figure 7).

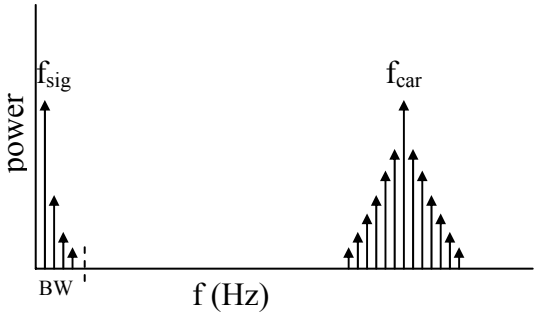

Figure 7: Modulation errors in a PWM with feedback

- In an ideal PW modulator the input is compared with an ideal triangular carrier signal. In the feedback system shown in Figure 6 the carrier signal is a block wave inserted at the input of the last integrator of the loop filter to create the triangular signal at the input of the comparator as will be seen in §6.1. This means the feedbacked signal is affected by the loop filter, while the carrier signal is not affected by the loop filter. Due to the loop filter the feedbacked signal will have a different phase shift than the carrier signal at the input of the comparator, thus the comparison is not ideal anymore from the ideal point of view. As will be seen in paragraph 4.5 the carrier signal can be inserted at the input of the loop-filter to get a better comparison. But this also introduces its drawbacks as will be discussed in paragraph 4.5.
- Another point of concern for feedback systems is the stability issue.
    - The first logic step to avoid instability is to place the loop filter zeros in the left halve of the s-plane. This is considered as basic knowledge.
    - Another source of instability and more specific for this system, is clipping of the PW Modulator. Clipping in this context is when, in a period of the carrier signal, the output doesn't switch. Clipping of the modulator occurs when the error triangle signal V_e (Figure 6) is larger than the carrier triangle frequency V_t. One can say the system is overloaded in this case. As explained in [2] the criterions for avoiding instability in a feedback loop are as follow:
        - The carrier triangle signal should be twice as big as the triangle error signal

$$V_t > 2V_e \qquad \textbf{(2-1)}$$

- The unity-gain frequency should be smaller than the carrier frequency divided by π.

$$\omega_{UG} < \frac{\omega_{car}}{\pi} \qquad \textbf{(2-2)}$$

- For higher order loop filters the LHP zero frequency should be sufficiently lower than the unity-gain frequency (ω_{UG}) in order to obtain sufficient phase margin and acceptable peaking of the closed-loop transfer.

o Another point to avoid instability is that open loop transfer function has a 1st order slope at the unity gain frequency. If the slope is a higher order the NTF will have an overshoot and which can result in an instable system.

- In practice the comparator is also not ideal. The comparator suffers from a delay which translates into an extra phase-shift. In a feedback system this affects the performance of the system. Because the input signal is low frequency, it can be considered as quasi-static. The input signal can be considered as a very slow changing signal (almost constant) with respect to the carrier signal. If the comparator delay is very small the input signal can be still considered as an almost constant value. If this is the case the comparator delay can be neglected. If the comparator delay is bigger the input signal has to be considered as less constant and so the comparison is less accurate. The result is that the error signal (V_e) will be bigger and so it has to be taken into account in the stability analysis.
- As mentioned in §2.1.1, clock jitter corrupts the triangular carrier signal, which results in wrong comparator decisions. The triangular carrier signal is created by integrating a block signal ([4]). Clock jitter in the block signal not only creates a variable phase shift, but it also affects the amplitude of the triangular carrier signal from period to period (see Figure 8, in the figure the jitter is very severe in order to show its effect). Jitter causes noise in the audio bandwidth. This so called jitter noise could be suppressed by the feedback loop. It depends were the carrier signal is inserted. (This will be explained in this report). Also jitter could result in clipping of the PWM. The jitter noise will add a little voltage to the internal signal and if this is not proper analyzed, this extra voltage could cause clipping.

Next chapter will go more into the loop filter and calculate the optimum filters.

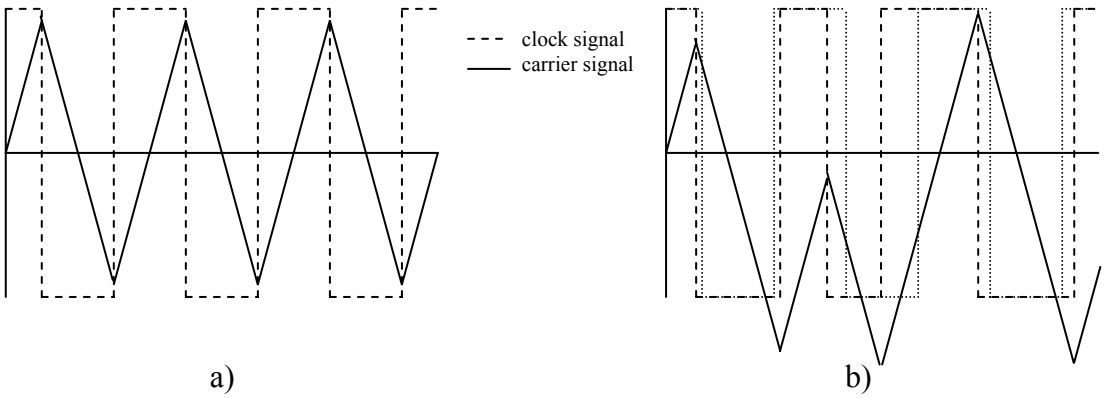

Figure 8: Carrier signal: a) ideal, b) with jitter

2.2 2nd order feedback loop for a Class-D audio amplifier by Philips

Philips has developed a good working 2nd order feedback loop for a Class-D audio amplifier ([2]). The amplifier is realized in a silicon-on-insulator (SOI)-based technology called A-BCD. This technology allows creating low voltage and high voltage circuits on the same wafer without latch-up phenomena. This way a 60 Volt output stage could be realized on the same wafer as the 12 Volt internal circuitry.

The PWM method used in this amplifier is also double-side natural sampling. This method was explained in §2.1.1. Conceptually, the input signal is compared with a triangular reference wave. When the input signal is converted to a PWM signal the output stage amplifies it to high power levels. The PWM output is then filtered by an output filter to extract only the audio content. A simple LC filter can be used for the purpose.

The amplifier uses a 2nd order feedback loop to suppress the supply voltage ripple and pulse-shape errors in the switching power stage. As input VI-converter a Gm is chosen because it has some advantages over a resistor:

- The input impedance is independent of the feedback loop.
- It has a differential input.
- The amplifier can be muted without influencing the feedback loop
- The noise and offset of the first integrator in the loop are not amplified by the closed-loop gain

Still the input gm and the feedback resistor have to be very linear to achieve a good closed-loop performance.

The reference triangle is realized by injecting a square-wave current into the virtual ground of the second (last) integrator. By doing this the duty-cycle errors or jitter from the oscillator is suppressed by the feedback loop. This allows one to use a less accurate oscillator.

The focus in this design was to reduce the effect of deadtime and supply-voltage modulation. This distortion is generated at the output stage. Using the feedback loop this distortion is being suppressed according to the noise transfer function.

The amplifier achieved a good result with a THD+N of 0.017% for 1 watt output power

Some terms mentioned above are maybe unknown to some readers. But these elements will be explained in the course of this report. One can also read [2] to get a basic idea.

2.3 Project Goals

The amplifier mentioned in the previous paragraph used a second order feedback loop. It is interesting to research if a higher order feedback loop improves the PWM significantly. Therefore the focus in the project is on the loop-filter. There are many different ways the loop filter can be designed. Different choices can be made on different levels.

System level:

- The **filter type** determines the shape of the noise transfer function (NTF). As will be seen, in this report the filter is designed on the basis of the NTF (how the noise and distortion generated at the end of the feedback loop is filtered). There exist many filter types like: Butterworth, Chebyshev, Elliptic and many hybrid filters. Due to the time limit for this project the focus is reduced to only the Butterworth and Chebyshev type filter because of their flat pass-band. The best type is used for implementation.
- The **filter order** determines the amount of filtering. A higher order filter results in more aggressive filtering of the noise generated inside the feedback loop. This is visible in the NTF. Higher order filters result in steeper slopes in the stop-band. The orders 1 till 5 are investigated
- The **loop gain and corner frequencies** are important factors for the loop filter. First it also determines the amount of filtering. A high loop gain results in more aggressive filtering of the noise generated inside the feedback loop. But the loop gain and corner frequencies cannot be set freely. If the loop gain is chosen too big or if the corner frequencies are put on a too high frequency, the system can become unstable due to equations (2-1). In the first part of this project an optimum for the loop gain and corner frequencies is investigated.
- The **frequency of the carrier signal** is also very important in the design of the loop filter. The carrier frequency set restrictions to, for example, the loop gain. By increasing the carrier frequency a higher loop gain can be chosen without the system becoming unstable.

It is not possible or even advantageous to ever increasing things like the filter order or loop gain. There are optimums in these parameters. These optimums depend on different points. The most important point is **stability of the system**. For example as already mentioned before, one cannot choose the loop gain too high. This results in an unstable system.

The choices to make as mentioned above also depend on the amount and types of noise or distortion. There are big differences between how to filter different types of noise or distortion. The noise- and distortion-sources investigated in project are:

- Supply voltage error
- Carrier jitter noise

And in lesser extend:

- Output stage noise

The systems were modeled at system level in simulation software. The software used is Matlab and Simulink.

Implementation of the loop-filter:

The level of implementation depended on the available amount of time. It was not possible to develop an implementation ready for production in the given amount of time for this project.

Again at component level there are many choices to make. The focus at the component level is on:

- There exist different **structures of the loop filter** for the same NTF. The differences in those structures are for example: the signal transfer function, power consumption and the specifications of the components inside. A subject of the structure of the loop filter is how the gain factors are implemented. For this implementation one can think about the trade-off between linearity and tunability
- Because the foundation of the loop filter is its integrators, the **structure of the integrators** is also an important issue. At first the integrators are considered as ideal, but in practice the integrators as far from ideal. Integrators suffer from many non-idealities like: **parasitic zeros and poles**, **finite gain** and **load impedances**. One can live with these non-idealities only when the integrator is properly designed. The different structures of the integrators differ from each other in: linearity, frequency range, power consumption, area consumption and tunability.

The values of the components are calculated. During the calculation of the components there are some things to be taken into account:

- **Voltage swing**: Signals in the actual systems cannot be limitless. One limit is the internal supply voltage. Signals cannot exceed the supply voltage. So the gain of the integrators has to be scaled in order that the signals will not clip to the supply voltage.
- It is important to **place the parasitic zeros and poles** on a place of desire. It can lead to instability or the function of the filter can heavily decrease if these parasitics lie at the wrong places. By choosing the right values of the components the parasitic can be placed on a place where they do no harm.

The implementation design is made in Cadence and is suitable for Philips' ABCD3 process.

Table 1 shows the specifications used in this project. Some of the specifications are already mentioned above. Others were also given in the assignment.

Parameter	**Specification**	
Filter types	Butterworth or Chebyshev	
Filter order	1 t/m 5	
Carrier frequency	350 kHz or 700 kHz	
Input frequency range	20 Hz – 20 kHz	
Input voltage	2 Volt peak-peak	Amplification = 30
Output voltage	60 Volt peak-peak	
Internal supply voltage	12 Volt peak-peak	
Comparator delay	30 ns	

Table 1: Specifications

In next chapters the subjects mentioned above are investigated, design choices are made and with those choices a beginning of a loop filter implementation is made. There was not enough time to completely out-develop the loop-filter, but a good start is made, which could be picked up by a successor.

3 Loop filters

Feedback systems are able to improve the output signal very much in comparison to a feedforward system.

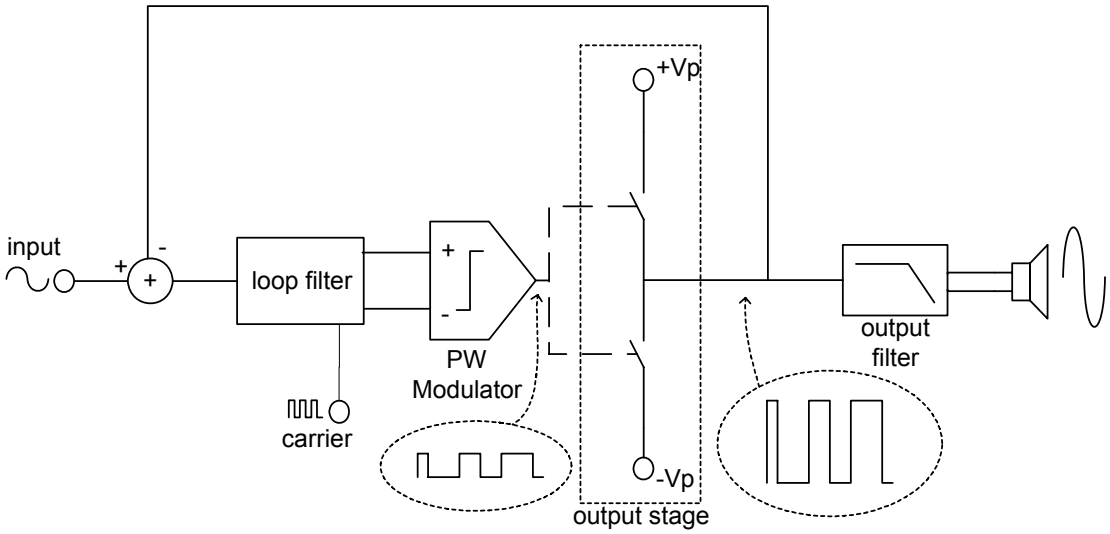

Figure 9: Basic feedback Pulse Width Modulator Model

With feedback it is possible to suppress noise and unwanted signals in a desired frequency range which are inserted or generated inside the feedback loop, while the input signal at these frequencies are passed through unaffected. While the noise or unwanted signals are suppressed in the signal-band, at other frequencies they are not suppressed and sometimes even amplified. This is sometimes also described as noise-shaping. If this is done the unwanted signals and noise can be filtered out of the system, without affecting the input signal. Only the unwanted signals and noise introduced inside the feedback loop can be shaped. Unwanted signals and noise inside the desired frequency band, introduced outside the feedback loop, are not seen by the feedback loop and so it is not be affected by it.

The way the noise is shaped can be determined by the loop-filter. The loop filter determines the signal transfer function (STF) and noise transfer function (NTF) of the system.

In the next chapter the different type loop filters are introduced and calculated. In this project the noise will only be suppressed as in a high-pass filter. It is possible to transfer noise from a certain pass-band, but that is not further discussed in this project.

3.1 Loop filter calculations and conditions

The loop filter can be seen as a function with zeros and poles:

$$H(s) = \frac{Z_H(s)}{P_H(s)} \qquad \textbf{(3-1)}$$

The open loop transfer is given by:

$$H_{open}(s) = G_{PWM} H(s) = G_{PWM} \frac{Z_H(s)}{P_H(s)} \qquad \textbf{(3-2)}$$

And the closed loop transfer or signal transfer function (STF):

$$H_{ST}(s) = \frac{H_{open}(s)}{1 + H_{open}(s)} = \frac{G_{PWM} Z_H(s)}{P_H(s) + G_{PWM} Z_H(s)} \quad \textbf{(3-3)}$$

With G_{PWM} as the gain of the feed-forward PWM, $Z_H(s)$ as the zeros of the loop filter transfer and $P_H(s)$ as the poles of the loop filter transfer.

In this project the field of research is higher order filters. When the order of the loop filter is an order higher than two the calculations will become very complex very rapidly. So it becomes difficult to calculate the optimal filter. Because of the feedback loop, this PW modulator can be considered as noise-shaper. The shape of the noise spectral density is of our interest. So why not specify a certain desired noise transfer function and calculate the loop filter from that noise transfer function. (see [5])

The noise transfer function of the system is given by:

$$H_{NT}(s) = \frac{1}{1 + H_{open}(s)} = \frac{P_H(s)}{P_H(s) + G_{PWM} Z_H(s)} \quad \Rightarrow \quad H_{open}(s) = \frac{1}{H_{NT}(s)} - 1 \quad \textbf{(3-4)}$$

Looking at equation (3-4) it can be noticed that the poles of loop filter will translate to the zeros of the noise transfer function while the poles, the zeros and the PWM gain are responsible for the poles of the noise transfer function.

To have a good noise reduction in a feedback system it's desired that the feedback loop has a high loop gain. The loop gain will determine the amount of noise reduction. If the loop gain is high the system has more noise reduction (see equation (3-4)), while the STF stays unity (see equation (3-3))

Related to the filter design, a design constrain has to be followed. The order of the denominator of the loop filter transfer has to be higher than de numerator. This is to avoid an algebraic loop in the system ([5]). Together with equation (2-4) one can see that the order the nominator and denominator of the NTF are both the same order as the denominator of the open loop transfer. In other words, the NTF has the same amount of poles as zeros and this is the same as the amount of poles in the open loop transfer. This can be summarized to the following equation:

$$order(P_H) > order(Z_H) \quad \Rightarrow \quad order(P_{NTF}) = order(Z_{NTF}) = order(P_H) \quad \textbf{(3-5)}$$

With this in mind the desired noise transfer can be designed. The simplest approach is to take a high-pass version of a standard filter (like a Butterworth or Chebyshev) as the base of the noise transfer function. Equation (3-4) shows how to calculate the loop filter from the noise transfer function.
In the next paragraphs two different prototypes are discussed. The Butterworth type (§3.2) and the Chebyshev type (§3.3)

3.2 Butterworth type Noise transfer function

3.2.1 Noise transfer function

A high-pass Butterworth characteristic is calculated by placing poles in the origin of the s-plane. The order of the zeros must be the same the order of the poles in order to have a flat pass-band.
According to [7] a low-pass Butterworth transfer function has the following magnitude:

$$\left|H(j\frac{\omega}{\omega_c})\right| = \frac{1}{\sqrt{1+\left(\frac{\omega}{\omega_c}\right)^{2n}}} \quad \textbf{(3-6)}$$

Where n is the order of the system and ω_c is the angular cutoff frequency or the *-3·n dB* point. The low-pass Butterworth transfer function will have the following form.

$$H_{but\_low}(s) = \frac{\omega_c{}^n}{s^n + a_1\omega_c s^{n-1} + \ldots + a_{n-1}\omega_c{}^{n-1}s + \omega_c{}^n} \quad \textbf{(3-7)}$$

The value of parameter a_i can be found in appendix 10.1.
To translate it to a high-pass filter next substitution has to be applied:

$$\frac{\omega}{\omega_c} \Rightarrow \frac{\omega_c}{\omega} \quad \textbf{(3-8)}$$

Using (3-6) and (3-8) the high-pass version of a Butterworth transfer function will look like this:

$$H_{but\_high}(s) = \frac{s^n}{s^n + a_1\omega_c s^{n-1} + \ldots + a_{n-1}\omega_c{}^{n-1}s + \omega_c{}^n} \quad \textbf{(3-9)}$$

NTF's from order 1 to 5 are calculated their bode-plots are shown in Figure 10. As can be seen from the amplitude plot, higher order filters will suppress the noise at low frequencies more than the lower order filters. But equation (2-2) has to be kept in mind. At the unity gain frequency of the open loop transfer function there has to be enough phase margin. This is why the corner frequency shifts to the left for higher filter orders. When we take a better look at the open loop filter we can see how the corner frequency is determined for every order of filter and what the actual phase margins are. This will be discussed in next paragraph.

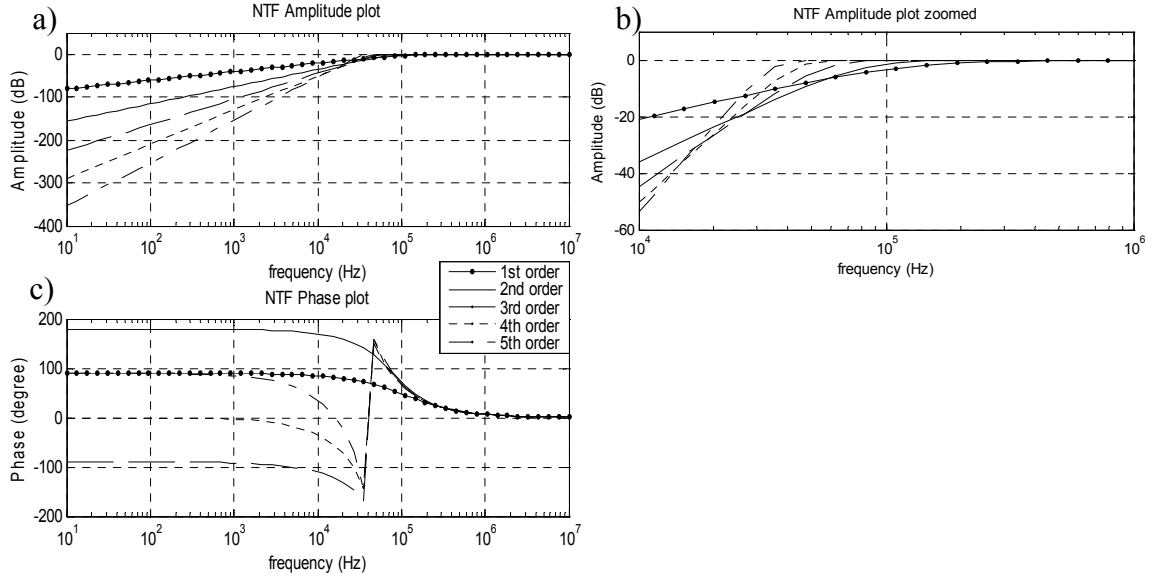

Figure 10: Bode plots of NTF's with Butterworth characteristics: a) amplitude, b) amplitude zoomed in, c) phase

3.2.2 Open loop transfer function

Now this high-pass transfer function is taken as the prototype for the NTF (3-9). With this as starting point it's easy to calculate the open-loop transfer function using equation (3-4). The result is in following form:

$$H_{open}(s) = \frac{a_1\omega_c s^{n-1} + \ldots + a_{n-1}\omega_c{}^{n-1} s + \omega_c{}^{n}}{s^n} \qquad \textbf{(3-10)}$$

From this formula it can be seen what the loop filter has to be and with what the loop gain. From equations (3-2) and (3-10) it can be seen that for Butterworth type filter the loop gain is:

$$G_{PWM} = a_1\omega_c \qquad \textbf{(3-11)}$$

and the loop filter has to look like:

$$H(s) = \frac{Z(s)}{P(s)} = \frac{s^{n-1} + \ldots + \frac{a_{n-1}\omega_c{}^{n-2}}{a_1} s + \frac{\omega_c{}^{n-1}}{a_1}}{s^n} \qquad \textbf{(3-12)}$$

Better insight in stability can be obtained from the root locus plots (see Figure 11 for 2nd till 5th order filters). As can be seen from the formula as well from the root locus plots of Figure 11 the poles of the open loop transfer function with Butterworth characteristics lie in the origin.

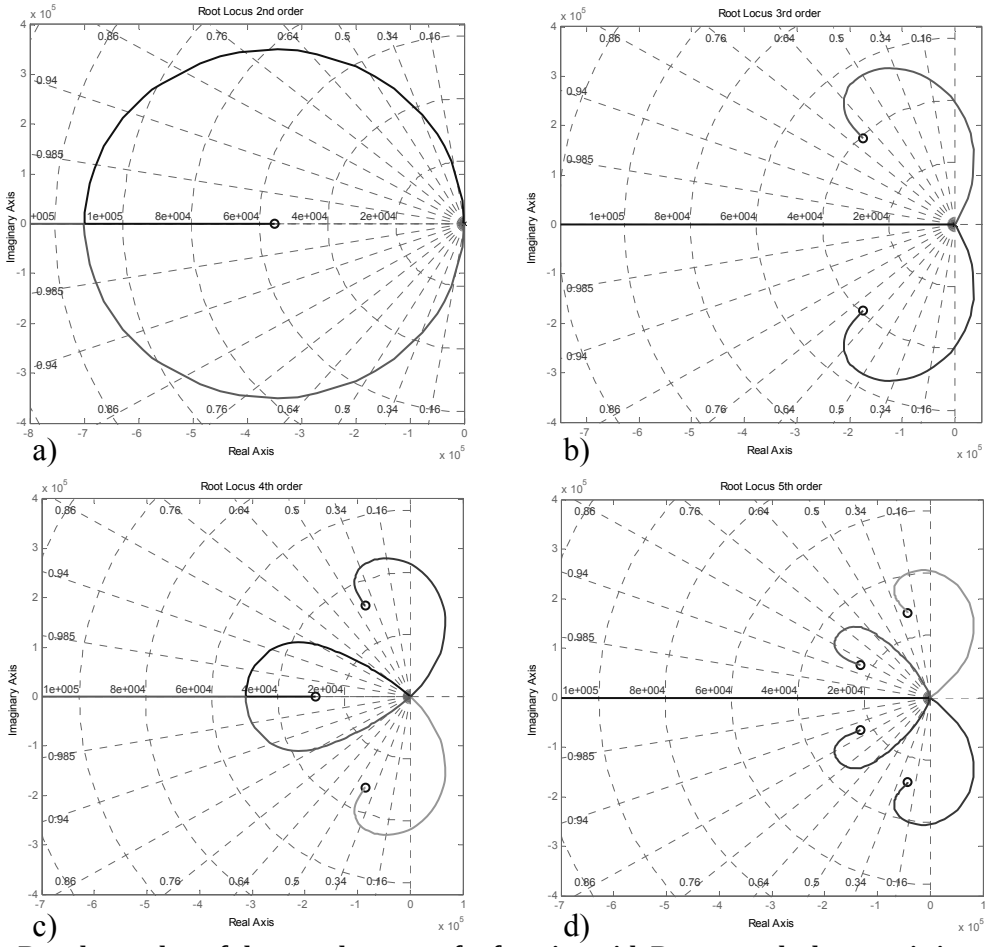

Figure 11: Root locus plots of the open loop transfer function with Butterworth characteristics for a: a) 2nd order, b) 3rd order, c) 4th order and d) 5th order loop filter

This results in the high gain at dc level as shown in the amplitude bode plot of Figure 12a. Because the NTF is calculated as a perfect Butterworth function the open loop transfer will be a little bit deformed and shows not a perfect Butteworth filter, this is visible because the zeros in the left half plane don't lie in line with a circle around the origin, characteristic for Butterworth. If the order is higher than 2, a too low loop gain will result in an instable feedback system. Looking at the root locus plots, some poles will travel first through the right half plane before entering left half plan. If a pole lies in the right half plane the system will be unstable.

As already mentioned the corner frequency of the desired NTF can be determined by looking at the open loop transfer function. From chapter 2.1.2 it's known that the unity gain frequency of the feedback loop should be sufficiently lower than the carrier frequency. See equation (2-2).

A carrier frequency of 352.8 kHz is used in the simulations. 352.8 kHz is multiple of 44.1 kHz (a well-known sample frequency in audio) and thus useful for the Fourier analysis.
Using a carrier frequency of 352.8 kHz the unity gain frequency should be less than $352.8/\pi$ kHz (or 705600 rad/sec). For a 1st order system it's easy to see that a loop gain of 700000 satisfies this condition. As mentions in paragraph 2.1.2 the slope of the amplitude plot has to be 1st order at the unity gain frequency. So a higher order loop-filter needs zeros at a frequency lower than the unity gain frequency in order to have a 1st order slope at unity gain. The frequency of the transition from higher order slope to the open loop transfer (ω_{c_o}) is related to the corner frequency (ω_c) of the NTF (equation (3-10)). To have the best noise suppression it is desirable to choose ω_c as high as possible. But one cannot choose the unity gain frequency from equation (2-2) as the ω_{c_o}. This way the *-3·n dB* point at ω_{c_o} is put at this frequency and thus the actual unity gain frequency of the system (ω_{UG}) will be higher, which results in an unstable system. In order to satisfy (2-2) the ω_{c_o} have to shift a little bit to a lower frequency.

As can be seen from equation (3-11), the PWM gain (G_{PWM}) is directly related to ω_c. It is only multiplied by the constant a_1. From appendix 10.1 it can be seen a_1 increases when the order of the filter increases. If one uses a constant G_{PWM} and increases the order of the filter, ω_c decreases (keeping in mind the NTF has to be a ideal Butterworth type). Because ω_{c_o} decreases when ω_c decreases, if the G_{PWM} is held constant, ω_{c_o} decreases when a higher order is chosen. This is exactly what is needed.

Now look at a 1st order filter. No ω_{c_o} is present and G_{PWM} could be calculated using equations (2-2) and (3-11). It turns out if this same G_{PWM} is also used for higher order filters, the ω_{c_o} of these filters will be placed low enough to have a 1st order slope of the open loop transfer at unity gain. The actual values for ω_{c_o} are not calculated in this project. The actual could be calculate with equation (3-12).

As can be seen in appendix 10.2.1 the loop gain of the 1st order filter is the same as the unity gain frequency (in radials).

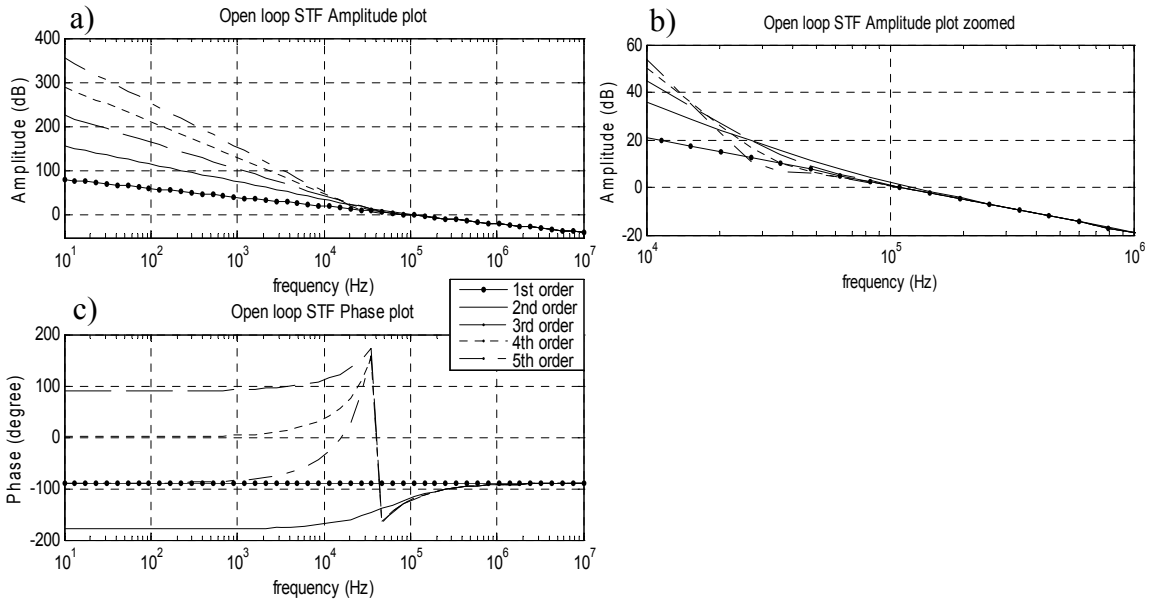

Figure 12: Bode plots of open loop transfer functions with Butterworth characteristics: a) amplitude, b) amplitude zoomed in, c) phase

Appendix 10.2 shows the Butterworth filter calculations until 3rd order filter. Higher order filters are becoming too complex to put in this report and are easy to be calculated by Matlab. See Figure 13 for the Matlab code.

```
[zn,pn,kn] = butter(n,2*ftri/a1,'high','s');
Hntf=zpk(zn,pn,kn)
Hopen=1/Hntf-1
Hcl=feedback(Hopen,1)
```

Figure 13: Matlab code: Butterworth filter calculations

In this code the function `butter()` returns the zeros, poles and gain for a high pass Butterworth transfer function of `n`'th order and with a corner frequency of `ftri/a1`. `ftri` is the frequency in Hz of the triangular carrier and `a1` is taken from the table of appendix 10.1 to shift the ω_{c_o} for higher order filters. The rest of the functions calculate the NTF, open loop transfer function and STF, but they don't need any explanation.

3.2.3 Signal transfer function

Finally according to (3-3) the STF is:

$$H_S(s) = \frac{a_1\omega_c s^{n-1} + \ldots + a_{n-1}\omega_c{}^{n-1}s + \omega_c{}^n}{s^n + a_1\omega_c s^{n-1} + \ldots + a_{n-1}\omega_c{}^{n-1}s + \omega_c{}^n} \qquad \textbf{(3-13)}$$

Figure 14 shows the bode plots of the STF. As can be seen the amplitude shows a flat characteristic over the audio bandwidth. Higher order systems show an overshoot at the corner frequency. If this peaking is too severe the system can overload if the input signal has frequency components at these frequencies. When overloading the filter, equation (2-1) doesn't hold and it leads to instability of the system. For now it is assumed that the input signal doesn't contain these frequency components. Another reason why it's not the biggest reason of concern, if the loop filter is implemented the STF of the feedback system can be altered by the way of applying the feedback.

This issue will be discussed later in this report when the filter will actually be implemented.

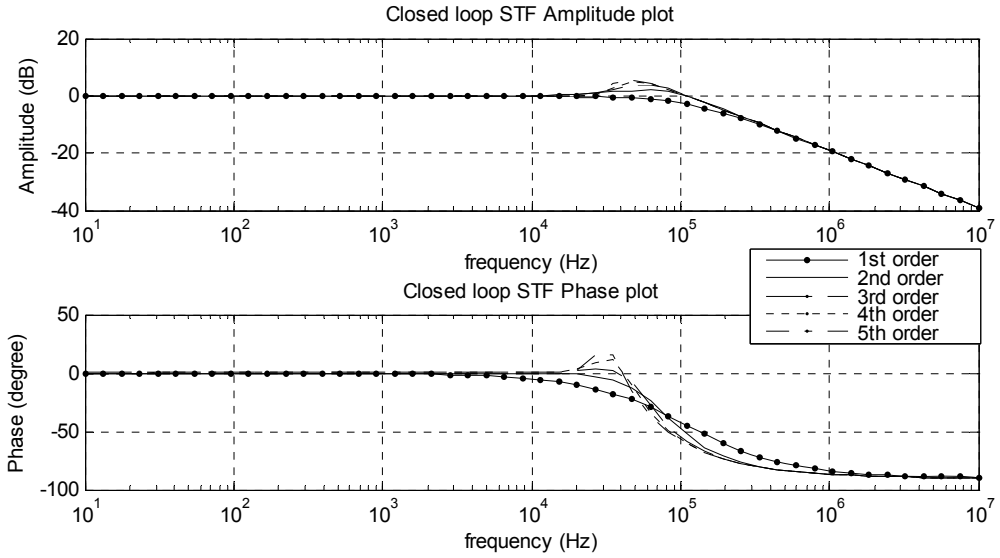

Figure 14: Bode plots of the STF of feedback system with Butterworth characteristics

3.3 Chebyshev type Noise transfer function

In previous paragraph a Butterworth type filter is used as loop filter. By placing the open loop poles in the origin, it has a very high DC-loop-gain and dropping along the frequency axis. As a result it has a very high DC- or low frequency noise suppression, but less noise suppression at higher frequencies.
Now another filter type is discussed which will have a more flat transfer function and overall a better signal to noise ratio (SNR) at the output of the system. This is done by placing the open loop poles on the imaginary axis instead of only in the origin as in case of a Butterworth filter. The maximum loop gain is not at DC anymore but at some given frequency. The consequence is that the filter has a steeper roll-off. But it also creates a ripple in the stop- or pass-band. The name of this filter is the Chebyshev filter.

The Chebyshev filter comes in two types. Type 1 and Type 2 or sometimes called inverse Chebyshev. De difference between the two filters is that the type 1 filter has a ripple in the pass-band, while the type 2 filter has a ripple in the stop-band. (see Figure 15).

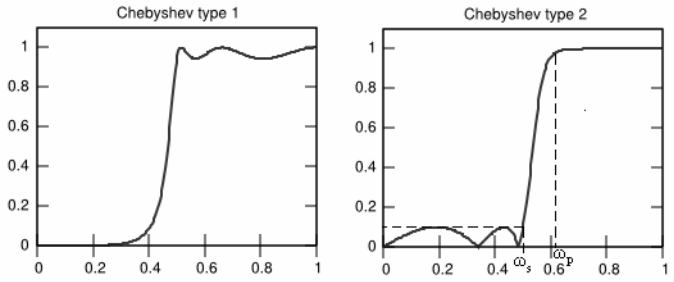

Figure 15: Two types of Chebyshev filters

3.3.1 Noise transfer function

To have the best noise reduction at lower frequencies, it's desired to use the Chebyshev type 2 filter as prototype. The Chebyshev calculations here are based on the Inverse Chebyshev Normalized Approximation Function described in [7].
The following magnitude response function is true for a low-pass type 2 Chebyshev filter:

$$\left|H(j\tfrac{\omega_s}{\omega})\right| = \sqrt{\frac{\varepsilon^2 C_n{}^2(\tfrac{\omega_s}{\omega})}{1+\varepsilon^2 C_n{}^2(\tfrac{\omega_s}{\omega})}} \qquad \textbf{(3-14)}$$

Where $C_n()$ is the Chebyshev polynomial and ε is related to the stop-band ripple (see appendix 10.3).
To translate it to a high-pass filter the same substitution as with the Butterworth filter has to be applied (see equation (3-8)). Resulting in the magnitude response function for the high-pass version:

$$\left|H(j\tfrac{\omega}{\omega_s})\right| = \sqrt{\frac{\varepsilon^2 C_n{}^2(\tfrac{\omega}{\omega_s})}{1+\varepsilon^2 C_n{}^2(\tfrac{\omega}{\omega_s})}} \qquad \textbf{(3-15)}$$

In [7] the calculated poles and zeros are inversed to get the actual poles and zeros. For a high-pass filter this is not necessary. Now ω_s is the stop-band bandwidth (Figure 15). The optimal Chebyshev type NTF for even functions will look like:

$$H_{NT}(s) = \frac{\prod_m \left(s^2 + A_{2m}\right)}{\prod_m \left(s^2 + B_{1m}s + B_{2m}\right)} \qquad \textbf{(3-16)}$$

$$m = 1, 2 \ldots \left[n/2\right] - 1 \quad (n \text{ even})$$

and for odd functions:

$$H_{NT}(s) = \frac{s\prod_m \left(s^2 + A_{2m}\right)}{\left(s+\sigma_R\right)\prod_m \left(s^2 + B_{1m}s + B_{2m}\right)} \qquad \textbf{(3-17)}$$

$$m = 1, 2 \ldots \left[\left(n-1\right)/2\right] - 1 \quad (n \text{ odd})$$

See appendix (10.4) for its calculations
Again the bode-plots of the NTF's from 1st to 5th order are plotted. Figure 16 shows the typical Chebyshev characteristics. The dip before the corner frequency is cause by the imaginary zeros in the transfer function. Even order filters have a flat spectrum until the dip before the corner frequency, while odd order filters have a 1st order slope. This is due to the zero in the origin of the odd order filters. So from this point of view the odd order filters are preferred because they have a better DC noise suppression. For the same reason as with the Butterworth type filters (paragraph 3.2), the corner frequency will shift to lower frequency if the order gets higher in order to satisfy equation (2-2).

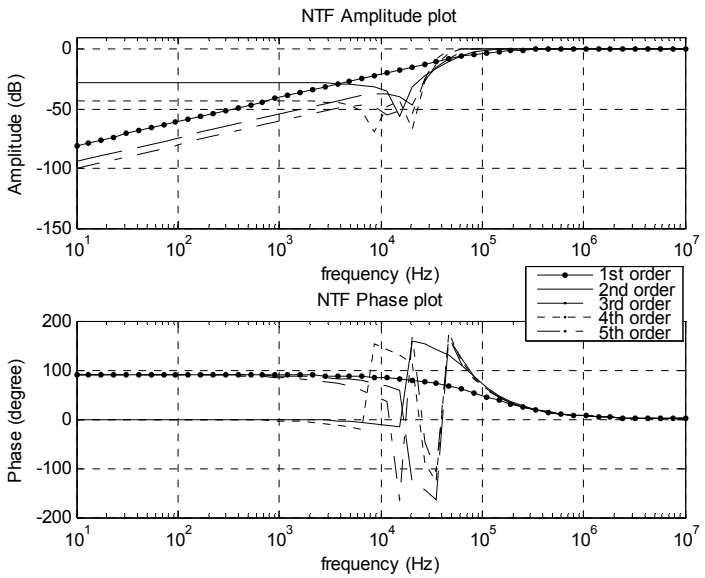

Figure 16: Bode plots of NTF's with Chebyshev characteristics: a) amplitude, b) amplitude zoomed in, c) phase

3.3.2 Open loop transfer function

From these preferred NTF's and equation (3-4) the open-loop transfer functions can be calculated and will look for even functions:

$$H_{open}(s) = \frac{\prod_m \left(s^2 + B_{1m}s + B_{2m}\right) - \prod_m \left(s^2 + A_{2m}\right)}{\prod_m \left(s^2 + A_{2m}\right)} \qquad \textbf{(3-18)}$$

$$m = 1, 2 \ldots \left[n/2\right] - 1 \quad (n \text{ even})$$

and for odd functions:

$$H_{open}(s) = \frac{\left(s + \sigma_R\right)\prod_m \left(s^2 + B_{1m}s + B_{2m}\right) - s\prod_m \left(s^2 + A_{2m}\right)}{s\prod_m \left(s^2 + A_{2m}\right)} \qquad \textbf{(3-19)}$$

$$m = 1, 2 \ldots \left[\left(n-1\right)/2\right] - 1 \quad (n \text{ odd})$$

In this formulation it's a little bit difficult to see how you can split it in the loop filter and PWM gain. But if you would explode these functions it will have the form of:

$$H_{open}(s) = \frac{G_{PWM}s^{n-1} + \ldots + b_1{\omega_s}^{n-1}s + {\omega_s}^n}{s^n + a_{n-2}{\omega_s}^2 s^{n-2} + \ldots + a_2{\omega_s}^{n-2}s^2 + {\omega_s}^n} \quad (n = \text{even}) \qquad \textbf{(3-20)}$$

for even function and:

$$H_{open}(s) = \frac{G_{PWM}s^{n-1} + \ldots + b_1{\omega_s}^{n-1}s + {\omega_s}^n}{s^n + a_{n-2}\omega_s s^{n-2} + \ldots + a_1{\omega_s}^{n-2}s + {\omega_s}^n} \quad (n = \text{odd}) \qquad \textbf{(3-21)}$$

for odd functions.

Combining the equations (3-18) to (3-21) the important PWM gain be calculated:

$$G_{PWM} = \sum_m B_{1m} \qquad \textbf{(3-22)}$$

$$m = 1, 2 \ldots \left[n/2\right] - 1 \quad (n \text{ even})$$

for even functions and for odd functions:

$$G_{PWM} = \sigma_R + \sum_m B_{1m}$$
$$m = 1, 2 \ldots \left[(n-1)/2 \right] - 1 \quad (n \text{ odd}) \qquad \textbf{(3-23)}$$

Again let's take a look at the root-locus plots of these open-loop functions in Figure 17. Looking at the root-locus plots of Figure 11 and Figure 17 the major differences between Butterworth and Chebyshev filters are: First Butterworth has all his poles in it's origin, creating a very high DC loop-gain. Chebyshev on the other hand has his poles on the imaginary axis. The result of this is a peak of the loop gain away from DC and a more flat spectrum at the lower frequencies. Only if it is a case of an odd order Chebyshev filter, it will have 1 pole in its origin, giving a higher DC gain, but this is not as much as with Butterworth.

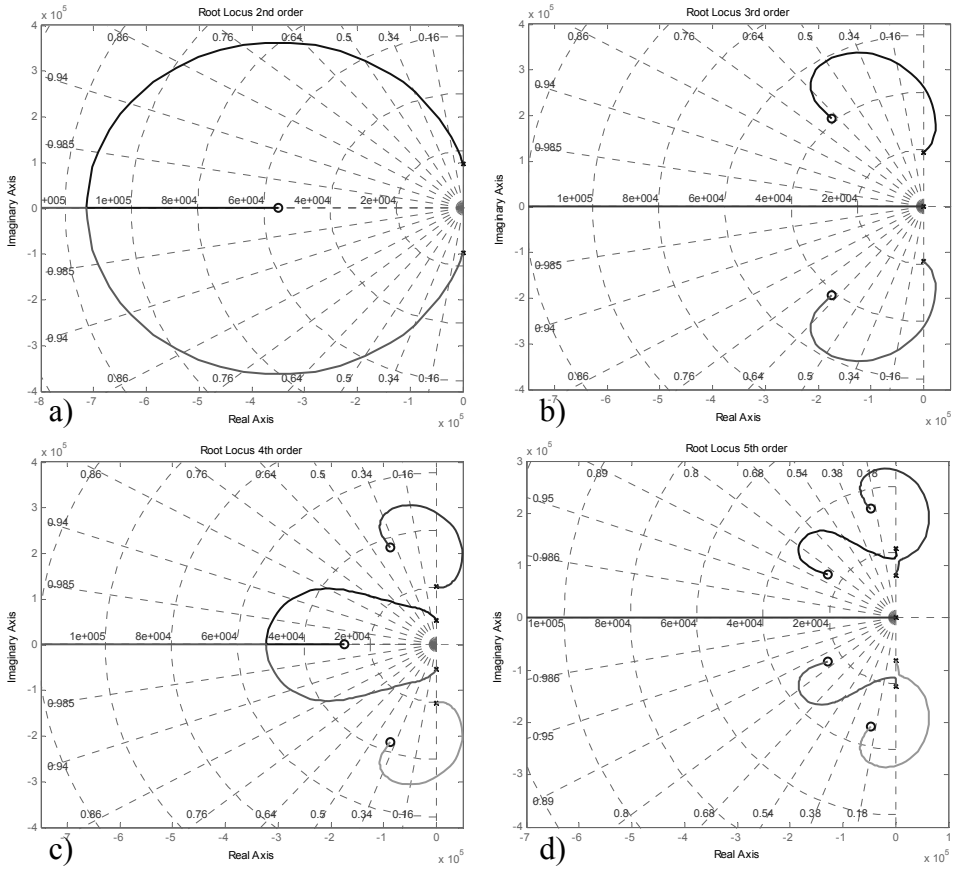

Figure 17: Root locus plots of the open loop transfer function with Chebyshev characteristics for a: a) 2nd order, b) 3rd order, c) 4th order and d) 5th order loop filter

A further examination on the open-loop transfer bode plot (Figure 18) shows the typical Chebyshev characteristics. Even order filters have the flat transfer for low frequencies, while odd order filters have a 1st order slope for low frequencies. The global maximum created by the poles on the imaginary axis is clearly visible. These maxima are caused by the poles of the open loop transfer which are the same as the zeros of the NTF. According to the calculations in appendix 10.4 the place of this maximum is only related to the stop-band bandwidth (ω_s, Figure 15) and if the order of the filter is odd or even. In this example ω_s is put at the end of the audio bandwidth

(20 kHz), to create a sort of flat (or 1st order slope) spectrum over the audio bandwidth. But it's of course possible to put the maximum somewhere in the audio bandwidth to suppress noise on the frequency most irritating for hearing.

The same conditions as for the Butterworth filters have to be applied on the Chebyshev filters to create a stable feedback system. Again to avoid the system from clipping and thus becoming unstable, equation (2-2) has to be obeyed. So for higher order filters the pass-band corner frequency (ω_p in Figure 15) has to shift to lower frequencies. In a Chebyshev filter ω_p is related to ω_s and the stop-band ripple. ω_p is a result of the zeros of equations (3-18) and (3-19). ω_s is put at the end of the audio bandwidth so that the filtering in the audio bandwidth is optimal. In this point of view ω_s is therefore fixed and ω_p can only be shift by the chosen stop-band ripple. The loop gain is also based on the stop-band ripple.

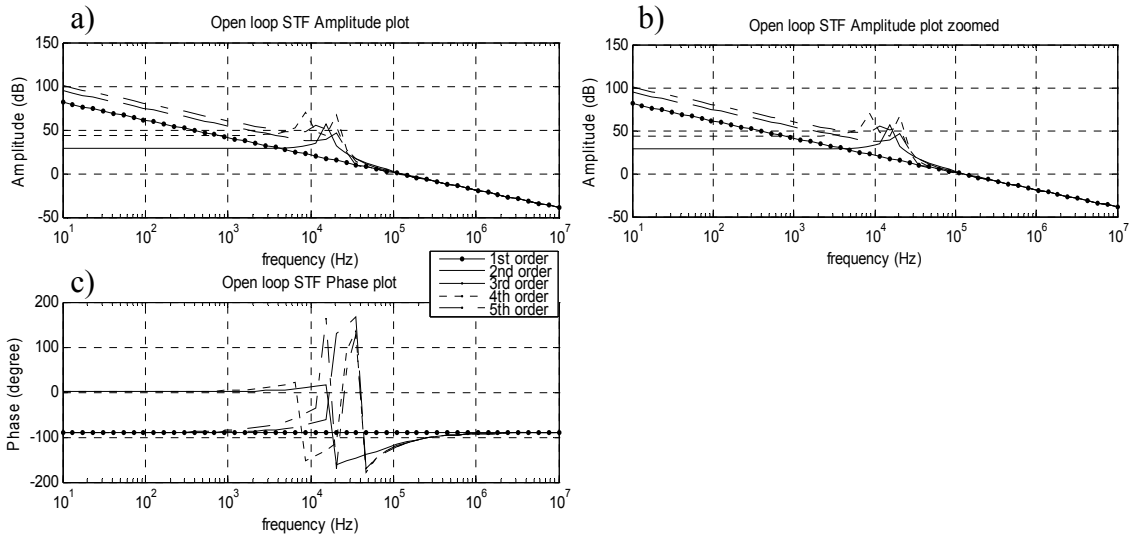

Figure 18: Bode plots of open loop transfer functions with Chebyshev characteristics

The same as with the Butterworth filters it turns out if the loop gain is held at the value of the loop-gain of the 1st order filter the unity gain frequency will stay on the same place. To calculate the loop filter appendix 10.4 can be used, but again as with the Butterworth the calculations will be too big to put in this report and it's very easy to calculate with Matlab. The source code is given in Figure 19.

```
[zn,pn,kn] = cheby2(n,Rb,Ws,'high','s');
Hntf=zpk(zn,pn,kn)
Hopen=1/Hntf-1
Hcl=feedback(Hopen,1)
```

Figure 19: Matlab code: Chebyshev filter calculations

In this code the function `cheby2()` returns the zeros, poles and gain for a high pass Chebyshev type 2 transfer function of `n`'th order and with a angular stop-band bandwith of `Ws`. `Rb` represents the ripple in dB in the stop-band. This is in this case the important parameter to keep the system stable.

3.3.3 Signal transfer function

What only rests now is signal transfer function:
For even order functions:

$$H_{ST}(s) = \frac{\prod_m \left(S^2 + B_{1m}S + B_{2m}\right) - \prod_m \left(S^2 + A_{2m}\right)}{\prod_m \left(S^2 + B_{1m}S + B_{2m}\right)} \qquad \textbf{(3-24)}$$

$$m = 1, 2 \ldots \left[n/2\right] - 1 \quad (n \text{ even})$$

and for odd order functions:

$$H_{open}(s) = \frac{\left(S + \sigma_R\right)\prod_m \left(S^2 + B_{1m}S + B_{2m}\right) - S\prod_m \left(S^2 + A_{2m}\right)}{\left(S + \sigma_R\right)\prod_m \left(S^2 + B_{1m}S + B_{2m}\right)} \qquad \textbf{(3-25)}$$

$$m = 1, 2 \ldots \left[\left(n-1\right)/2\right] - 1 \quad (n \text{ odd})$$

The bode plots of the STF are shown in Figure 20. Here you'll see the same overshoot as with the Butterworth filter (paragraph 3.2). So it's not relevant to repeat it here.

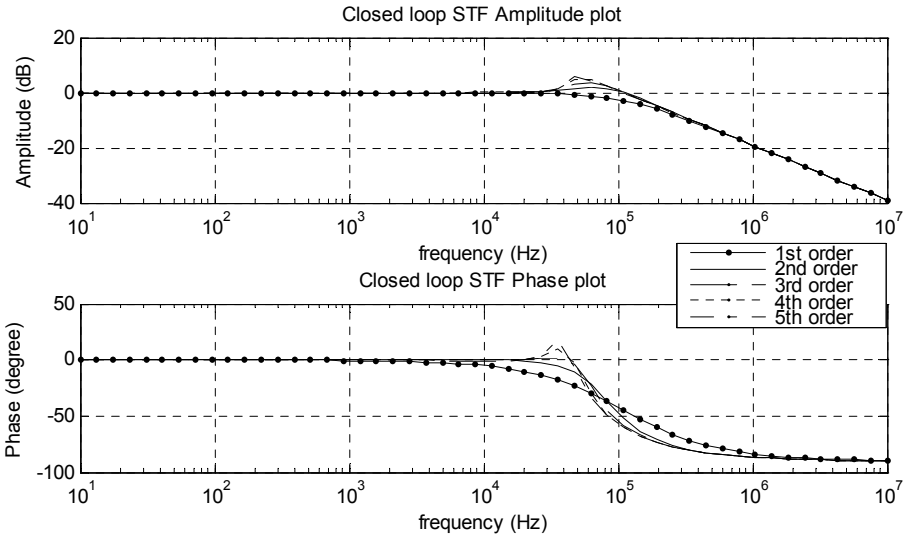

Figure 20: Bode plots of the STF of feedback system with Chebyshev characteristics

3.4 Loop filter conclusions.

Until now only the characteristics of the different type of loop filters were analyzed. It depends on the type of noise and distortion which is introduced in the loop to choose which type of filter is best. But some conclusions can already be drawn. When the noise and distortion has a white spectrum, the Chebyshev type filter is preferred. The Chebyshev type filter creates higher SNR of the system. The Butterworth type filter creates a much better noise suppression at low frequencies. So if the noise and distortion is more dominant at the lower part of the desired frequency range, the Butterworth type filter is preferred. It is also possible to design the filter more to the frequency response of the human ear. One can choose a Chebyshev type filter but with a smaller stop-band frequency range and so creating a sort hybrid filter between a Chebyshev and Butterworth type filter. This is outside the scope of this report and thus will not be further discussed.
In next chapter the noise and distortion sources of a PW modulator are analyzed. After these analyses we can choose the best type and order of the loop filter for this project.

4 System Model

In previous chapters the pulse width modulator system was explained and also how the loop filter could be calculated. In this chapter a model will be presented which is used to simulate the PWM at system level.
Because in practice the idealized system is a utopia it's necessary to include the most important sources of noise and distortion. The source include is this model are:

- Supply voltage error (4.3)
- Comparator delay (4.4)
- Jitter in the carrier signal (4.6)
- Output stage noise and distortion (4.7)

The system model is created in Simulink. Because Simulink is a graphic based tool for simulation it's easy to distinguish the components of the system and extract signals desired to be examined. This increases the ease in understanding the system. Simulink is combined with Matlab, because Matlab has some powerful tools to calculate for example the desired loop filter.

4.1 System Model

First of all let's take a look at the Simulink model itself. It is displayed in Figure 21. The loop filter is already discussed in chapter 3. The non-ideal effect like: supply voltage error, comparator delay, jitter in the carrier signal and noise of the output stage will be discussed in next paragraphs.

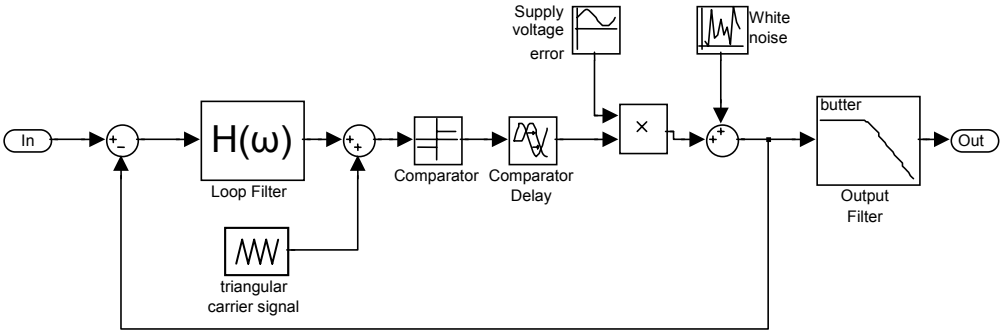

Figure 21: Simulink Model of the PW Modulator

The system will be simulated for different design choices at different conditions. This will give a good idea about the effect of the design choices. The design choices are:

- Filter order:
  - 1st order
  - 2nd order
  - 3rd order
  - 4th order
  - 5th order
- Filter type (NTF characteristics):
  - Butterworth
  - Inverse Chebyshev
- Carrier frequency:
  - 350 kHz
  - 700 kHz

The simulation parameters are given in appendix 10.6.

4.2 Ideal system

First let's take a look at the ideal system. In this case it means no voltage supply error, no comparator delay, no jitter and no other sources of noise. In this case only the intrinsic modulation errors will be visible (the higher harmonics mentioned in §2.1.2). Other noise visible is due to simulation error. As long as the simulation error does not exceeds the noise or distortion of interest it is not a problem.
Figure 22 shows the PSD's of systems with Butterworth type filters (a) or with Chebyshev type filters (b).

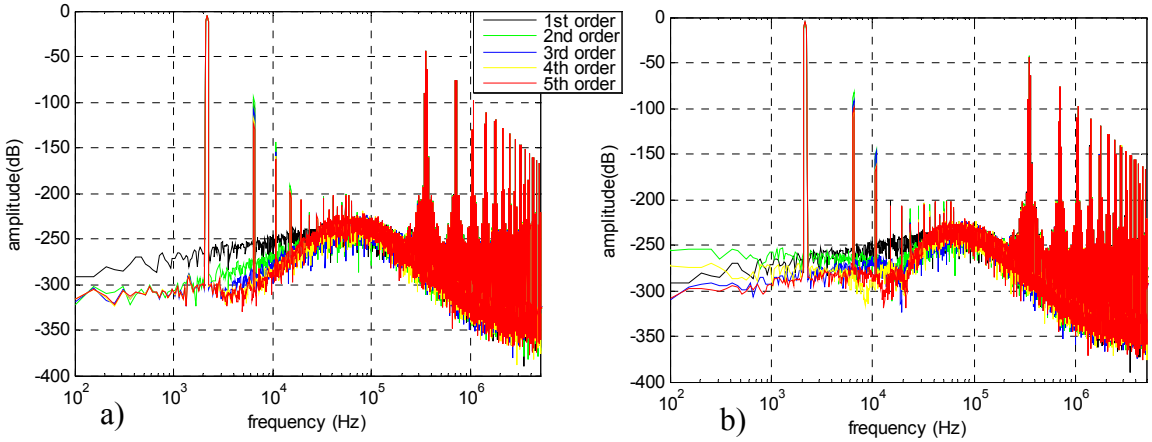

Figure 22: Simulation results: PSD plots of a ideal PWM model, type filter: (a) Butterworth, (b) Chebyshev.

In these plots it's hard to see the difference between the characteristics of the different filter types. This is because there is no white noise in the system and it's hard to see the NTF characteristics. But it is still visible when looking at the harmonics of the input signal. It's clearly visible that the 2nd harmonic has a lower peak in the Butterworth case in comparison to the Chebyshev case (see also appendix 10.7.1). This is all in line with the theory, as Butterworth type filters suppress disturbance at lower frequencies better than Chebyshev.
Another point of interest is that the harmonics of the 2nd order filter have a higher power than that of the 1st order filter. As mentioned in section 2.1.2, due to the loop filter a phase difference is present between the feedbacked signal and the carrier triangle. A higher order filter has more phase shift than a lower order, so the carrier triangle will be more corrupted. For a filter order of 3 or higher the suppression of the disturbance (including the disturbance due to this phase difference) will compensate it again, but in case of the 2nd order filter the disturbance suppression is not enough and thus the higher harmonics have a higher power.

4.3 Supply voltage error

A disturbance which has a high influence on the system's performance is the supply voltage error. Supply voltage error can be a low frequency disturbance like a 50/60 Hertz component in a DC supply from a converted AC source. These components will be modulated around the input signal (or multiplied on the output signal (Figure 21)). In this simulation a little higher frequency is chosen for the supply voltage error (458.6 Hz), this is due to the resolution of the FFT which is 51.4 Hz. In case a 50 Hz disturbance would have been chosen the individual components would not been visible very well. With a 458.6 Hz supply voltage error there will be components visible at: $\Delta n \cdot 458.6$ Hz (n=natural number) around the input signal and it's harmonics.

In these simulations the supply voltage error is considered the same for the positive as for the negative supply. In practice the positive and negative supply are separated and therefore their errors not correlated for a single-ended output stage.
Because this error is introduced after the loop-filter and inside the feedback-loop, this will be suppressed according to the NTF of the feedback loop. The simulation results showed in Figure 23 confirm this.

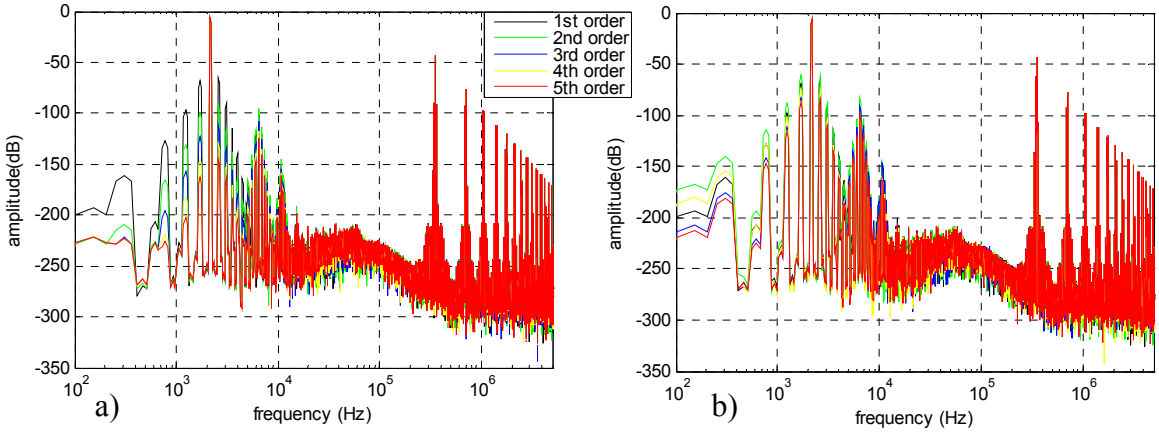

Figure 23: Simulation results: PSD plots of a PWM model with supply voltage error, type filter: (a) Butterworth, (b) Chebyshev.

Clearly visible is the modulation of the supply voltage error around the input signal and its harmonics. It's also clearly visible that a Butterworth type filter gives much better result in suppressing the supply voltage error disturbance than the Chebyshev type filter in this case (appendix 10.7.2). This is due to that the Butterworth filter suppresses the noise and distortion at low frequencies very good.
The result of the supply voltage error depends on the input signal. If the input signal has a higher frequency, the supply voltage error is also visible at higher frequencies. So it's possible, e.g. if the frequency of the input signal lies in the optimal noise suppression spike of the Chebyshev type filter, that the Chebyshev type filter is better than the Butterworth type. But because the optimal noise suppression spike of the Chebyshev type filter lies at the outer region of the audio bandwidth, in most cases the Butterworth type filter is better for supply voltage error suppression.

4.4 Comparator delay

Another non-ideality which can cause trouble is the comparator delay. One can imagine when the comparator delay is bigger than a period of the carrier signal the comparator will definitely give a wrong decision which will be seen in the output.
If the comparator delay is very small in comparison to a period of the carrier signal it will only result in a very small phase shift which can be neglected.
To simulate a comparator delay Simulink offers a couple of possibilities. But be careful with the decision. On possibility is to use a transient delay block. This is a very dangerous block especially if the comparator has a delay which is not a multiple of the simulation step width. *'When output is required at a time that does not correspond to the times of the stored input values, the block interpolates linearly between points. When the delay is smaller than the step size, the block extrapolates*

from the last output point, which can produce inaccurate results'[1]. This is not a good and reliable option.
The next option is to use a low pass filter with a pole (or more poles) far away from origin. As we look at the transfer function this filter we can see why this is a good solution:

$$H(j\omega) = \frac{k}{j\omega + p} \qquad \textbf{(4-1)}$$

If the pole lies far away from the origin the amplitude plot of the filter is constant for low frequencies and with a correct chosen gain for the filter the amplitude plot is almost equal to 1 for low frequencies:

$$|H(\omega)| = \frac{k}{\omega^2 + p} \xrightarrow{\omega << p} \frac{k}{p} \xrightarrow{k=-p} 1 \qquad \textbf{(4-2)}$$

Also if the pole lies far away from the origin, the phase-shift of the filter is almost equal to 0:

$$\phi(\omega) = \tan^{-1}\left(\frac{-\omega}{p}\right) \xrightarrow{\omega << p} 0^\circ \qquad \textbf{(4-3)}$$

Now it is shown that the amplitude plot and the phase-shift of this filter have no influence on the signal if the pole lies far away enough from the origin. The group-delay (or time delay) is the derivative of the phase-shift:

$$delay(\omega) = \frac{d\arg(\phi(\omega))}{d\omega} = \frac{d\arg\left(\tan^{-1}\left(\frac{-\omega}{p}\right)\right)}{d\omega} = \frac{-p}{\omega^2 + p^2} \xrightarrow{\omega << p} \frac{-1}{p} \qquad \textbf{(4-4)}$$

The group-delay depends only on the pole (for low frequencies and if the pole lies far from the origin).
It is possible to improve this filter to have a more accurate time-delay, a more constant amplitude plot and more constant phase-shift. It is possible to use more poles and lay them further away from the origin. But as we can see later this is not necessary in this case. More poles will result in slower simulations and is not desired

The comparator in this project will have a delay of 30 ns. This means a pole has to be laid at -3.333e7. The filter has its corner frequency at 5.305 MHz this about 15 times more than the carrier frequency at 350 kHz (or 7.5 times at 700 kHz). This will be enough and more poles further away are not necessary

The carrier signal has a period of 2.86 µs (@350 kHz) or 1.43 µs (@700 kHz). The comparator delay will be only 1% respectively 2% of period time of the carrier signal. This is very small so the prediction is that this will not have a big influence on the performance of system. Simulations will verify there predictions. The simulations are done for a series of comparator delays ranging from 0 to 50 ns. No other sources of noise of distortion, like supply voltage error, are introduced.

[1] Form the help of Matlab/Simulink

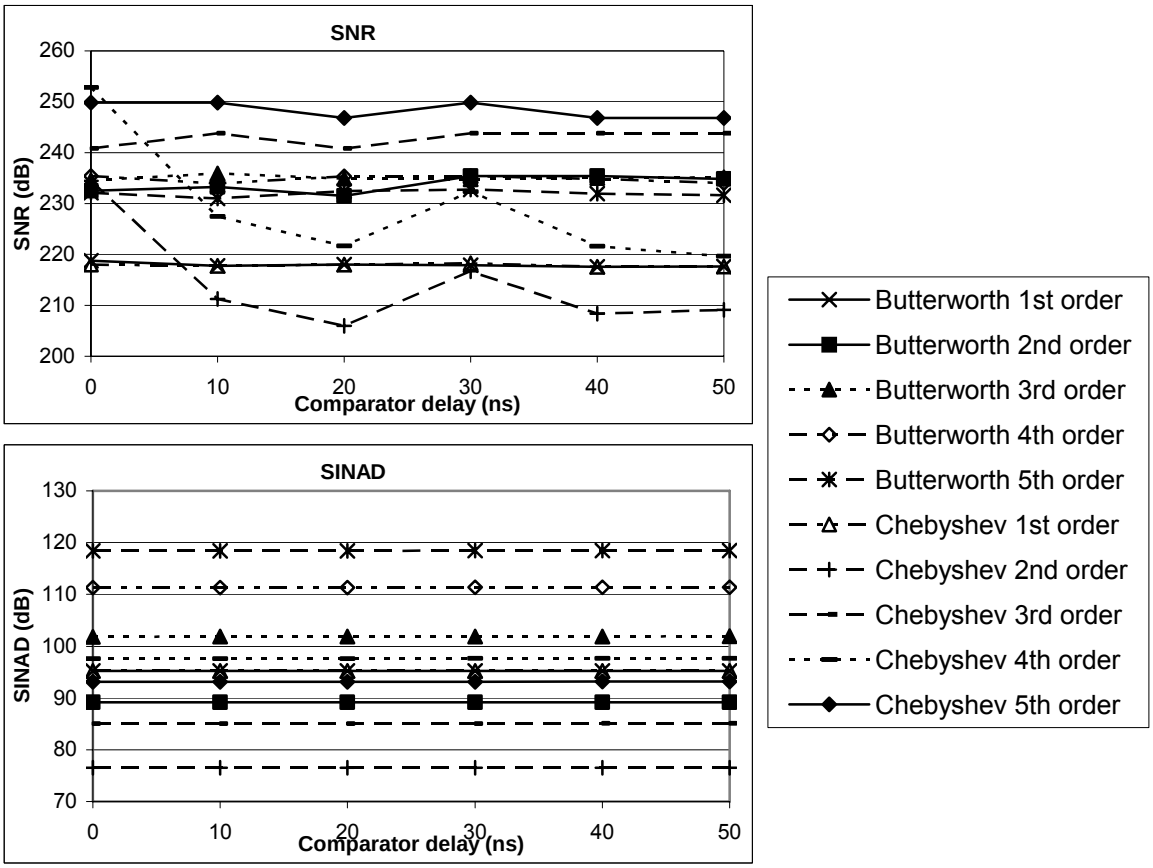

Figure 24: Simulation results of comparator delay simulations

Figure 24 shows the results of the simulations with a 350 kHz carrier signal. Looking at the SNR only some differences are seen at the even order Chebyshev type filters. In all these cases the SNR is very high so it's assumed that the differences here are the result of the simulation artifacts. The reason this only happens with the Chebyshev type filters is that they are more difficult to simulate. Looking at the SINAD in which the modulation components are included, there is no difference at all.
It seems the delay has as expected almost no influence on the system if the delay is very small in comparison to the period time of the carrier signal. Because of this the delay will not be used in further simulations, because it has almost no effect on the system and it only decreases the speed of the simulations.

4.5 Placement of the Carrier signal

The carrier signal can be integrated in the system at different positions. Every position has its pros and cons. In all previous chapters the carrier signal was integrated at the end of the loop filter as shown in Figure 21. A disadvantage of this topology is that, as described in paragraph 2.1.2, due to the feedback loop the error signal will be corrupted and therefore the comparison with the carrier signal is less accurate. Another disadvantage is the stability of the signal (see also paragraph 2.1.2). The amplitude of the error triangle may not be larger than the one of the carrier signal. This gives a limit to the aggression of the noise shaping ability of the feedback loop.
It's also possible to integrate the carrier signal in front of (or outside) feedback loop. In this project this will be referred a type 2. The model of this type 2 system is shown in Figure 25.

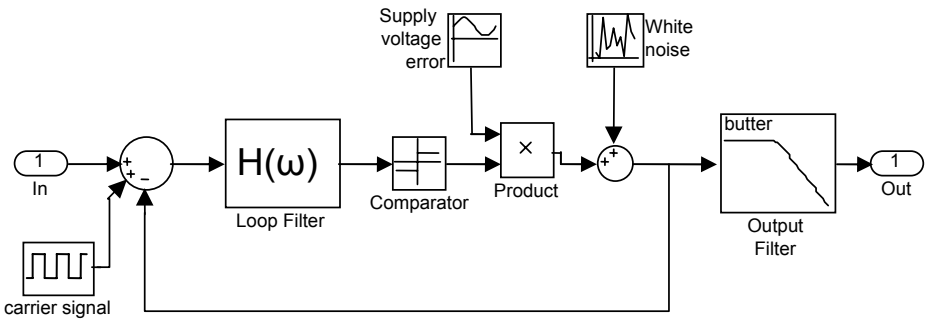

Figure 25: Simulink Model of the PW Modulator type 2

The first improvement of this system is that as long as the carrier signal has at least 2 times the amplitude of the output, the system will never clip as long as the input signal is not above its maximum (= amplitude of the output divided by closed-loop gain). Therefore it doesn't become unstable this way. This is because the output is directly compared with the carrier signal. The amplitude output together with the input signal never exceeds 2 times the amplitude of the output signal (as long as the input amplitude is not bigger than that of the output). So if the carrier signal has at least 2 times the amplitude of the output signal the amplitude of the error triangle never exceeds the amplitude of the carrier triangle, as both signals pass through the same filter. This allows to create a filter which can noiseshape much more aggressive. In this case equation (2-2) is not an issue any more. Equation (2-1) is now achieved only by the choice of amplitudes of the input, carrier and output signal.
Another point of difference is the phase difference between the error and the triangular carrier signal. As mentioned in paragraph 2.1.2 the feedback loop will phase-shift the error signal which will be analyzed by the comparator. In the type 1 system (the carrier signal inserted at the end of the loop filter) only the error signal is phase-shifted by the loopfilter and not the carrier triangle. In other words the error- and the carrier triangle are not matched to each other. By inserting the carrier triangle before the loop filter the carrier triangle will be phase-shifted by the loopfilter the same way as the error signal, so both signals are better matched to each other. This way the comparator will decide more accurately. Figure 26 shows the actual signals for a second order system which are compared in the comparator. It shows the error signal (if input = 0) and the unfiltered (for a type 1 system) or filtered (for a type 2 system) carrier signal. As can be clearly seen the error signal is bend due to the second order filter. If the carrier signal is not filtered (in type 1) the carrier has no bend. If the carrier signal is filter, as in a type 2 system, the carrier signal gets the same bend. So this signal is better matched and the comparison is more accurate.

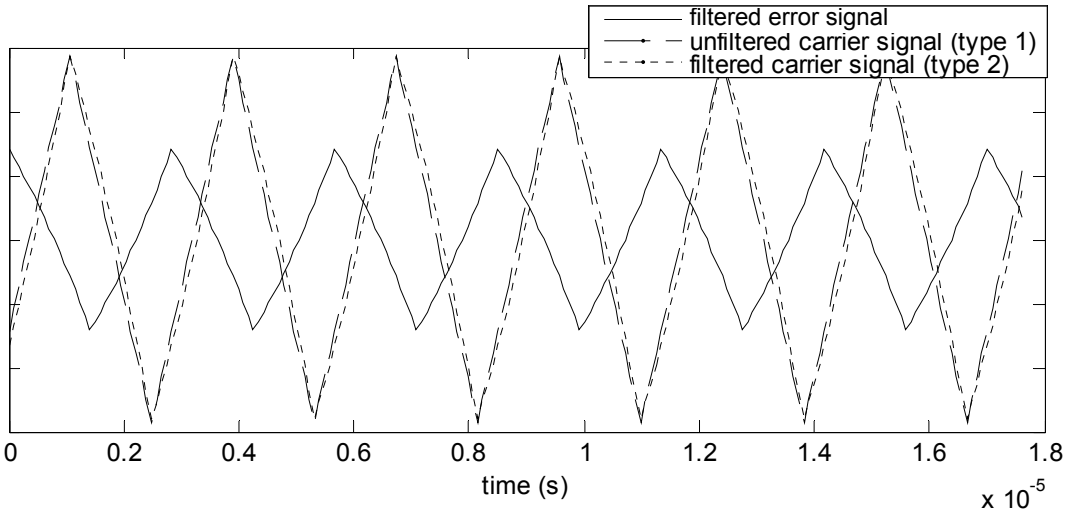

Figure 26: Filtered error signal and carrier signal of type 1 and type 2 systems at the input of the comparator (input = 0)

Appendix 10.7.3 shows if no noise-sources are present the SINAD and SFDR are about 12 dB better for higher order filters in case of the type 2 system in comparison with the type 1 system. This is because the type 2 system has less modulation error due to the better comparison of the feedbacked output signal and carrier signal at the input of the comparator (modulation error, see §2.1.2).

The biggest reason not to input the carrier signal in front of the loop filter is the noise and distortion in the carrier signal, e.g. jitter. In the case of the type 1 system noise from the carrier signal is inserted within the feedback loop. Therefore this noise will be shaped by the feedback loop. In case of the type 2 system the carrier signal is inserted outside the feedback loop, so the noise within this signal is also inserted outside the feedback loop. This means this noise will not be seen by the feedback loop as unwanted and will not be shaped. The result will be that this noise will simply pass the system and will be seen at the output of the feedback loop without alteration. While the carrier signal in the type 1 system can contain some noise, as it will be filtered out, the carrier signal type 2 system as to be very clean, so the noise from it is not the dominant disturbance.

4.6 Jitter in the carrier signal

Jitter in the carrier signal can be a serious problem for the performance of the system, especially for the type 2 system mentioned in previous paragraph. First let's take a look how the jitter itself can be modeled. In this explanation the jitter will be examined from the frequency spectral point of view. Considering an ideal sine wave oscillator, the frequency spectrum will be only a Dirac pulse at the frequency of the oscillator (Figure 28a). [8] explains that jitter in an oscillator can be identified as a shaped white noise folded around the oscillator. Figure 27 shows a jitter noise spectrum which is folded around the oscillator frequency. This is a simplified version of the spectrum given in [8], in order to simplify the model. This spectrum only shows the -20 dB/dec slope of the noise.

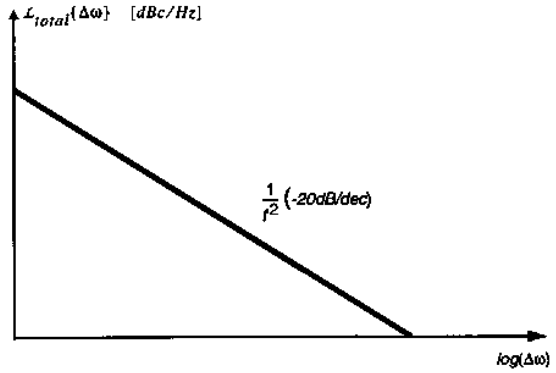

Figure 27: Simplified jitter noise spectrum of an oscillator which is folded around the oscillator frequency

Figure 28 shows how this spectrum is folded around the oscillator frequency. (Beware, Figure 27 has a logarithmic x-axis, Figure 28 has a linear x-axis)

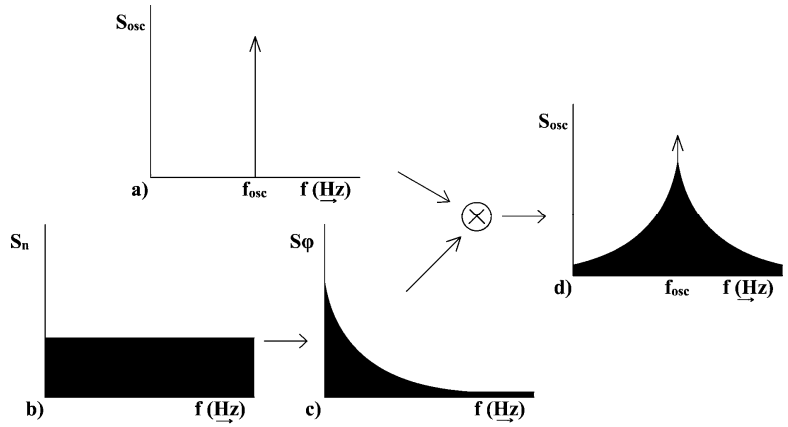

Figure 28: Evolution from ideal oscillator to oscillator with jitter (frequency spectral view)

Now the question is, how to model such a oscillator with jitter. How such a model has to behave is already shown Figure 28. A Gaussian white noise is filtered to the shape as given in Figure 28c (remember this plot has a linear x-axis). This filtered noise should have the spectrum of Figure 27. Because the spectrum of Figure 27 has a -20 dB/dec slope, one can use a first order low-pass Butterworth filter. This will represent the phase noise of the oscillator. Now this phase noise can be modulated around the oscillator frequency. From this explanation it's easy to derive the equations for this model. The equations are:

$$output = \sin(\omega t + \varphi) \quad \textbf{(4-5)}$$

$$S_{\varphi} = \left|H_{lowpass}\right|^2 \cdot S_{N_o} \quad \textbf{(4-6)}$$

$$S_{N_o} = \frac{N_o}{2} \quad \textbf{(4-7)}$$

To create a square wave the sine wave will be put through a comparator. And to create a triangular wave the square wave is put though an integrator. Now this model can be created in simulink as shown in Figure 29.

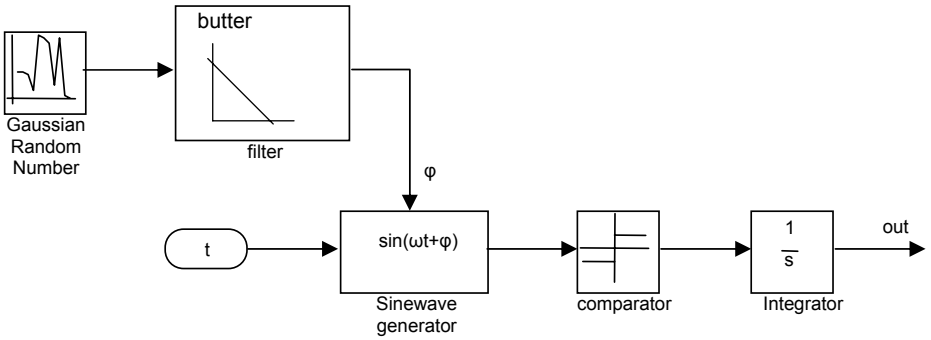

Figure 29: Simulink: Oscillator with jitter model

The problem is still how to create the correct jitter noise spectrum (Figure 27). In papers about oscillators normally one gives the amount of noise-power in a bandwidth of 1 Hz at a certain distance from the oscillator frequency. This number is for an oscillator with certain frequency. The oscillator used in this analysis has a noise-density ($L(\Delta f)$) of -102 dBc/Hz at 10 kHz distant from the oscillator frequency when the oscillator has a frequency of 1.5 MHz. ([9]). But the oscillator has to have a frequency of 350 kHz for this system. [10] provides an equation to calculate the noise-power at the same distant from the oscillator frequency but when the oscillator oscillates on a different frequency. With this equation the noise-power at 10 kHz distant from the oscillator frequency is calculated for an oscillator oscillation at 350 kHz:

$$L(\Delta f)_{@350kHz} = L(\Delta f)_{@1.5MHz}\left(\frac{f_{o_{@350kHz}}}{f_{o_{@1.5MHz}}}\right)^2 = 10^{-10.2}\cdot\left(\frac{3{,}5\cdot 10^5}{1{,}5\cdot 10^6}\right)^2 = -114{,}64\,\text{dBc/Hz}_{@10\text{kHz}} \quad \textbf{(4-8)}$$

Looking at Figure 27, if the noise is -114,64 dBc/Hz at 10kHz and the slope is -20 dB/dec, it means that noise is 1 (0dB) at 0.0185 Hz ($10^{-1.732}$ Hz, Figure 30). If a white noise source is used with a noise power of 1 W/Hz, a 1st order low-pass Butterworth filter has to be used with a gain of $2\pi\cdot 0.0185$ to create the right jitter noise spectrum.

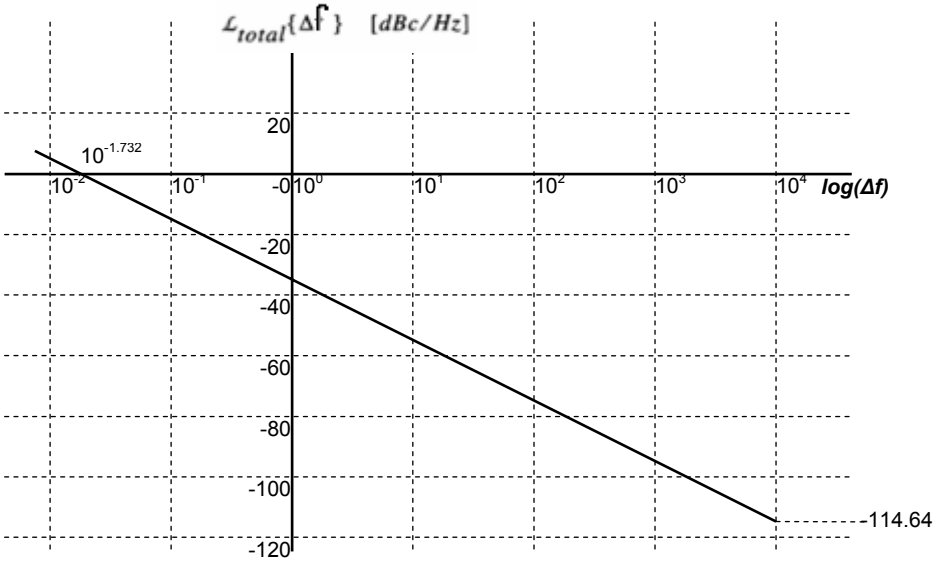

Figure 30: Jitter noise spectrum of an oscillator which is folded around the oscillator frequency use in model

Jitter noise of the oscillator is very important in the choice where the carrier signal is inserted. If the carrier signal is inserted at the end of the loop-filter (type 1 in §4.5) the jitter noise will be suppressed by the feedback loop. If the carrier signal is inserted at the beginning of the loop-filter (type 2 in §4.5) the jitter noise is not suppressed at all and will be fully visible at the output. In other words, the amount of jitter-noise from the oscillator is important in the choice of where to insert the carrier signal.
Using the jitter noise calculated in this paragraph both systems of §4.5 are simulated with only jitter as noise source and a Butterworth type NTF.

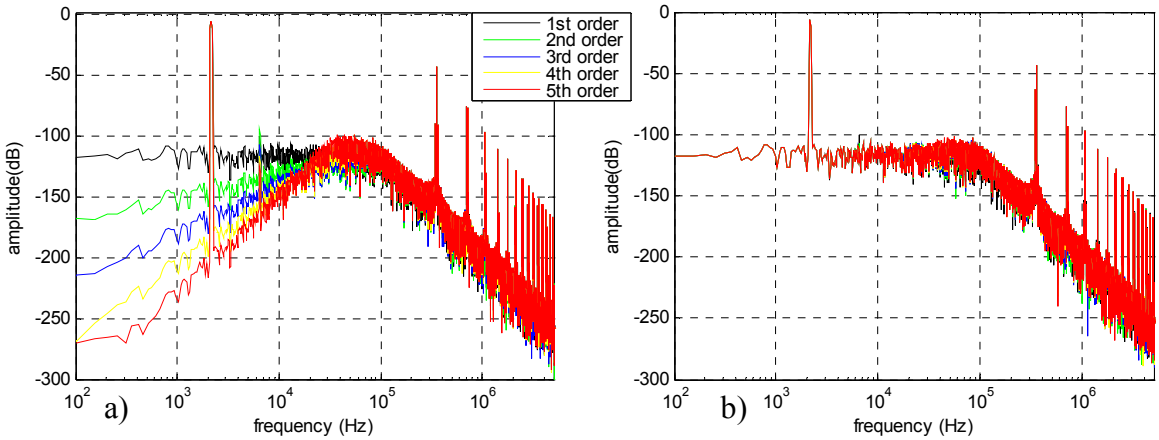

Figure 31: Simulation results: PSD plots of a PWM model with jitter noise, Butterworth type NTF, (a) type 1 and (b) type 2 system.

Figure 31 shows the results of the simulations. As can be seen with a type 2 system (Figure 31b) the jitter is not suppressed at all, while the type 1 system (Figure 31a) nicely suppresses the jitter as a Butterworth type filter. If jitter is one of the dominant noise sources, type 1 system is definitely the best choice for implementation. Appendix 10.7.4 shows the SNR and SINAD of the simulation results. At the type 1 system a optimum filter order is visible (3^{rd} or 4^{th} order). The reason is that for a higher order Butterworth type filter the corner frequency of the NTF shifts towards the bandwidth of interest. If the corner frequency lies too close to the bandwidth of interest the noise at the higher reagon of the bandwidth of interest is less suppressed. This will be explained in §4.8.
In this case the type 2 system has a SNR (for the audio-band) of about 84 dB in the audio band when the modulation depth is 50%. According to the calculations in appendix 10.8 this is correct. Choosing a higher carrier frequency doesn't affect the SNR for the audio-band due to the noise-jitter. If the carrier frequency is doubled the noise spectrum (Figure 30) will shift up with 3 dB, due the larger carrier frequency. But because the carrier frequency is twice as far from the audio band the SNR in the audio band will also increase with 3 dB. Both these effects cancel each other out so the SNR in the audio band remains the same.

4.7 Output stage noise and distortion

The last noise source discussed in this report is the output stage. The output stage has numerous sources for the creation of noise and distortion. Think about slewing, deadtime, etc. It is too much work for this project to analyze all these sources independently. The modeling of the output stage would be a nice project for further research. In this report the noise created by the output stage is summarize as a Gaussian white noise source at the output of the system. The noise source has a

variance of 0.001. In this case this means the mean noise voltage is 3.16% of the output amplitude. The bandwidth of the noise is 16x the carrier frequency. These values are not based on any paper. It is merely an intuitive chosen value. This noise should not be used for a quantitative analysis. It is used to see if the NTF is as calculated in chapter 3.
Figure 32 shows two simulations plots when the only noise source is the output stage noise. In these simulations again a carrier frequency of 352.8 kHz is used. Using an open-loop gain of 700000 as mentioned in paragraph 3.2 the corner frequency of the NTF of a Butterworth type NTF could be calculated with equation (3.11). For a 5th order butterworth filter the corner frequency is 34.4 kHz. Using this fact Figure 32a can be consider as corrected, because the corner frequency lies at the same frequency. Furthermore Figure 32a shows also the Butterworth NTF slope belonging to the order of the filter.

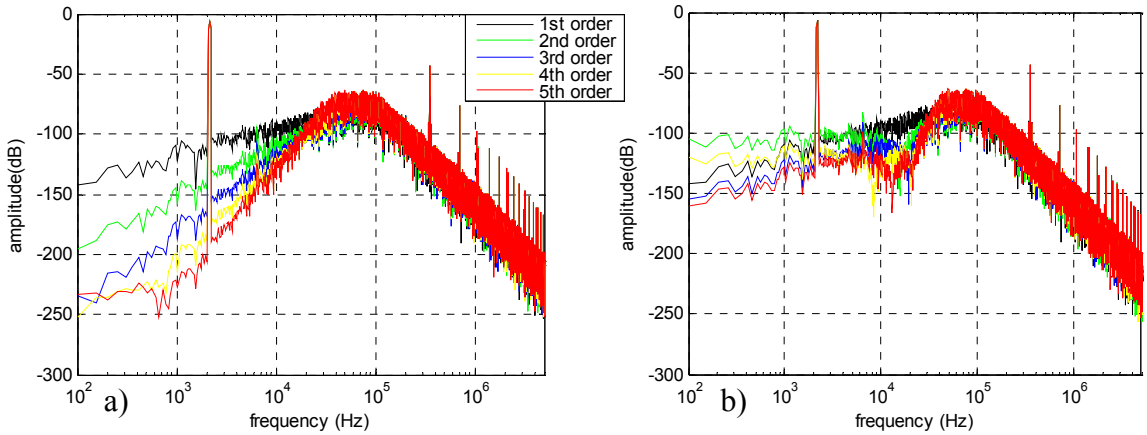

Figure 32: Simulation results: PSD plots of a PWM model with output stage noise with a) Butterworth or b) Chebyshev type NTF.

From the SNR and SINAD values showed in appendix 10.7.5, the Chebyshev type filter is much better in this case. This was also concluded in Chapter 3.
When looking at the Butterworth type filter again the optimum filter orders are 3 and 4. The cause is the same as mentioned in previous paragraph and will be explained in next paragraph.

4.8 700 kHz carrier

In previous paragraphs the Butterworth type filter had an optimum filter order of 3 or 4 in case of the presence of jitter noise or output stage noise. The reason is that those noise sources have a white noise characteristic in the bandwidth of interest (audio bandwidth) and when a higher order is used the corner frequency of the NTF is shifted towards this audio bandwidth. If the corner frequency lies too close to the audio bandwidth, the frequencies in the higher region of the audio bandwidth are less suppressed. Figure 33 shows that from about 18 kHz the 5th order filter has a lower suppression than the 3rd and 4th order filter.

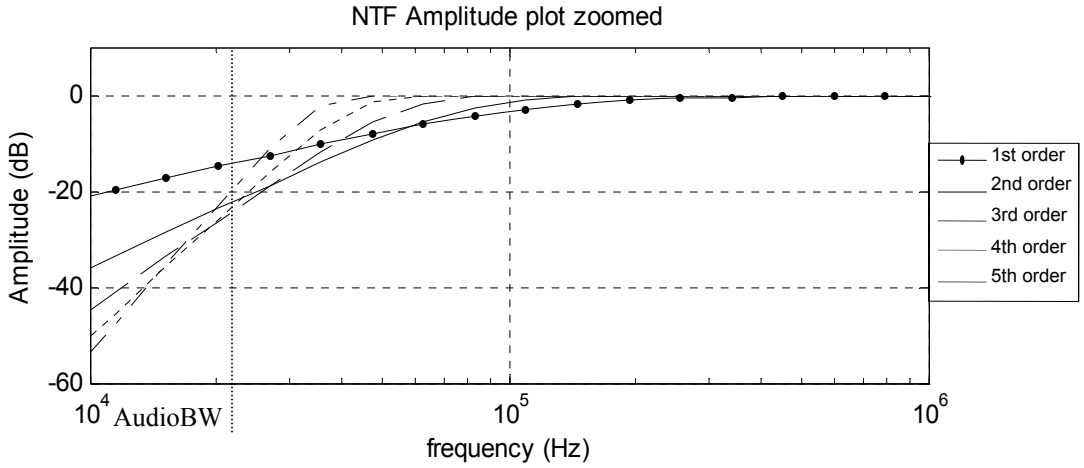

Figure 33: Butterworth NTF of a feedback loop with a 350 kHz carrier

For a Butterworth filter this effect is more severe than for a Chebyshev filter, because the slope of the transition band of a Chebyshev filter is much steeper than the slope of a same order Butterworth filter. Therefore the pass-band corner could lie closer to the audio bandwidth before this effect appears.
A way to solve the problem that the NTF pass-band corner lays too close to the audio bandwidth is to increase the carrier frequency. By increasing the carrier frequency the corner frequency of the NTF can be put further away from the audio bandwidth. As can be seen in Figure 34 in case of the 700 kHz carrier, at least until the 5th order, a higher order gives always a better noise suppression in the audio bandwidth.

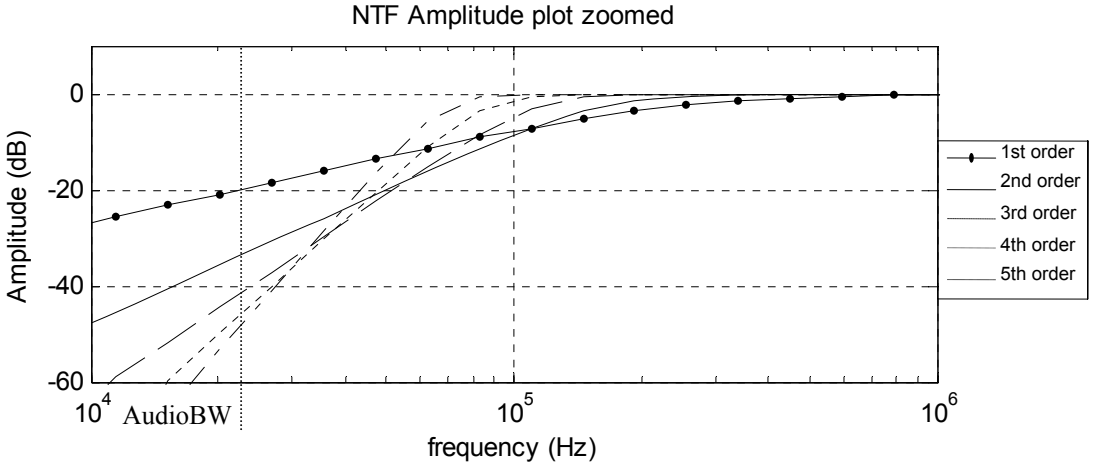

Figure 34: Butterworth NTF of a feedback loop with a 700 kHz carrier

Besides this advantage a higher carrier frequency gives an overall better noise reduction. When the carrier frequency doubles the SNR in the audio bandwidth increases with $n \cdot 6$ (where n is the order of the filter). This is analog to a discrete noise shaper [11].

4.9 Final system model simulations and conclusions

Now only rest some final simulations from which we can decide which type of filter is the best choice for implementation. In these simulations all noise sources which have some influence on the performance of the system are included. The included noise sources are the supply voltage error and jitter noise. The output stage noise is not included because no good quantitative model for this noise source is analyzed in this report and so no verified conclusions could be drawn from simulations including this noise source.

With the included noise sources mentioned above we will look at de difference between:

- Butterworth and Chebyshev type filter
- 350 kHz and 700 kHz carrier

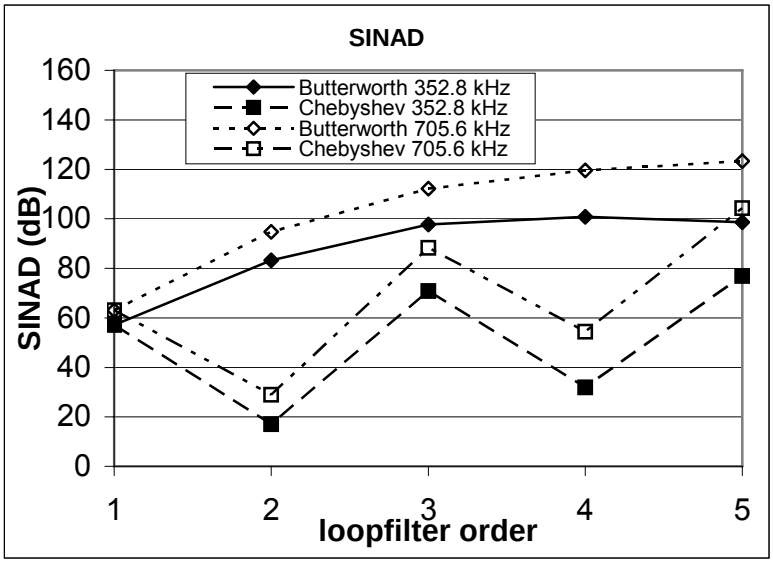

Figure 35: Simulation results: SINAD for systems with supply voltage error and jitter error with 50% modulation depth

Figure 35 shows the final SINAD results of the mentions filter types and carrier frequencies with 50% modulation depth. As can be seen using a 700 kHz carrier is a big improvement in comparison to the 350 kHz carrier. The improvement start with $n \cdot 6$ (where n is the order of the filter) as mentioned in §4.8. But at higher order filter the improvement becomes less. Because the jitter noise suppression is not linear to the filter order due to the shift of the corner frequency of the NTF (see §4.8). The improvement of the SINAD due to jitter noise is $(n\text{-}1) \cdot 6$ (where n is the order of the filter), because the carrier signal is inserted at the input of the last integrator (will be explained in Chapter 6.1).

Looking at the simulation results it seems that the supply voltage error is the most dominant noise/distortion source. This can be concluded because the Butterworth type filter turns out to be the filter with the best performances. Also the fact that the even order Chebyshev type filters have a very low SINAD confirms that the supply voltage error (low frequency) is the dominant noise/distortion factor. It is possible that, if the output stage noise is included, the difference between the Butterworth and Chebyshev type filter becomes smaller or even that the Chebyshev type filter becomes a better filter, because the Chebyshev type filter suppresses white noise better. But for now it

is predicted that the output stage noise is not that severe. Thus the Butterworth type filter is preferred for implementation. In Chapter 5 it will also be explained that the Butterworth type filter is easier to implement than a Chebyshev type filter.
For implementation a 3rd order filter is chosen. Using a 700 kHz carrier the improvement of the SINAD is about 29 dB in comparison of the 2nd order filter, according to the simulations. A 3rd order filter is probably already quite complicated to implement and due to the time span of this project this is supposed already complicated enough.
Now the last decision is where to input the carrier frequency. From the simulations, using a 3rd order Butterworth type filter with a carrier frequency of 700 kHz the SINAD is about 112 dB in the audio bandwidth when the carrier is inserted in the last integrator and de modulation depth is 50%. In §4.6 it was stated that the SINAD is always about 84 dB if the carrier is inserted at the beginning of the feedback loop when only jitter noise present. The difference is very big so it can be concluded that the carrier signal has to be inserted in the last integrator of the loop-filter.

This concludes the first part of the project. With the design choices mentioned above we can start the research of the implementation of the loop-filter. In next chapter we take a closer look at the implementation of the loop-filter.

5 Filter Implementation

In the previous chapters we have looked at the pulse width modulator at system level. From those analyses the first design choices could be made for the system. Those design choices are:

- 3rd order loop-filter.
- Butterworth type filter.
- 700 kHz carrier.
- Insert the block wave at the end of the loop-filter

From this point we can take a better look at the implementation of the loop-filter. In the previous chapters we considered the loop-filter to be ideal. Ideal in this context means that ideal integrators are used and only the poles and zeros are present which contribute to the optimal filter type. In this case it is a Butterworth type filter.
In practice the filter is not ideal. The first reason is because the integrator can not be made ideal. Furthermore parasitic elements will introduce extra poles and zeros.
In next chapters we will take a look at the topology of loop-filter (§5.1) and the integrators (§5.2). There are a lot of choices which can be made. These considerations have to do with issues like linearity, parasitic poles and zeros, power consumption etc. First let's take a look at the topology of the loop-filter.

5.1 Loop-filter topology

A couple of loop-filter topologies have already been presented in the course of time. The most common topologies can be found in [11]. Although in [11] the filters are presented in a discrete time representation, the continuous time is analogous to it and will be discussed in this report. The differences between the topologies influence mainly the STF and NTF of the filter and give some specifications to the integrators which should be used in the loop-filter.
Because some choices concerning the NTF are already made in previous chapter, some of the topologies can already be left out of the design considerations. As type of the NTF the Butterworth type was chosen because it was considered that errors like supply voltage modulation were the main point of concern. By doing so, the topologies with resonators can be left out. Those only apply for Chebyshev type filters. A benefit is that topologies without resonators are easier to implement. These Chebyshev type loop-filter topologies will not be further discussed in this report. The only three common topology types which will remain now are:

- Chain of Integrators with Weighted Feedforward Summation
- Chain of Integrators with Distributed Feedback
- Chain of Integrators with Distributed Feedback and Distributed Feedforward Inputs

As starting point let's take the NTF as we already specified it in previous chapters. It happens, that for all three topologies mentioned above the NTF's are the same. This is because the open loop transfer is the same. For this analysis the loop is cut right after the comparator. The input is tied to ground and the open loop transfer is calculated with the input at the cut and the output at the input of the comparator. Now in all cases the open loop transfer is:

$$L(s) = -\sum_{k=1}^{n} \frac{a_k}{s^k} \qquad \text{n=order of the filter} \qquad \textbf{(5-1)}$$

And the NTF will be:

$$NTF(s) = \frac{1}{1+L(s)} = \frac{1}{1-\sum_{k=1}^{n} \frac{a_k}{s^k}} = \frac{s^n}{s^n - \sum_{k=1}^{n} a_k s^{n-k}} \qquad \text{n=order of the filter} \qquad \textbf{(5-2)}$$

So the NTF is for all topologies above the same. And by choosing the right parameters you will have a Butterworth NTF. The STF can be different for the 3 topologies. In next paragraphs the differences are discussed.

5.1.1 Chain of Integrators with Weighted Feedforward Summation (CIFF)

The main characteristic of a chain of integrator with weighted feedforward summation (Figure 36) is that the STF and NTF are highly related to each other:

$$STF(s) = 1 - NTF(s) = \frac{\sum_{k=1}^{n} a_k s^{n-k}}{s^n - \sum_{k=1}^{n} a_k s^{n-k}} \qquad \text{n=order of the filter} \qquad \textbf{(5-3)}$$

As can be seen from (5-3) the STF is totally dependent on the NTF. So this means the STF is fixed when the NTF is determined. A drawback of this topology is the same as already seen in chapter 3. The STF will peak at high frequencies, which means the input has not to contain these high frequencies otherwise the filter could overload and become instable. This could mean one has to pre-filter the input.

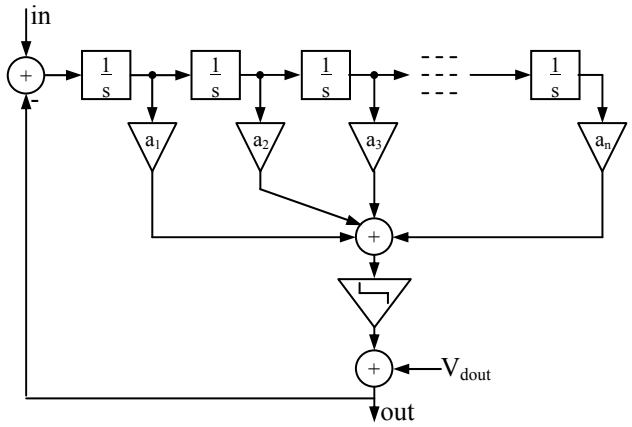

Figure 36: Chain of Integrators with Weighted Feedforward Summation

Another important issue concerning the topology is the linearity of the integrators. In the CIFF case all output signal is fed back to the summation point at the input. The output voltage in a closed loop consists of $STF*V_{in}+ NTF*V_{dout}$, where V_{dout} represents all output distortion. This means the signal voltage at the input of the first integrator is:

$$(1 - STF) \cdot V_{in} - NTF \cdot V_{dout} = NTF \cdot (V_{in} - V_{dout}) \qquad \textbf{(5-4)}$$

From this point of view we can assume that this signal contains only a small part of the input signal (low frequency) and a large quantity of high frequency output distortion (switching error). Going through the loop filter the low frequencies are

amplified and the high frequencies are attenuated by the integrators. This means that the signal at the first integrator contains only very little input signal and a lot of switching error signal. The signal at the last integrator contains a lot of input signal and much less switching error signal.
The first integrator needs to be very linear because low frequency noise or distortion generated in the first integrator is almost not suppressed by the feedback loop. The low frequency distortion generated due to non-linearity in the first integrator comes from the high frequency switching error signal. Due to non-linearity of the integrator the switching error signal folds back to the baseband. The nonlinearity of the next integrators will generate less distortion from the switching error signal because the switching error signal is less present at the other integrators. The nonlinearity of the other integrators will generate more distortion related to the input signal, but this will be shaped by the loop-filter and the overall distortion power is much less than for the 1st integrator. Therefore the nonlinearity of the other integrators is less important.

5.1.2 Chain of Integrators with Distributed Feedback (and Distributed Feedforward Inputs) (CIFB)

The biggest drawback of the last topology (CIFF), the peaking of the STF at high frequencies, can be helped by choosing a chain of integrators with distributed feedback. The STF of the CIFB topology (Figure 37a) is as follow:

$$STF(s) = NTF(s)L_o(s) = \frac{b_n}{s^n - \sum_{k=1}^{n} a_k s^{n-k}} \qquad \text{n = order of the filter} \qquad \textbf{(5-5)}$$

$$L_o(s) = \frac{b_n}{s^n} \qquad \textbf{(5-6)}$$

The poles of the STF will always be the same as those of the NTF but in comparison to the CIFF topology the STF has no zeros as could be seen in equation (5-5). Because the STF has only poles, the STF has the form of a low-pass butterworth filter and has no peaking.
The STF could be altered by inserting distributed feedforward inputs. This changes $L_0(s)$. Adding more feedforward-inputs can be done when a wider STF equal to unity bandwidth is required. If all feedforward-inputs are inserted (Figure 37b) and the b-factors are the same as the a-factors, the STF is again the same as in case of the CIFF topology.

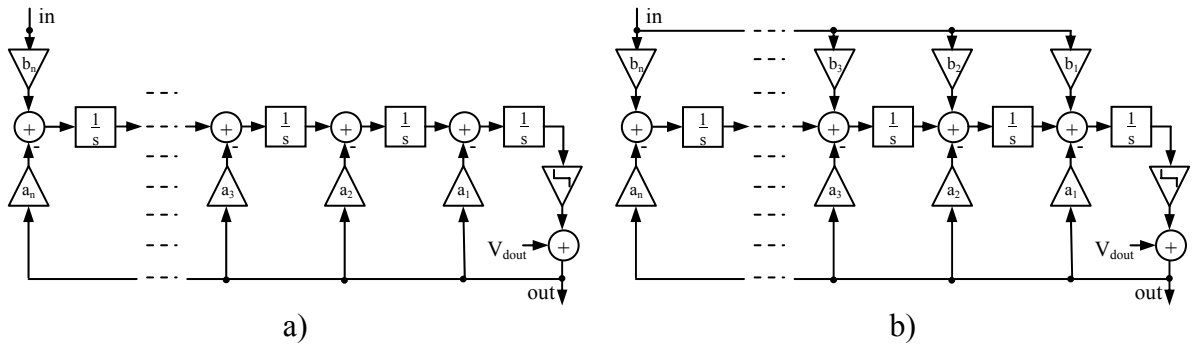

Figure 37: a) Chain of Integrators with Distributed Feedback, b) and Distributed Feedforward Inputs

In the CIFB case equation (5-4) is not valid. Less input signal is subtracted in the input summation point but also less output noise is present at this point. This leads to a larger input signal and a lower output distortion contribution at the input of the first integrator in comparison with the CIFF topology. [12] shows that non-linearity of the first integrator of both topologies has almost the same effect. Now because of the distributed feedback the input signal contribution for the other integrators doesn't change much. The integrator amplifies the input signal from the previous stage and the feedback branch subtracts a part. This means non-linearity of the integrator give always about the same distortion. Because the distortion is less shaped at the earlier integrators it means that those have to have also a certain linearity. Nonlinearity of the first integrator has still the most influence on the loop-filter performance, but the difference in comparison to the CIFF is that the non-linearity of the second integrator of the CIFB has much more influence on the loop-filter performance ([12]). Although the required linearity is less than of the first integrator, the input signal contribution of the second integrator is much larger than in case of the CIFF. Because this is earlier in the chain, the in-band noise created by the nonlinearity of this integrator is shaped less by the loop-filter.
In the CIFF topology only the linearity of the first integrator is important and the linearity of the other integrators has much less effect. In case of a CIFB topology the linearity of all integrators have effect on the filter performance. Most effect for the first integrator and decreasing effect towards the last integrator. [12] shows some nice results in this field. An advantage of this topology is that it doesn't have so much output distortion at the input of the first integrator. The output distortion is added at every integrator, but is also attenuated by the integrators. This means less output distortion is present in the loop filter in comparison to the CIFF topology.
Previous analysis on the loop filter topologies are mainly based on [12]. No actual simulations are done to verify the conclusions. For this some more research has to be done.

5.1.3 Power dissipation of the loop-filter topologies

First let's take a look at the CIFB topology. As mentioned in the previous paragraph, the input signal has a relative big contribution at the input of all integrators and so the linearity of all integrators has to be quite well in order to have a good performance. As we will see in chapter 5.2, higher linearity of the integrators means more power consumption. So if we assume that for the CIFB topology all integrators consume a considerable amount of power, while for the CIFF topology only the first integrator consumes a considerable amount of power and the other integrators a lot less, we can state that in this case the CIFF is a better choice concerning power consumption.
Distortion in the output stage causes a higher voltage swing of integrators. In order to stay in the limits of the supply voltage, this means bigger capacitors are needed. This will increase the power consumption of the integrator. In this case the CIFB is a better choice concerning the power consumption, because it has less output distortion inside the loop filter. A trade-off between linearity and output distortion should be made.

5.2 Integrators

In the loop-filter designs discussed in previous chapters the integrators were considered ideal. In this context it are integrators with only a pole in the origin. Unfortunately as for everything in the real world, nothing is ideal. Real integrators suffer from parasitic poles and zeros created by for example parasitic components, load impedances and finite gain of the OpAmp/Gm.

In this chapter we will take a look at different integrator implementations, discuss their advantages and drawbacks and take a look at what the effect of their non-idealities is on their performance for at least one of the implementations.

Figure 38 shows four different types of integrator implementations. The integrator implementations of Figure 38 are discussed in a variety of papers, e.g. [12], [13], [14], [15]. The names of the implementations do not always concur in some papers. In this report the following names will be used.

- Figure 38a: RC integrator
- Figure 38b: Miller integrator
- Figure 38c: Gm-C integrator
- Figure 38d: Gm-Miller integrator

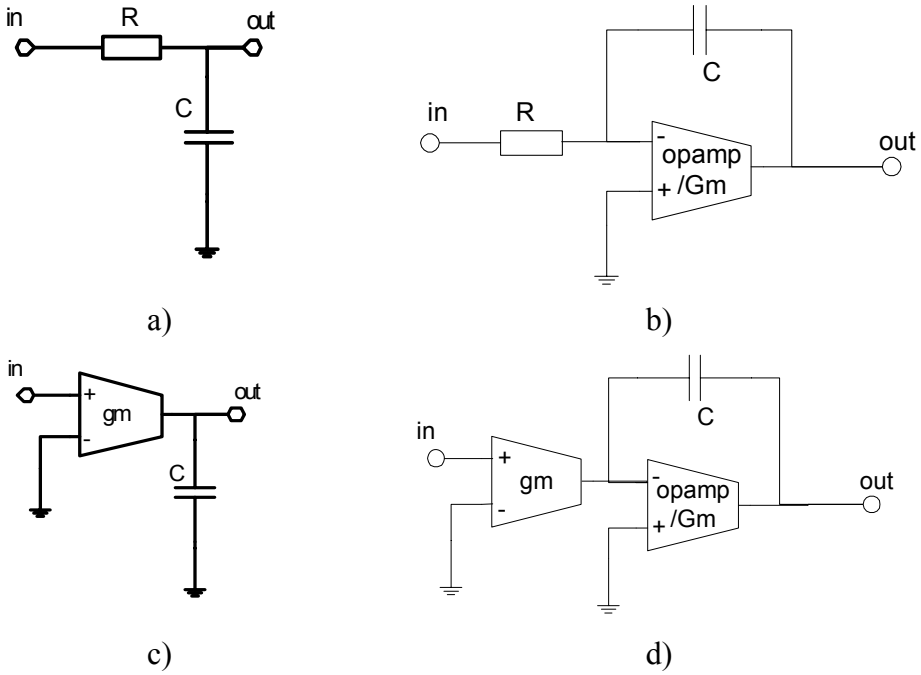

Figure 38: Continuous-time integrators

In this paragraph the four types are discussed and together with previous paragraph the best type/types for the filter implementation are chosen.

- RC integrator

The RC integrator (Figure 38a) is not a serious candidate for implementation. First of all it doesn't have its pole in the origin of the s-plane. Furthermore, loading this integrator will have a lot of effect on its transfer function.

- Miller integrator

The Miller integrator (Figure 38b) is considered as the integrator with the highest dynamic range and lowest power consumption ([14]). But the Miller integrator has also its drawbacks:

- Reduced frequency range: The integrator has a local feedback loop. This can cause a 180º phase shift, which could result in an instable loop-filter.

- Resistors: It uses resistors which use a relative large area. Furthermore large resistor values are difficult to implement. If small resistor values are used the capacitors values will be large and thus the power consumption increases.
- Difficult to tune: Tuning of this implementation type is difficult in an integrated circuit.

- Gm-Miller integrator

Some of the drawbacks of the Miller integrator can be solve by using a Gm-Miller integrator (Figure 38d). Gm-Miller type looks like the Miller type, but the resistor is replaced by an Gm giving the following advantages:

- Less area consumption: The area of a Gm is much smaller than of a resistor.
- Tunable: In addition a Gm is easy to tune, so the integrator becomes tunable.
- High input impedance: The input impedance of a Gm is very large. When cascading integrators this can be desired.

But again this integrator has its drawbacks:

- Reduced frequency range: Same as with the Miller integrator
- Poor linearity: The input transconductor has a non-linear behavior if it has to be tunable.

- Gm-C integrator

When a high frequency range is desired the Gm-C integrator (Figure 38c) is the best option. The Gm-C integrator also adopts the advantages of the GM-Miller integrator. De advantages of the Gm-C integrator are:

- High frequency range: Due to it feedforward structure it will not have a 180º phase shift of its own.
- Less area: Same as the Gm-Miller integrator the Gm-C type doesn't use resistors so its area consumption is small.
- Tunable: The Gm makes the integrator easy tunable.
- High input impedance: The input impedance of a Gm is very large.

The biggest drawback of this integrator type is it poor linearity. The output resistance non-linearity of the Gm is the cause of this. The Gm-Miller integrator has still a feedback structure after the Gm stage. This creates a virtual ground for the output of the Gm, so there will be output related nonlinearity. The Gm-C type has no compensation and additional linearization circuitry has to be added.

5.3 Filter implementation conclusions

In previous paragraph a good overview of possibilities is given of how the loop-filter implementation would look like.

At first **the loop-filter topology**:

The chain of integrators with feedforward summation (Figure 39a) seems to be the best choice in this case. It gives more ease and freedom for the implementation of the integrators. Only the first integrator has to have a good linearity. The other integrators have less strict specifications, thus more freedom in design.

In this report the distortion from the output stage has not been researched. So no real power estimation can be given. For now it is assumed that the linearity of the integrators has more influence on the power consumption of the integrators than the effect of the output distortion.

The main drawback of the feedforward topology, the peaking of the STF at high frequencies, is not of mayor concern. In this report the input signal is considered clean

with an audio-range bandwidth, so no signal at high frequencies. From this point of view the peaking at high frequencies would not have effect on the stability of the system (due to overloading).

Next **the integrator implementations:**
From the choice of the loop-filter topology it is known that the linearity of the first integrator is important. This immediately brings one to use a Miller integrator (Figure 39b) for the first integrator. Also, because of the large output voltage, the first integrator has to have a resistor as V-I converter. A Gm cannot handle such high voltages. The fact that this type has the best power consumption is a nice addition. Later in this report it will be explained that it is not a big issue if the first integrator is not tunable. This integrator has to be designed carefully so the reduced frequency range will not affect stability of the system. If this is all designed properly the only issue is the relatively large area consumption. This is a fact we should have to live with. The other integrators are until now still free of choice.

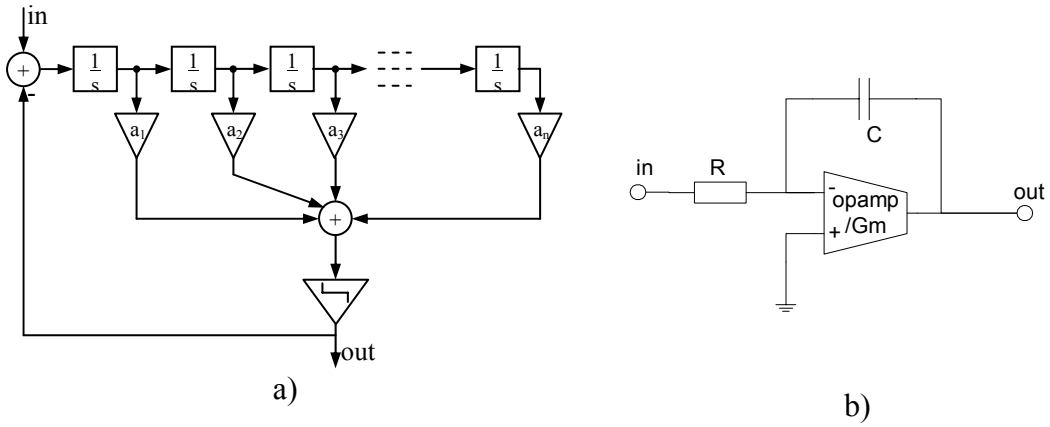

Figure 39: a) CIFF loop-filter; b) Miller integrator: best choices for implementation

6 Loop-filter realization

From the choices made in the previous chapter a loop-filter can be realized in Cadence software. As starting point the CIFF loop-filter topology is chosen. In this Chapter the implementation of this loop-filter on circuit-level will be discussed. As will be seen, also on this level different design choices can be made.
In previous chapter the implementation of the first integrator was already chosen. In this chapter also the implementation of the other integrators are chosen. The next thing will be how the gain factors ($a_{...}$) of the loop-filter topology are implemented (paragraph 6.1). Here one can think of tunability of the gains and the influences of the gains as loads on the integrators. The influence of spread and mismatch of the RC values on the loop-filter are discussed in paragraph 6.2. It should be nice if one could choose a carrier frequency and the loop-filter would adjust itself to an optimal filter. Paragraph 6.3 will take a look at the possibilities. Next the integrator implementations will be examined more close. Integrators suffer from undesired zeros and poles (paragraph 6.4). These zeros and poles specify the limitations on the integrators. For example they limit the DC-gain and frequency range of the integrator. In order to calculate practical values one should know the voltage swing of every stage, otherwise the internal voltages will clip to the supply voltage. These calculations are discussed in paragraph 6.5. Finally before calculating the real values of the passive components and gm's a noise analysis is done in paragraph 6.6

6.1 Loop-filter topology

The loop-filter topology of desire is already thoroughly discussed. The first choice is the chain of integrators with feedforward summation (Figure 39a). Only the first integrator is already chosen to be a Miller type integrator. To simplify the analysis for now, it is assumed that all integrators will be of the Miller type. Later on these integrators could be changed to maybe more desired implementations. For now the part of interest is the implementation of the gain factors.
Two options for the implementation of the gain factors are presented in Figure 40. The differences between the two options is that the gain factors of Figure 40a are formed by resistors and those of Figure 40b are formed by transconductors. Using resistors creates a better linearity of the gain factors. But the errors are created at the end of the loop-filter so linearity is not the biggest issue. Signals created at the end of the loop-filter will be shaped according to the NTF, so this applies for these errors.
The use of transconductors to form the gain factors has some advantages over the use of resistors. At first, the very high input impedance of the transconductors is very desirable. It means it doesn't influence the dc gain of the integrator which it loads very much, as will be seen in paragraph 6.4.1. What also makes the use of transconductors very desirable is that they are electrically tunable. This tunability is a nice tool to compensate for mismatch and even to create an optimum loop-filter if the carrier frequency changes. This will be all explained in next paragraph.
When resistors are used the comparator has to compare voltages. If transconductors are used the comparator has to compare currents.
Concluding from the arguments mentioned above it seems the use of transconductors (Figure 40b) is preferred. From this part on the implementation using resistors will not be further analyzed.

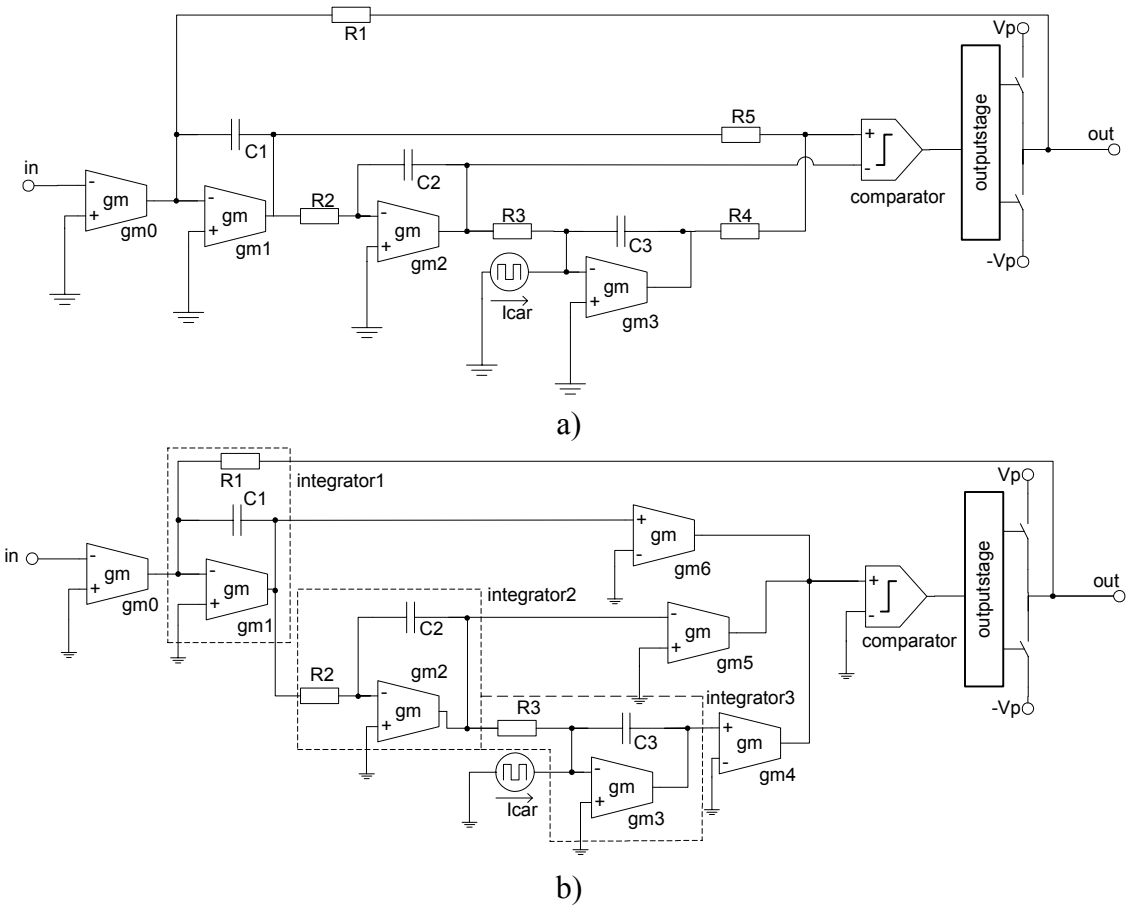

Figure 40: Loop-filter implementations with gain factors consisting of: a) resistors; b) transconductors

For the first analysis of the loop-filter implementation let's assume that the gain of the transconductors (*gm1*, *gm2 & gm3* in Figure 40b) is very high. This case the transfer functions of the integrators can be simplified to (see paragraph 6.4.1):

$$H_{\text{int}}(s) \approx \frac{-1}{sR_xC_x} \qquad \textbf{(6-1)}$$

With this simplification it is easy to calculate the open loop transfer function of the system. For this calculation the loop is cut between R_1 and the output and the side of R_1 is used as input. This is allowed because the input impedance of this new input is much larger than the impedance which will finally load the Class-D amplifier (4 to 16 ohms) (see [16]). Figure 41 shows the schematic used for the open loop calculations.

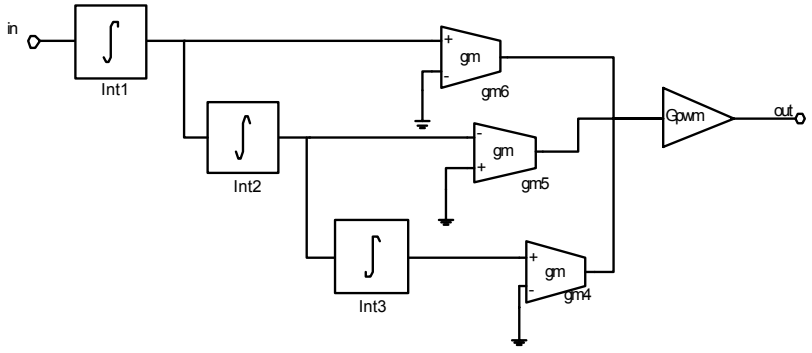

Figure 41: schematic for the loop-filter's open loop calculations

The integrators are here represented by a black box with the transfer function (6-1). G_{pwm} is the gain coming from the PW modulator. This gain is described in [2] as the ratio between the amplitude of the output PWM signal (V_p in Figure 40b) and the amplitude of the reference triangle at the input of the comparator. Because in this case the carrier signal is injected at the input of the last integrator the reference triangle at the input of the comparator will be the same as the reference triangle mention in [2]. A small difference is that the reference triangle is amplified by the transconductor after the integrator. Using all this, the gain of the PW modulator is:

$$G_{PWM} = \frac{4 f_{car} V_p C_3}{I_{car} gm_4} \qquad \textbf{(6-2)}$$

Using Figure 41 it is easy to calculate the open loop transfer function of the loop-filter. In appendix 10.9 these calculations are shown. The open loop transfer function of the loop-filter is.

$$H_{open-loop}(s) = \frac{G_{PWM}\left(s^2 R_2 R_3 C_2 C_3 gm_6 + s R_3 C_3 gm_5 + gm_4\right)}{s^3 R_1 R_2 R_3 C_1 C_2 C_3} \qquad \textbf{(6-3)}$$

This equation can be rewritten in the following form:

$$H_{open-loop}(s) = G\frac{\left(s^2 + sA + B\right)}{s^3} \qquad \textbf{(6-4)}$$

$$\text{with:} \quad G = \frac{gm_6 G_{PWM}}{R_1 C_1}, \quad A = \frac{gm_5}{R_2 C_2 gm_6}, \quad B = \frac{gm_4}{R_2 R_3 C_2 C_3 gm_6}$$

This form can be used together with equations (3-11) and (3-12) from chapter 3.2.2 to calculate to optimal loop-filter with a NTF as:

$$NTF(s) = \frac{s^3}{s^3 + G\left(s^2 + sA + B\right)} = \frac{s^3}{s^3 + s^2 G + sGA + GB} \qquad \textbf{(6-5)}$$

The amplification, or also called closed loop gain, of this system is for audio frequencies:

$$Gain_{closed-loop} = \frac{V_{out}}{V_{in}} = R_1 gm_0 \qquad \textbf{(6-6)}$$

This can be easily derived. At low frequencies all current generated by the input gm flows through R_1, because it cannot go through C_1. If gm1 is high enough the input of the gm in the first integrator can be considered as a virtual ground. So the output voltage will be the same as the voltage over R_l.

6.2 RC Spread

During production it is very likely that spread and mismatch of the RC components occur. This is an unwanted side-effect of production which should be taken into account during this analysis. It is very well possible for the system to become unstable if spread and mismatch are neglected.
Spread is considered as occurring most severe, in the order of percents possible, while mismatch can be made very small, depending on the size of the components ([16]).

In this paragraph the influence of spread on the system is discussed as well how it could be cancelled.

Spread will affect the gains of the integrators. Using equation (6-5) the effect of spread on the NTF can be analyzed. Let's consider a spread factor Δ is present only in the resistors of the loop-filter. Equation (6-5) will become:

$$NTF(s) = \frac{s^3}{s^3 + s^2\frac{G}{\Delta} + s\frac{GA}{\Delta^2} + \frac{GB}{\Delta^3}} \qquad \textbf{(6-7)}$$

In chapter 3.2 the Butterworth NTF was discussed. It was shown that a 3rd order Butterworth NTF will look like:

$$NTF(s) = \frac{s^3}{s^3 + s^2 2\omega_c + s2\omega_c^2 + \omega_c^3} \qquad \textbf{(6-8)}$$

Comparing equations (6-7) and (6-8), one can see the Butterworth characteristic of the NTF remains. Only the corner frequency (ω_c) shifts (Figure 42a). It can be seen that if the spread increases the RC values ($\Delta>1$) the noise suppression will be less, while if the spread decreases the RC values ($0<\Delta<1$) the noise suppression will be larger. The danger of spread can be seen in the open loop transfer function (Figure 42b). In this case an increasing spread is acceptable considering the stability of the system. Decreasing spread leads to a higher unity gain frequency. This higher unity gain frequency results in an instable system as was explained in chapter 2.1.2. (The spread factor used for Figure 42 is extremely high. This is done to get a better view what the effect of spread is)

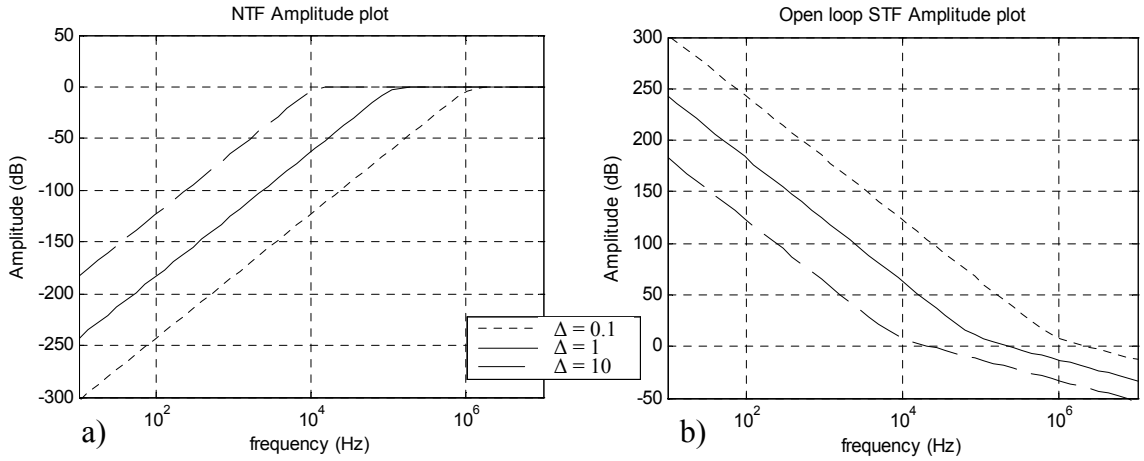

Figure 42: Effect of component spread on (a) the NTF and (b) the open loop transfer function when the open loop gain is independent of spread

In theory one can compensate in this case using the transconductors of the gain factors (gm_4, gm_5, gm_6) and the amplitude of the carrier signal (I_{car}).

In the previous analysis only the resistors of the integrators suffer from spread, but when the same carrier is used as the one used in [4] the amplitude of the carrier signal (I_{car}) also suffers from spread. Here, I_{car} is depending on the oscillator frequency, the

supply voltage and a resistor. The resistor used to create I_{car} also suffers from spread. When I_{car} is dependent on spread the NTF look like:

$$NTF(s) = \frac{s^3}{s^3 + s^2 G + s\frac{GA}{\Delta} + \frac{GB}{\Delta^2}} \qquad \textbf{(6-9)}$$

where: $G \propto \frac{gm_6}{R_1 gm_4 I_{car}}, \quad A \propto \frac{gm_5}{R_2 gm_6}, \quad B \propto \frac{gm_4}{R_2 R_3 gm_6}$

Figure 43 shows the NTF and open-loop transfer if also I_{car} suffers from spread. The dependency of I_{car} on spread causes that the NTF will not be a real Butterworth form anymore. In case of decreasing spread factor the NTF will have an overshoot at the corner frequency. Because this will be outside the audio band this is not a real problem for the system performance. Actual the dependency of I_{car} on spread is only positive. When the spread factor is more than 1, the noise suppression (at low frequencies) is less than intended. But because of the spread in $I_{car,}$ the open-loop gain increases and so the noise suppression is becoming better again. If the spread factor is less than 1, the unity gain frequency becomes too high and equation (2-2) is not valid any more. If in this case I_{car} is also dependent on spread, the open-loop gain decreases and the unity gain frequency becomes lower. So if I_{car} is dependent on spread, more spread is allowed before the system becomes unstable. If the spread factor is much less than 1 the open-loop transfer doesn't have a 1st order slope at unity gain. This leads to an overshoot in the NTF. This can also lead to instability according to equation (2-1).

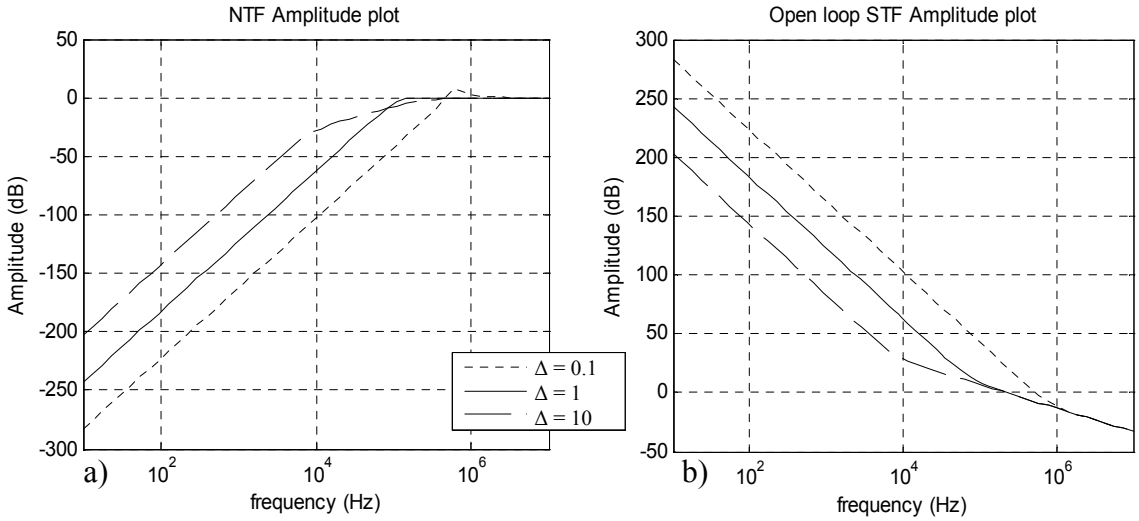

Figure 43: Effect of component spread on (a) the NTF and (b) the open loop transfer function when the open loop gain is dependent of spread

Now to compensate for the spread, an option would be:

$$gm_4 = \Delta gm_4'$$
$$gm_6 = \frac{gm_6'}{\Delta} \qquad \textbf{(6-10)}$$
$$I_{car} = \frac{I_{car}'}{\Delta^2}$$

I_{car} is already dependent to spread. Besides this, it needs to have an additional quadratic dependency to compensate for the spread (equation (6-10)). In total it needs to be to the power 3 dependent to spread. This could be very difficult to create in practice. It is also possible to make adjustable resistors by splitting a large resistor in a number of small resistors and so no quadratic dependency is needed, but this is outside the scope of this report.

6.3 Changeable Carrier Frequency

It would be very nice if one could change the carrier frequency and the loop-filter will adjust itself to an optimal filter. Due to the tunability of the transconductors and amplitude of the carrier signal (I_{car}) this should be in theory possible.

The first thing which have to be said, when the carrier frequency changes also the limits to the unity gain frequency of the open loop transfer function changes. A high carrier frequency means a higher unity gain frequency of the open loop transfer function is possible without the system becoming unstable (This was explained in chapter 2.1.2).

From a NTF point of view (equation (6-5)) a change of the carrier frequency (δ) only affects the gain of the open loop function (G). So only changing the carrier frequency (δ) results in the following NTF:

$$NTF(s) = \frac{s^3}{s^3 + s^2 G\delta + sG\delta A + G\delta B} \qquad \text{(6-11)}$$

where: $G \propto \frac{gm_6}{gm_4 I_{car}}, \quad A \propto \frac{gm_5}{gm_6}, \quad B \propto \frac{gm_4}{gm_6}$

In order to create an optimal loop-filter the gain factors and carrier signal amplitude should be changed as follow:

$$gm_4 = \delta gm_4'$$
$$gm_6 = \frac{gm_6'}{\delta} \qquad \text{(6-12)}$$
$$I_{car} = \frac{I_{car}'}{\delta^2}$$

If this is possible to create, the NTF and open loop transfer function will look like:

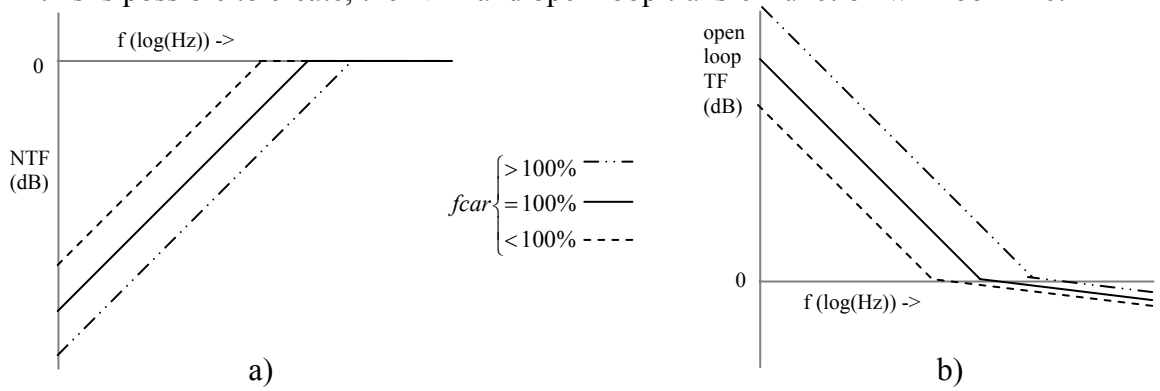

Figure 44: Change of NTF and open loop TF if transconductor and carrier signal amplitude if adjustment is possible

As can be seen the NTF will be optimized after the change in carrier frequency. Again one can look at using adjustable resistors as mentioned before to get rid of the quadratic dependency. The feasibility of these specifications is outside the scope of this report.

6.4 The integrator

The integrators are the core of the loop-filter. In 5.2 the different type of integrators were already discussed and in paragraph 6.1 it was stated that only miller integrators are used to simplify the analysis for now.

6.4.1 Miller integrator

In this paragraph a closer look will be taken on the miller integrator (Figure 45a). To calculate the transfer function, a small signal model is used (Figure 45b). In this model C_p represents the parasitic gate capacitance of the input of the transconductor. Z_l represents the load impedance of the integrator due to the next stage.

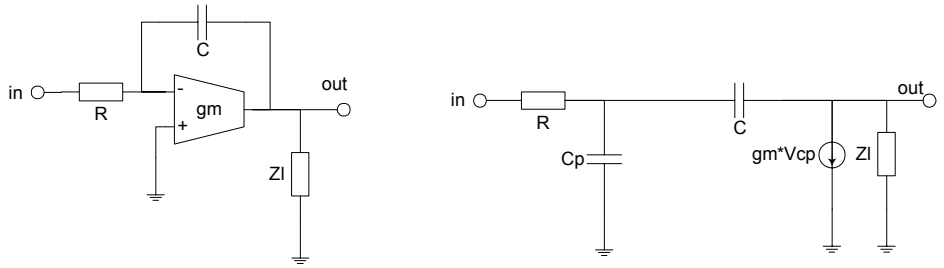

Figure 45: Miller integrator: a) implementation; b) small signal model

Appendix 10.10.1 shows the calculations of the transfer function of the miller integrator. The transfer function is:

$$H(s) = \frac{Z_l(sC - gm)}{s^2 RCZ_l C_p + s\left(CR(gmZ_l + 1) + Z_l C + RC_p\right) + 1} \quad \textbf{(6-13)}$$

Assume Z_l is very high the transfer function will become:

$$H(s) = \frac{(sC - gm)}{s^2 RCC_p + sC(Rgm + 1)} \quad \textbf{(6-14)}$$

This case one of the poles lies in the origin. Now also assume gm is very high and the transfer function will become as mentioned in paragraph 6.1:

$$H(s) \approx \frac{-1}{sRC} \quad \textbf{(6-15)}$$

To simplify the analysis the load impedance, Z_l, is considered as only a resistive load:

$$Z_l(s) = \Re\left(Z_{in\_next}(s)\right) = R_{next} + \frac{1}{gm_{next}} \quad \text{(see appendix 10.10.1)} \quad \textbf{(6-16)}$$

The first thing standing out is the RHP zero:

$$Zero = \frac{C}{gm} \quad \textbf{(6-17)}$$

One should be very careful with RHP zeros. They will change the output polarity of the integrator. Thus one should take care that this zero lies further away than the unity gain frequency of the system. Otherwise the system becomes unstable.
There is a way to eliminate this RHP zero. This will be discussed in next paragraph.

An ideal integrator has only 1 pole in the origin and no zeros. From equation (6-13) it can be seen a miller integrator has 2 poles and, if a load-impedance is present, not one pole is actually in the origin.

The poles are located at:

$$Pole_1 = \frac{1}{CR(gmZ_l + 1) + Z_l C + RC_p}, \quad Pole_2 = \frac{CR(gmZ_l + 1) + Z_l C + RC_p}{RCZ_l C_p} \qquad \textbf{(6-18)}$$

Or for a fast analysis, if *gm* is large enough:

$$Pole_1 = \frac{1}{RCgmZ_l}, \quad Pole_2 = \frac{gm}{C_p} \qquad \textbf{(6-19)}$$

When designing the integrator, the placement of the poles is also a point of concern. One pole is desired close to the origin, to create a high dc gain. The second pole has to be further from the origin than the unity gain frequency of the open loop transfer function, otherwise the system will become unstable. If the second pole is closer to the origin, the open loop transfer function will not have a 1st order behavior at the unity gain frequency. Chapter 2.1.2 explained the system becomes unstable in this situation. Figure 46 gives the ideal and the actual integrator transfer function.

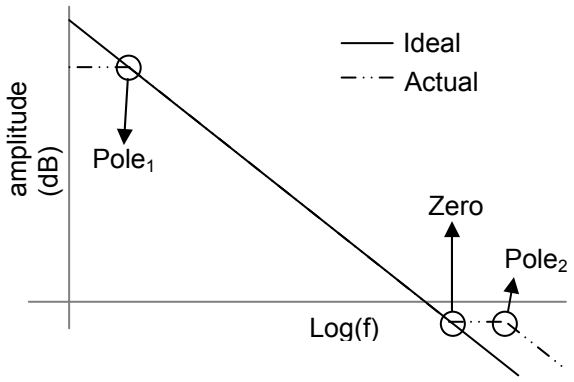

Figure 46: Integrator transfer functions

6.4.2 RHP zero cancellation.

In the analysis of the previous chapter a RHP zero is present. If this zero ends up closer to the origin of the s-plane than the unity gain frequency of the system, the system could become unstable. So one have to take care this zero lies beyond the unity gain frequency of the system. But there are also known approaches to completely cancel this zero ([17]). This can be done by inserting a resistor in series with the feedback capacitor (Figure 47).

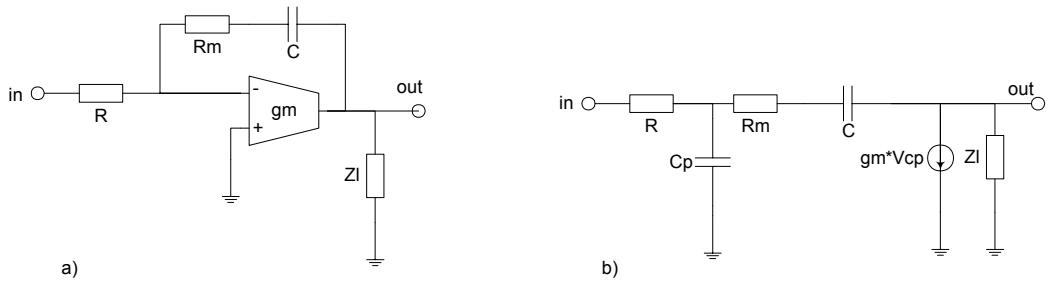

Figure 47: Miller integrator with RHP zero cancellation: a) implementation; b) small signal model

The transfer function of this modified integrator is (see appendix 10.10.2):

$$H(s) = \frac{Z_l\left(sC\left(1 - gmR_m\right) - gm\right)}{s^2 CC_p R\left(Z_l + R_m\right) + s\left(CR\left(gmZ_l + 1\right) + Z_l C + R_m C + RC_p\right) + 1} \qquad \textbf{(6-20)}$$

Still considering Z_l is a resistive load. Now the zero could be cancelled by choosing

$$R_m = \frac{1}{gm} \qquad \textbf{(6-21)}$$

In this case the poles will be:

$$Pole_1 = \frac{gm}{gm\left(CR\left(gmZ_l + 1\right) + RC_p\right) + \left(gmZ_l + 1\right)C},\ Pole_2 = \frac{gm\left(CR\left(gmZ_l + 1\right) + RC_p\right) + \left(gmZ_l + 1\right)C}{RCC_p\left(gmZ_l + 1\right)} \qquad \textbf{(6-22)}$$

If $gm \cdot Z_l >> 1$ the poles will not change in comparison to the integrator without compensation. The input impedance becomes:

$$Z_l(s) = \Re\left(Z_{in\_next}(s)\right) = R_{next} + \frac{2}{gm_{next}} \qquad \text{(see appendix 10.10.2)} \qquad \textbf{(6-23)}$$

Also the input impedance of the integrator will not change very much if $R_{next} >> \frac{1}{gm_{next}}$.

6.5 Voltage swing

In simulations, voltages and currents don't have to be bound to limits. Unfortunately this is not the case in a real practical circuit. For example voltages are bound to the supply voltage (Vdd). Therefore for the circuit implementation one should take care, the voltage swing of the amplifiers (in this case the integrators) will not exceed the supply voltage.
First take al look at the signals in the system. Take a look at Figure 48:

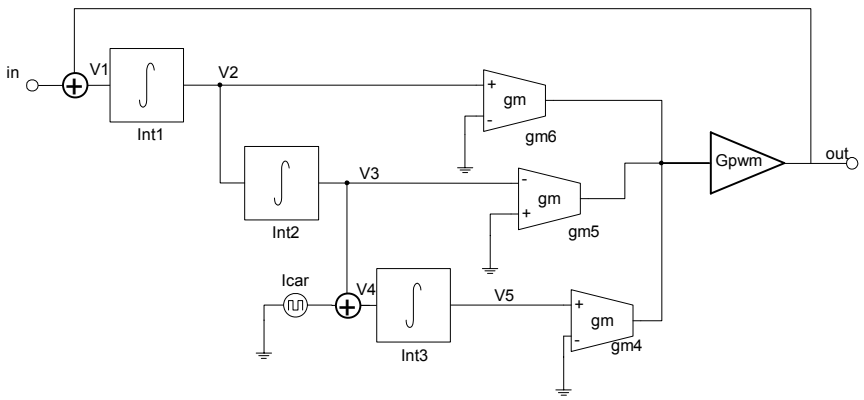

Figure 48: 3rd order loop-filter for a PW modulator

The output of this system is:

$$V_{out} = V_{in} \cdot STF + V_{n\_out} \cdot NTF + V_{car\_out} \quad \textbf{(6-24)}$$

Where V_{n_out} is the output referred noise voltage and V_{car_out} is all signal at the output created by only the carrier signal. This is the signal at the carrier frequency and its harmonics.

In paragraph 5.1.1 I already stated that in a feedforward topology "1-*STF = NTF*" (equation (5-3)). So the signal at the input of the first integrator is:

$$V_1 = V_{in} - V_{out} = V_{in} \cdot (1 - STF) + V_{n\_out} \cdot NTF + V_{car\_out} = (V_{in} + V_{n\_out}) \cdot NTF + V_{car\_out} \quad \textbf{(6-25)}$$

When traveling again to the output, this signal is processed by the integrators. As already was determined in paragraph 5.1.1, the input signal contribution is only very small at the first integrators and increasing when traveling further trough the system. The opposite is true for the V_{car_out} because its frequencies are higher than the corner frequency of the loop filter. Figure 49 shows a possible representation of the signals, V_{in} and V_{car_out}, at different stages in the loop-filter. From these drafts one can clearly see that at first V_{car_out} is dominant part for the voltages swing. So the swing of the first integrator can be determined by only looking at V_{car_out}. For the second integrator the input signal will have more influence on the maximum swing. At the third integrator the carrier is put in, so this will have influence again on the maximum swing. When the input signal is dominant for the voltages swing, one should look at the worst case. Because the transfer has a high pass filter characteristic, one should look at the highest frequencies of the input signal.

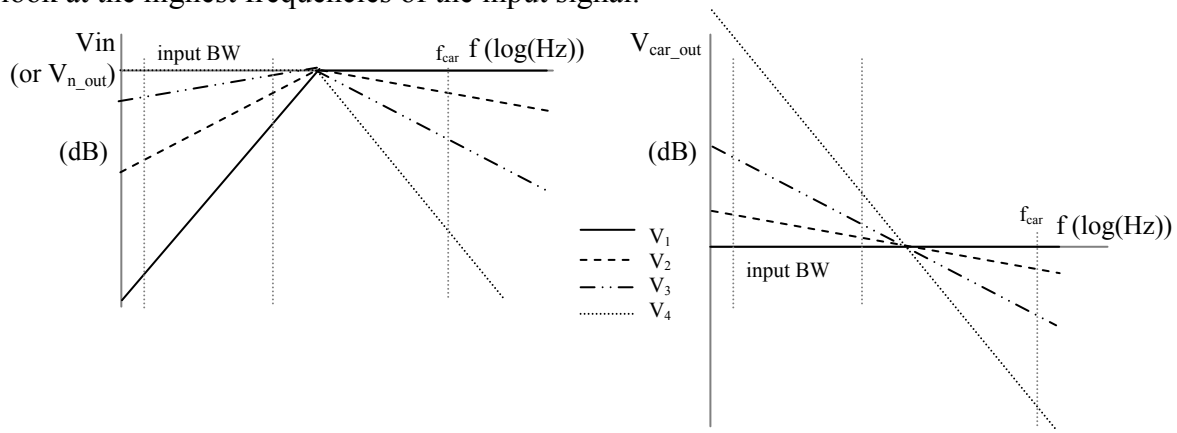

Figure 49: Transfer functions on different stage of the loop-filter

Now look at the integrators. The worst case frequencies for voltage swing are the carrier frequency or the highest input frequency (20 kHz). So looking at the Figure 46, the area of interest is the slope between 'Pole$_1$' and 'Zero'. For this analysis it is considered the frequency of Pole$_1$ is lower than the highest input frequency and the frequency of 'Zero' is higher than the carrier frequency.

6.5.1 1st integrator:

At the first integrator the dominant part for the maximum swing is V_{car_out}, so the integrator gain has to be designed that the swing due to V_{car_out} is smaller than the supply voltage. If the frequency of 'Zero' is higher than the carrier frequency the transfer function of the slope of the first two integrators is:

$$H'_{int}(s) = \frac{-Z_{lx} gm_x}{s\left(C_x R_x \left(gm_x Z_{lx} + 1\right) + Z_{lx} C_x + R_x C_{px}\right)} \overset{\substack{gm_x Z_{lx} >> 1 \\ C_{px} << C_x}}{\Longrightarrow} H'_{int}(s) \approx \frac{-1}{sC_x R_x} \quad \textbf{(6-26)}$$

Using this equation and suppose $gm_1Z_{l1} >>1$ and $C_{p1}<<C_1$, the swing at the carrier frequency is:

$$V_{car\_out@V_2@f_{car}} = \frac{1}{C_1 R_1}\frac{1}{2\pi f_{car}} \cdot V_{car\_out@f_{car}} \quad \textbf{(6-27)}$$

The carrier component is a square wave (when no input voltage is applied, the output is a square wave). So also the odd harmonics contribute to the amplitude of the voltage swing.
A square wave in mathematical form looks like:

$$V_{square} = \sum_{k=0}^{\infty} \frac{4V_{sq\_max}\sin\left(2\pi ft\left(2k+1\right)\right)}{\pi\left(2k+1\right)} \quad \textbf{(6-28)}$$

At the output of this PW modulator $V_{sq\_max} = V_p$. Using a square wave as input of the first integrator, the swing for the first integrator becomes:

$$V_{2\_max} = \frac{1}{C_1 R_1}\frac{2V_p}{\pi^2 f_{car}}\sum_{k=0}^{\infty}\left(\frac{1}{\left(2k+1\right)^2}\right) = \frac{1}{C_1 R_1}\frac{V_p}{4f_{car}} \quad \textbf{(6-29)}$$

6.5.2 2nd integrator:

In case of the 2nd integrator the input signal has much more influence on the maximum swing, while the influence of V_{car_out} becomes less. The gain at the carrier frequency can calculated in the same ways as with the 1st integrator mentioned above. The transfer function of the slope between $Pole_1$ and Zero is the same as (6-26):
The transfer function of V_{car_out} at the output of the 2nd integrator is the product of the 1st and 2nd integrator. This means the swing at the carrier frequency can be calculated by calculating the gains of both integrators at 1Hz and use a 40 dB falling slope to calculate the swing at the output of the 2nd integrator.

$$V_{car\_out\_max@V_3} = Gain_{int1@1Hz} \cdot Gain_{int2@1Hz} \cdot \frac{1}{4\pi^2 f_{car}{}^2} \cdot V_{car\_out\_max} \quad \textbf{(6-30)}$$

The gains of both integrators at 1 Hz are (using (6-26) if $gm_xZ_{lx} >>1$ and $C_{px}<<C_x$):

$$Gain_{int1@1Hz} = \frac{1}{C_1 R_1} \quad \textbf{(6-31)}$$

$$Gain_{int2@1Hz} = \frac{1}{C_2 R_2} \quad \textbf{(6-32)}$$

Now the swing at the carrier frequency is:

$$\begin{aligned} V_{car\_out\_max@V_3} &= \frac{1}{C_1 R_1}\cdot\frac{1}{C_2 R_2}\frac{V_p}{\pi^3 f_{car}{}^2}\sum_{k=0}^{\infty}\left(\frac{1}{\left(2k+1\right)^3}\right) \\ &= \frac{1}{C_1 R_1}\cdot\frac{1}{C_2 R_2}\frac{7V_p\zeta(3)}{8\pi^3 f_{car}{}^2} \end{aligned} \quad \textbf{(6-33)}$$

Where $\zeta(x)$ is the Riemann Zeta function.[2]
For the gain of the input signal at this stage the calculations are a bit more difficult. The transfer function for the input signal at the output of the 2nd integrator is:

$$H_{V_{in}@V_3} = NTF \cdot Gain_{closed-loop} \cdot H'_{int1}(s) \cdot H'_{int2}(s) \quad \textbf{(6-34)}$$

---

[2] The Zeta function is defined for Re(x)>1 by $\zeta(x) = \sum_{k=1}^{\infty}\frac{1}{k^x}$ (From Maple Help)

Considering an ideal integrator this transfer function will have a 20 dB rising slope from DC. To calculate the gain at the highest input frequency one could calculate the gain a 1 Hz and from here calculate what the gain is at the highest input frequency (20 kHz).

$$V_{in\_\max@V_3@f_{in\_\max}} = Gain_{NTF@1Hz} \cdot Gain_{closed-loop} \cdot Gain_{int1@1Hz} \cdot Gain_{int2@1Hz} \cdot 2\pi f_{in\_\max} \cdot V_{in\_\max@f_{in\_\max}} \quad \textbf{(6-35)}$$

The gain contributions at 1 Hz are:

$$Gain_{NTF@1Hz} = \frac{1}{f_{car}^3} \quad \textbf{(6-36)}$$

$$Gain_{closed-loop} = R_1 gm_0 \qquad \text{(same as equation (6-6))} \quad \textbf{(6-37)}$$

Give these gains now the maximum amplitude of the input signal at this output of the second integrator can be calculated (again if gm_xZ_{lx} >>1 and C_{px}<<C_x):

$$V_{in\_\max@V_3@f_{in\_\max}} = \frac{R_1 gm_0}{f_{car}^3} \frac{1}{C_1 R_1} \frac{1}{C_2 R_2} 2\pi f_{in\_\max} \cdot V_{in\_\max@f_{in\_\max}} \quad \textbf{(6-38)}$$

Finally the maximum swing could be calculated. The maximum swing at V_3 is:

$$V_{3\_\max} = V_{car\_out\_\max@V_3} + V_{in\_\max@V_3@f_{in\_\max}} \quad \textbf{(6-39)}$$

6.5.3 3nd integrator:

In case of the 3rd integrator the influence of V_{car_out} can be neglected. But instead of this I_{car} is put in the system and influences the swing.
The transfer function of the slope between Pole$_1$ and Zero for the 3rd integrator is:

$$H'_{int3}(s) = \frac{-gm_3}{sC_3(R_3gm_3+1)} \overset{R_3gm_3>>1}{\Longrightarrow} H'_{int3}(s) \approx \frac{-1}{sC_3R_3} \quad \textbf{(6-40)}$$

I_{car} has an extra gain due to R_3. Using the same calculations as before one can see that the swing due to the carrier signal is (if R_3gm_3>>1):

$$V_{car@V_5@f_{car}} = \frac{R_3gm_3}{C_3R_3gm_3} \frac{1}{2\pi f_{car}} I_{car@f_{car}} = \frac{1}{C_3} \frac{1}{2\pi f_{car}} I_{car@f_{car}} \quad \textbf{(6-41)}$$

I_{car} is also a block wave so the total contribution of I_{car} is:

$$V_{car\_\max@V_5} = \frac{1}{C_3} \frac{I_{car\_\max@f_{car}}}{4 f_{car}} \quad \textbf{(6-42)}$$

At the output of the 3rd integrator, the transfer function of the input signal has a flat spectrum at its bandwidth. The transfer function for the input signal to the end of the 3rd integrator is:

$$H_{V_{in}@V_5} = NTF \cdot Gain_{closed-loop} \cdot H'_{int1}(s) \cdot H'_{int2}(s) \cdot H'_{int3}(s) \quad \textbf{(6-43)}$$

Because the spectrum is flat one could use the products of all integrators and NTF at 1Hz.

$$V_{in\_\max@V_5} = Gain_{NTF@1Hz} \cdot Gain_{closed-loop} \cdot Gain_{int1@1Hz} \cdot Gain_{int2@1Hz} \cdot Gain_{int3@1Hz} \cdot V_{in\_\max} \quad \textbf{(6-44)}$$

The gain at 1 Hz for the 1st and 2nd integrator and NTF are already given above the gain at 1Hz of the 3rd integrator is (if R_3gm_3>>1):

$$Gain_{int3@1Hz} = \frac{1}{C_3R_3} \quad \textbf{(6-45)}$$

Now all ingredients are present to calculate the contribution of the input signal at the end of the 3rd integrator (using (6-31), (6-32), (6-36), (6-37), (6-44), (6-45), $R_x gm_x >> 1$ and $C_{px} << C_x$):

$$V_{in\_\max@V_5} = \frac{R_1 gm_0}{f_{car}^3} \frac{1}{C_1 R_1} \frac{1}{C_2 R_2} \frac{1}{C_3 R_3} \cdot V_{in\_\max} \quad \textbf{(6-46)}$$

Finally the maximum swing at the output of the 3rd integrator is:

$$V_{5\_\max} = V_{car\_\max@V_5} + V_{in\_\max@V_5} \quad \textbf{(6-47)}$$

In this analysis of the swing at different stages only the input signal and carrier signal were incorporated. Noise in the system was neglected. In practice the noise can be responsible for a system to overload and thus in this case could become instable. So for the actual calculations the contribution of the noise has also to be incorporated.

6.6 Noise analysis

If a system is not designed well, in-system noise could destroy the working of the system. In a feedback system noise could make the system unstable. This is why a proper noise analysis is necessary. A good way to analyze the noise is to calculate the contribution of a noise-source at the input of the system. This is called the input-referred noise ([16]).

Thermal noise generated due to the resistors and transconductors is important for the SNR of the system. Noise generated in the early stages of the loop filter will not be fully suppressed by the feedback loop.

For the noise generated by the resistors and transconductors the models showed in Figure 50 are used:

a) b)

Figure 50: Noise models

As noise sources the thermal noise is considered only. From [16] it is known the thermal noise of a resistor (Figure 50a) is:

$$\overline{I_{n\_R}^2} = \frac{4kT}{R} \quad \textbf{(6-48)}$$

k is Boltzmann's constant and T the temperature in Kelvin.

The noise source of the transconductor depends on the type of transconductor which is used. Because the implementation of the transconductor is out of the scale of this report, a simple ideal MOSFET is used as model for this analysis. The thermal noise of a MOSFET (Figure 50b) is:

$$\overline{I_{n\_gm}^2} = 4kT\gamma gm \qquad \textbf{(6-49)}$$

The coefficient γ is different for different MOSFETs.

Figure 51 shows the noise sources in an integrator.

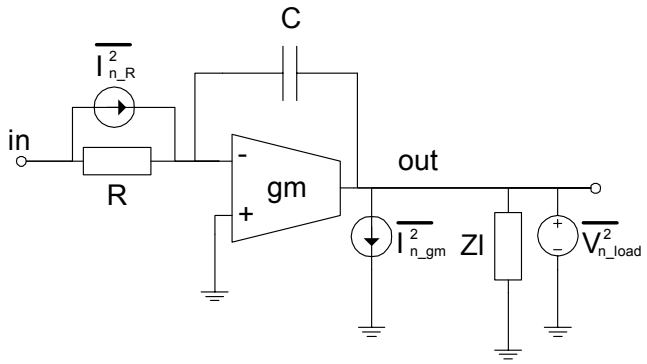

Figure 51: Noise in an integrator

From [16] it is known that one can shift the noise source through the circuit by using the following equation:

$$S_Y(f) = S_X(f)\left|H(f)\right|^2 \qquad \textbf{(6-50)}$$

Using superposition, the input referred noise voltage of all noise sources can be calculated. Appendix 10.11 shows the calculations of this. The total input referred noise this integrator is:

$$\overline{V_{n\_in}^2} = 4kT\left(R + \frac{\gamma}{gm}\right) + (\omega RC)^2 \overline{V_{n\_load}^2} \qquad \textbf{(6-51)}$$

One can see the noise of the load is suppressed by the integrator for low frequencies. When looking at the global system one can imagine the noise floor at low frequencies at the output of the system is mainly the sum of the noise sources of the first integrator and input transconductor. Due to this analysis the dominant input referred noise voltage at low frequencies of the total system are caused only by the first integrator and the input Gm (Figure 52).

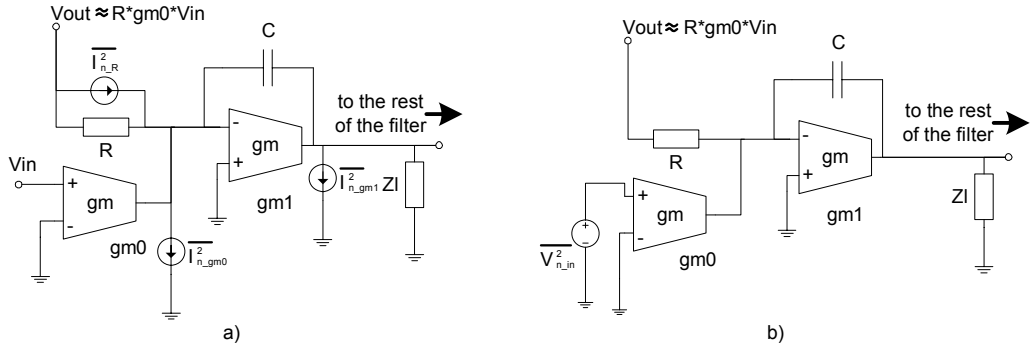

Figure 52: Dominant input referred noise of the system: a) with internal noise sources, b) input referred noise only

Together with Figure 52 one can calculate the dominant input referred voltage noise for the complete system:

$$\overline{V_{n\_in}^2} = 4kT\left(\frac{1}{R_1 gm_0^2} + \frac{\gamma}{R_1^2 gm_1 gm_0^2} + \frac{\gamma}{gm_0}\right) \quad \textbf{(6-52)}$$

If the closed loop gain ($R_1 gm_0$, §6.1) is larger than $1/\gamma$ and $R_1^2 gm_1 gm_0 > 1$, gm_0 is the dominant factor for the noise. The specifications tell that the amplification (or closed loop gain) is 30 and $R_1^2 gm_1 gm_0$ is probably also larger than 1. This means the gm_0 will be de dominant factor for the noise.
In that case the input referred voltage noise will produce a noise power inside the audio bandwidth of:

$$P_{noise\_in\_audioband@input} = 4kT\frac{\gamma}{gm_0}\cdot(20\cdot 10^3) \quad \textbf{(6-53)}$$

This noise power is not affected by the loop filter and will be completely visible in the output. The output referred voltage noise is for low frequencies even amplified by the closed loop gain. This results in a output referred noise power in the audio band of:

$$P_{noise\_in\_audioband@output} = 4kT\frac{\gamma}{gm_0}\cdot(20\cdot 10^3)\cdot Gain_{closed-loop}^2 \quad \textbf{(6-54)}$$

The noise is nice start to calculate the required parameter values.

In this analysis the thermal noise was only considered as white noise. In practice it also contains noise like 1/f noise. This was neglected for simplicity reasons. So in practice the noise power will be little bit higher, but the ratios of input referred voltage noise between the components remain the same.

7 Parameter calculations and system simulations

In previous Chapter it was shown how the parameter values could be calculated. In this chapter some actual values of the components are calculated in order to create an optimal loop-filter. In Cadence software this loop-filter will be simulated in a simple PWM model and some simulation results will be presented. In the research as described in the previous chapters some design choices concerning the loop filter are formulated:

- 3rd order loop filter with Butterworth type NTF
- 700 kHz carrier signal (f_{car})
- Carrier inserted in the last integrator
- Chain of Integrators with Weighted Feedforward Summation
- Internal supply voltage = 12 V peak-peak
- Output voltage (V_p) = 60 V peak-peak

7.1 Parameter calculations

In §3.2 a loop filter with a Butterworth type NTF is investigated. From appendix 10.2.3 it is known that if an ideal 3rd order Butterworth NTF is desired the open loop transfer function becomes:

$$H_{open-loop}(s) = -\frac{2\omega_c s^2 + 2\omega_c^2 s + \omega_c^3}{s^3} \qquad \textbf{(7-1)}$$

$$G_{PWM} = 2\omega_c$$

Were ω_c is the corner frequency of the NTF. As mentioned in §3.2 the G_{PWM} for a 3rd order filter should be same as for a 1st order filter. Using appendix 10.2.1 one sees G_{PWM} has to be the same as the unity gain frequency (ω_{UG}). ω_{UG} is determined with equation (2-2) and the open loop filter can be calculated for a 700 kHz carrier frequency with (7-1):

$$\omega_{UG} = \frac{\omega_{car}}{\pi} = 2f_{car} = 1.4 \cdot 10^6 \qquad \textbf{(7-2)}$$

$$G_{PWM} = \omega_{UG} = 1.4 \cdot 10^6 \qquad \textbf{(7-3)}$$

$$\omega_c = 7 \cdot 10^5 \qquad \textbf{(7-4)}$$

$$H_{open-loop}(s) = \frac{-1.4 \cdot 10^6 \left(s^2 + 7 \cdot 10^5 s + 2.45 \cdot 10^{11}\right)}{s^3} \qquad \textbf{(7-5)}$$

In §6.1 the relation between the Chain of Integrators with Weighted Feedforward Summation topology and open-loop transfer function were discussed. Together with equation (7-5) the relation is as follow:

$$H_{open-loop}(s) = -G\frac{\left(s^2 + As + B\right)}{s^3} \qquad \textbf{(7-6)}$$

Where:

$$G = \frac{4f_{car}V_p C_3 gm_6}{R_1 C_1 I_{car} gm_4} = 1.4 \cdot 10^6,\ A = \frac{gm_5}{R_2 C_2 gm_6} = 7 \cdot 10^5,\ \mathrm{B} = \frac{gm_4}{R_2 C_2 R_3 C_3 gm_6} = 2.45 \cdot 10^{11}$$

Concerning the parameters one cannot choose just any values. There are many trade-offs which have to been made:

- At first it is important that the **voltage swing** of the integrators stays within the limits of the internal supply voltage. This means in this case the maximum swing cannot exceed 12 V peak-peak, or an amplitude of 6 V. It is desired that the integrators have a gain as high as possible. But when the gain is too high the integrator will clip to the supply voltage. In these calculations a maximum amplitude of 5 V is chosen in order to allow some noise and distortion generated in the output stage and non-linearity of the gm.
- Placement of the **zeros and poles**. As could be seen in §6.4.1 the actual integrator has a zero. This zero should lie higher than the unity gain frequency of the open loop transfer, otherwise the system becomes unstable. If the zero could not be put on a higher than the unity gain frequency of the open loop transfer, the zero has to be cancelled. §6.4.1 also tells that there are 2 poles. One pole is preferably to be put as close as possible to origin in order to have a loop gain as high as possible for low frequencies. This gives the best noise reduction for low frequencies. The second pole has to be put further than the unity gain frequency in order to keep the system stable.
- Resistors and Gm's are known **noise** sources. It is preferable to keep the resistor values as low as possible and the Gm values as high as possible in this point of view. Low resistor and high Gm values create less noise but consumes more power.
- Large resistor and capacitor values require large areas. For resistors especially when also high linearity is desired.
- Of course also feasibility is an important point. There are limits for creating certain values. For example the gm value.

Through this way the RC components are calculated. To created the correct loop filter the gain factors (gm_4, gm_5 and gm_6) are adjusted according to equation (7-6). Now let's take a look at the integrators.

1st integrator:

According to §6.5.1 the maximum swing at the output of the first integrator (if $gm_1 Z_{l1} >> 1$) is:

$$V_{2\_\max} = \frac{1}{C_1 R_1} \frac{V_p}{4 f_{car}} \qquad \textbf{(7-7)}$$

Now some choices have to be made:

Let's first start with gm_0. This is the dominant factor for the thermal noise visible at the output. If a $gm_0 = 0.0003$ is chosen, according to equation (6-54) the noise power in the audio band at the output of the system will be -92 dBV. Because the maximum output amplitude of the system is 30 Volt (29.5 dB) the maximum dynamic range due to the thermal noise will be about 121.5 dB.

Now the closed loop gain and gm_0 are known, R_1 can be calculated using equation (6-6). Further more a choice should be made for gm_1 and Z_{l1}:

$$\begin{aligned} &- \quad R_1 = 100\ \text{k}\Omega \\ &- \quad gm_1 = 0.001 \\ &- \quad Z_{l1} \approx R_2 = 100\ \text{k}\Omega \end{aligned} \qquad \textbf{(7-8)}$$

Now $gm_1 Z_{l1} >> 1$ and together with the 700 kHz carrier frequency, 30 volt output voltage amplitude and 5 volt amplitude for the maximum swing. With equation (7-7) this leads to: $C1 = 21.03\ \text{pF}$

Suppose that all the parasitic capacitance at the input of the Gm's are (this is an educated guess):

- $Cp = 0.1\,\text{pF}$

Using equation (6-17) and (6-18) from §6.4.1, the zero and poles of the 1st integrator for these parameter values are:

- $Zero = -7.57\ \text{MHz}$
- $Pole_1 = -735\ \text{Hz}$
- $Pole_2 = -1.62\ \text{GHz}$

These zero and poles are place in order to maintain a stable system (see above). So it is not necessary to apply zero cancellation.
The capacitor has quite a large value and thus will require a large area. For now this is not considered as the biggest issue. It is possible to decrease the capacitor value but than the resistor value has to be increased. If this is the case the resistor will consume more area. The optimal values for area consumption are not investigated.

2nd integrator:

According to §6.5.2 the maximum swing at the output of the second integrator (if $gm_x Z_{lx} >> 1$) is:

$$V_{3\_\max} = \frac{1}{C_1 R_1 C_2 R_2}\left(\frac{7V_p\zeta(3)}{8\pi^3 f_{car}{}^2} + \frac{R_1 gm_0}{f_{car}^3} 2\pi f_{in\_\max} \cdot V_{in\_\max@\, f_{in\_\max}}\right) \qquad \textbf{(7-9)}$$

Again some choices have to be made:

- $R_2 = 100\ \text{k}\Omega$ (already given in in the first integrator calculations)
- $gm_2 = 0.001$ **(7-10)**
- $Z_{l2} \approx R_3 = 500\ \text{k}\Omega$

With a 1 volt input amplitude and 5 volt amplitude for the maximum swing and with equation (7-9) this leads to: $C2 = 12.72\,\text{pF}$

Now the zero and poles are:

- $Zero = -12.5\ \text{MHz}$
- $Pole_1 = -242\ \text{Hz}$
- $Pole_2 = -1.61\ \text{GHz}$

The same conclusions are valid for the 2nd integrator:

- The zero and poles lie on place where they do no harm
- It is not necessary to apply zero cancellation.
- Large capacitor

The noise produced here is not really of interest because it will be shaped by the feedback loop.

3rd integrator

According to §6.5.3 the maximum swing at the output of the third integrator (if $gm_x Z_{lx} >> 1$) is:

$$V_{5\_\max} = \frac{I_{car\ @\ f_{car}}}{C_3 4 f_{car}} + \frac{R_1 gm_0}{f_{car}^3} \frac{V_{in\_\max}}{C_1 R_1 C_2 R_2 C_3 R_3} \qquad \textbf{(7-11)}$$

The last choices have to be made:

- $R_3 = 500\ \text{k}\Omega$ (already given in in the 2nd integrator calculations)
- $gm_3 = 0.001$
- $I_{\text{car}} = 183\ \mu\text{A}$
- $Z_{l3} \approx \infty$

(7-12)

I_{car} comes for the open loop transfer calculations (7-6). I_{car} can already be calculated when C_3 is not yet known because C_3 can be chosen free from $I_{car.}$ The ratio between gm_4 and gm_6 compensate for this.

With a 1 volt input amplitude and 5 volt amplitude for the maximum swing and with equation (7-11) this leads to: – $C3 = 25.90\,\text{pF}$

Now the zero and poles are:

- $Zero = -6.14\ \text{MHz}$
- $Pole_1 = 0\ \text{Hz}$
- $Pole_2 = -1.59\ \text{GHz}$

The same conclusions are valid for the 3nd integrator:

- The zero and poles lie on place where they do no harm
- It is not necessary to apply zero cancellation.
- Large capacitor
- The noise produced here is not really of interest because it will be shaped by the feedback loop.

As last the gain factors can be calculated with equation (7-6) and the parameters mentioned above. The ratios for the gain factors are:

- $gm_4 : gm_5 : gm_6 = 1 : 0.24 : 0.25$

The actual values for gm_4, gm_5 and gm_6 can be chosen freely as long as the ratios are still valid.

7.2 Cadence simulations

Now all parameters are calculated, some simulations of the implementation could be done. In this paragraph it will be shown that the calculations of the previous paragraph and equations derived in this report are correct. This will be done by simulations. Appendix 10.12 shows the system models for the simulations Figure 62 shows the cadence model to simulate the complete system in a transient simulation. This is done to show the calculations for the swing are correct and if the noise at the output signal is the same as calculated.

The Gm's of the integrators in this model are represented as ideal voltage controlled current sources with a parasitic capacitance at the input and a noise current source at the output. The other Gm's are only represented as ideal voltage controlled current

sources due to simplicity. The resistors of the integrators are represented at an ideal resistor with a noise current source in parallel. The comparator is represented as an *arctan* function. An *if*-statement was not an option for transient simulations because of the integrating elements in the model. The infinite steep slope of an *if*-statement would lead to convolution problems. The *arctan* function with a very high slope in the origin comes very close to an *if*-statement and is even more representing an actual comparator

To check the correct voltage swings inside the loop filter, the voltages at the output of the integrators have to be checked. According to the calculations in next paragraph the maximum voltage swing should have a 5 volt amplitude if no noise sources are present. Because in this model noise sources are present the maximum voltage swing will be a little larger than 5 volt. As long as the voltage swing stays within an amplitude of 6 volt the system will be correct according to the specifications.

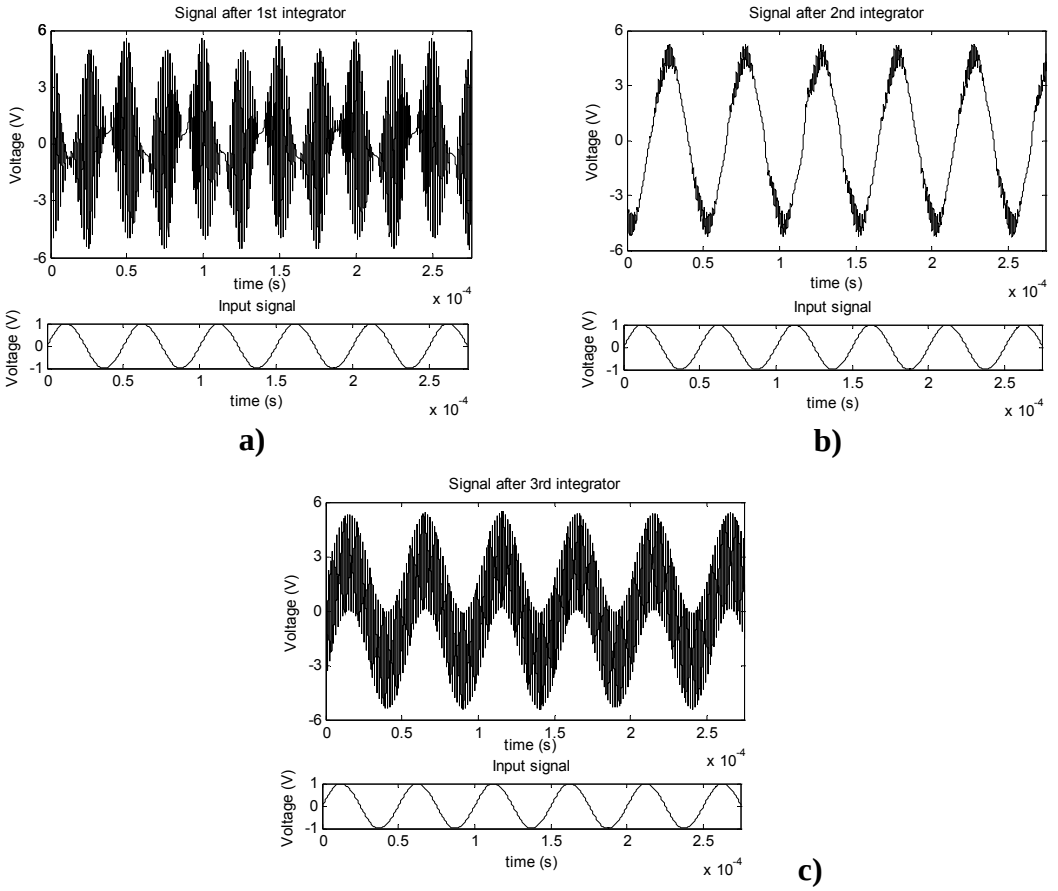

Figure 53: Signal inside the loop filter after the: a) 1st, b) 2nd and c) 3rd integrator

Figure 53 shows that the voltage swing at every stage has an amplitude of about 5 Volt. Because of the noise sources the actual voltage swing is a little more, but it stays under the 6 volt. Because of this it can be concluded that the voltage swing calculations from §6.5 are valid. Because the voltage stays below the 6 volt amplitude, the specifications for the voltage swing are obeyed.

Also a Fourier analysis is done to check the noise power in the system. For this analysis a 2.16 kHz input signal with an amplitude of 1 μV is applied to the system. This way the noise floor and dynamic range can be easily calculated from the

simulation results. The output PWM signal will be filtered by a simple 2nd order LC low-pass filter with a corner frequency of 25 kHz to get and actual representation of a system which could be used as a real audio amplifier. The system is also simulated with a low-pass output filter with a corner frequency of 1.57 MHz. This is done in order to see the corner frequency of the NTF which lays at 111 kHz according to the calculations.

Figure 54 shows the results of the Fourier analyses. The noise power in the audio bandwidth is -92.7515 dBV (for Figure 54a, in case of Figure 54b too much high frequency noise is folded back to the audio band due to sampling). According to the previous paragraph this is almost the same noise power in the audio bandwidth created by the input gm. This verifies the simulation results. Because the maximum output amplitude is 30 Volt. The dynamic range will be 122.2939 dB. This is a very good result. In Figure 54b one can see that the corner frequency of the NTF lays around 111 kHz as calculated.

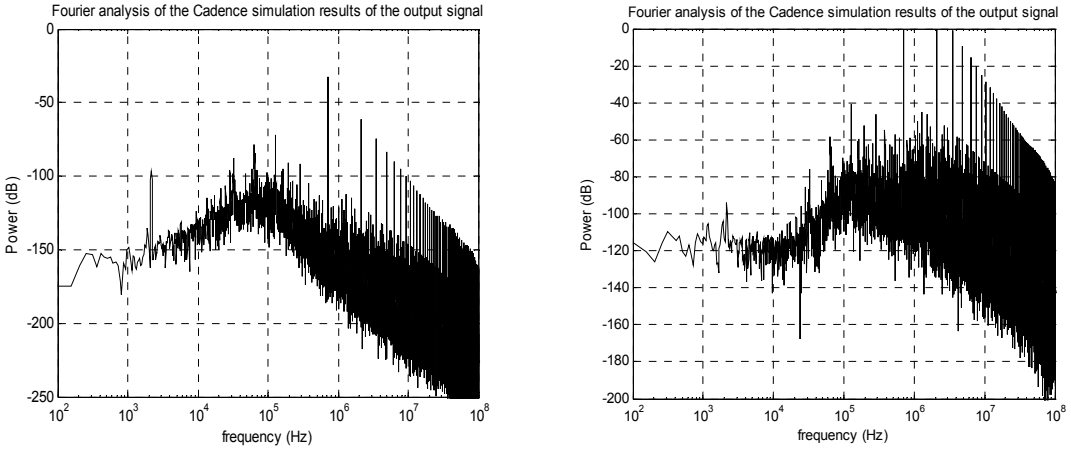

a) b)

Figure 54: Fourier analysis of a transient simulation of the PWM system in Cadence: a) 25 kHz output filter, b) 1.57 MHz output filter

The next thing to check is the transfer function of the integrators and the open loop. In this analysis the placement of the zeros and poles can be investigated and confirmed. The open loop transfer function is interesting because this is connected to the noise suppression. A high gain of the open loop transfer functions leads to a high noise suppression. Figure 55a shows simulation results of the transfer functions of the integrators.

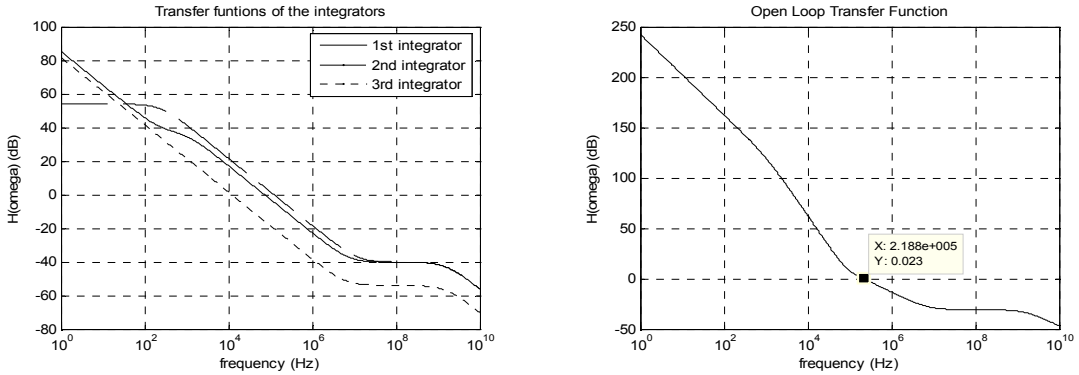

a) b)

Figure 55: a) Transfer functions of the integrators, b) open loop transfer function

According to the calculations of previous chapter the zeros and poles are placed at:

Integrator 1 :	Integrator 2 :	Integrator 3 :
– $Zero = -7.57$ MHz	– $Zero = -12.5$ MHz	– $Zero = -6.14$ MHz
– $Pole_1 = -735$ Hz	– $Pole_1 = -242$ Hz	– $Pole_1 = 0$ Hz
– $Pole_2 = -1.62$ GHz	– $Pole_2 = -1.61$ GHz	– $Pole_2 = -1.59$ GHz

This is exactly where they are also placed according to Figure 55a. This again validates the correctness of the calculations. But something unexpected happens in the transfer function of the 1st integrator. It appears that there exist a zero and a pole which are placed lower than $Pole_1$. The reason is that the load impedance of the 1st integrator (or the input impedance of the 2nd integrator) has a complex value (See appendix 10.10.1). Because the load impedance of the 2nd integrator is not infinite the input impedance becomes complex. This is only due to the model is simplified. In practice an integrator suffers also from the output resistance and capacitance of the Gm, which created more poles and zeros. These output impedances are in this analysis neglected due to simplicity.

Finally let's take a look at the open loop transfer function. With the calculated parameters the PWM gain (equation (6-2) is 101.5 dB. Together with the integrator transfer functions the simulations result in an open loop transfer function as showed in Figure 55b. Until 735 Hz the open loop transfer function has a 2nd order slope. This is because the second integrator has at this range a flat spectrum. After this the slope becomes a 3rd order slope until it becomes a 1st order slope before unity gain. At unity gain the slope is 1st order and the unity gain frequency lies below f_{car}/π. With these results the stability criteria mentioned in chapter §2.1.2 are obeyed.

From these results it can be concluded that the implementation functions like it supposed to.

8 Conclusion summary and Recommendations

This report was a record of the research on a higher order feedback loop for a Pulse Width Modulator and the implementation of a 3rd order loop-filter for this feedback loop. In this chapter some conclusion from the research and some recommendations for further research are given. Let's first start with the conclusions.

- **[Butterworth type loop filter]**

In the first part of this project the loop-filter for the feedback loop was analyzed. The Butterworth type loop filter is considered as the best filter if the noise and distortion is mainly low frequency. This is the case for voltage supply error and intrinsic modulation error. The Chebyshev type filter is considered if the noise and distortion has a more white noise behavior or high frequencies. From the simulations it turned out that the voltage supply error has the most effect on the noise and distortion. Therefore the Butterworth type filter is preferred.

- **[3rd order loop filter with a 700 kHz carrier frequency]**
- **[SINAD increases with 29 dB in comparison to the Philips' design]**

Different orders for the filters were analyzed. If a 350 kHz carrier signal is used the optimum filter order for a Butterworth type filter would 3rd of 4th order. By increasing the carrier frequency the optimum filter order is transferred to higher orders. Increasing the carrier frequency also improves the performance of the PWM very much. When a 3rd order filter with a 700 kHz carrier signal is used instead of a 2nd order filter with a 350 kHz carrier signal (as used in the Philips' design) the SINAD will increase with 29 dB according to the simulations. In the simulations only the voltage supply voltage error and jitter noise were incorporated. The output stage errors were not proper analyzed and therefore not weighted in this simulation.

- **[Carrier inserted in the last integrator]**

The simulations also showed that it is desired to insert the carrier signal in the last integrator instead of in the first integrator. Although the intrinsic modulation error is worst when the carrier signal is inserted in the last integrater, the jitter noise is shaped by the loop filter. The jitter noise is concerned as a bigger problem than the intrinsic modulation error.

- **[CIFF loop filter topology]**

In the second part of this project a start was made for designing an actual implementation for a 3rd order Butterworth type loop filter with a 700 kHz carrier signal inserted in the last integrator. For this design a CIFF topology is preferred. Except for the 1st integrator in a CIFF, the linearity of the other integrators is not of big importance. The advantage is that the requirements for those integrator implementations are much more relaxed. It also means that the power consumption of the integrators can be lower and thus the overall power consumption will be lower than in case of the CIFB topology. In this analysis it was assumed that linearity had more influence on the power consumption than the noise inside the loop filter. A drawback of the CIFF topology is that its STF has an overshoot at higher frequencies. In this case it is not big problem because the input signal is assumed to contain only components inside the audioband.

- **[Gm's as gain factors]**

Gm's are used for the gain-factors of the loop filter. This makes the gain-factors tunable. With tunable gain-factors it is easy to compensate for component spread and it is possible to adjust the loop-filter to an optimal filter is the carrier frequency is changed. The errors created in the Gm's due to nonlinearity will be shaped according to the NTF of the feedback loop.

- **[Miller integrators]**

The integrator topologies used in this project are Miller integrators. The choice is made because Miller integrators have the highest linearity and lowest power consumption. It is possible, for other than the 1st integrator of the loop-filter, to use integrators with lower area consumption and which are more tunable, but this requires further research.

- **[Simulations verify calculations]**

Finally parameter values for the implementation were calculated and the implementation model was simulated. The results were compared with the calculations. The simulation results are almost the same as the calculation which verify the simulation results and the calculations. It was showed that the designed implementation is able to achieve a dynamic range of 122 dB with only thermal noise and modulation error. The actual dynamic range will be probably less if all other noise/distortion sources and all parasitics are incorporated in the simulation model. But it can be concluded that until now a good system is designed.

Finally some ideas and recommendations for further research are given:

- Modeling of the output stage noise and distortion: In this report the output stage noise and distortion was assumed to be a global white noise. And also the noise power was not based on any research. It would be interesting to have a proper model for this output stage noise and distortion. It could turn out that it is better to use a Chebyshev type filter instead of the Butterworth type filter as used in the implementation of this project
- Inserting the carrier signal in the middle of the loop filter: In case of the placement of the carrier signal a trade-off should be made for the amount of suppression of the jitter noise from the carrier and the effect on the modulation error. In this report only the two extremes are analyzed: Inserting the carrier signal in first integrator, or inserting the carrier signal in the last integrator. If the carrier signal is inserted in the middle of the loop filter it will probably have an averaged function of both extremes.
- Using other integrator topologies for other integrators than the 1st one: In this project only Miller integrators are use. They have the best linearity and lowest power consumption, but they are hard to tune and have a large area consumption. Other integrator topologies are maybe better tunable which makes it easier to compensate for component spread and to adjust the loop-filter to an optimal filter if the carrier frequency is changed Also other topologies could have a smaller area consumption
- Implementation of the Gm's. In this project the Gm's were considered as ideal voltage controlled current sources with only a parasitic capacitance at the input and a thermal noise source at the output. When an actual implantation of a Gm is used one will see that there will be much more parasitic components. For example a parasitic impedance at the output. These other parasitics could cause trouble when they are neglected while the system is designed. Furthermore an actual implementation will also show the limits to linearity of the Gm.
- Including the output filter in feedback loop: In this project the output filter was not part of the feedback loop. When the output filter is inside the feedback loop the noise and distortion generated in the output filter is also suppressed.

A good start has been made for the implementation of an actual 3rd order feedback loop for a Pulse Width Modulator. Still there is a lot more to be done before a real device can come out of a factory. This could be a nice challenge for further research on this subject.

9 References

[1] N. Anderskouv, K. Nielsen & M.A.E. Andersen
"High Fidelity Pulse Width Modulation Amplifiers based on Novel Double Loop Feedback Techniques"
Presented at the 100th Convention AES, Copenhagen, Denmark, 1996 May 11-14, Preprint 4258

[2] M. Berkhout
"An Integrated 200-W Class-D Audio Amplifier"
IEEE Journal of Solid-Stae Circuits, Vol. 38, No.7, July 2003

[3] M. Berkhout
"A class D output stage with zero dead time"
IEEE International Solid-State Circuits Conference. Digest of Technical Papers. 2003.

[4] M. Berkhout
"TDA8920 Class D Amplifier"
Philips, 2006

[5] D. Schinkel
"High-accuracy and High-resolution ΣΔ Converters, Using novel topologies for Mismatch Shaping and PWM signaling"
Faculty of Electrical Engineering of the University of Twente, January 2003

[6] H.K. Kim
"Some Prominent Aspects of the Inverse Chebyshev Functions"
IEEE Transactions on circuits and systems, Vol. 38, No.3, March 1991

[7] L. Thede
" Practical Analog and Digital Filter Design"
Artech House, Inc., 2004

[8] A. Hajimiri & T.H. Lee
" The Design of Low Noise Oscillators"
Kluwer Academic Publishers, 1999

[9] S.L.J.Gierkink
"A Coupled Sawtooth Oscillator Combining Low Jitter With High Control Linearity"
IEEE Journal of Solid-State Circuits, Vol. 37, No. 6, June 2002

[10] K. Kundert
"Modeling Jitter in PLL-based Frequency Synthesizers"
The Designer's Guide Community, Version 4f, November 2005

[11] S.R.Norsworthy, R. Schreier, & G.C.Temes
"Delta-Sigma Data Converters: Theory, Design and Simulations"
WileyInterscience, 1997

[12] A. Leuciuc
"On the Nonlinearity of Integrators in Continuous-Time Delta-Sigma Modulators"
Proceedings of the 44th IEEE 2001 Volume 2, 14-17 Aug. 2001

[13] G. Groenewold
"Optimal dynamic range integrators"
IEEE Transactions on Circuits and Systems I: Fundamental Theory and Applications,
Vol. 39, No. 8, Aug. 1992

[14] J.P. Moreira & M.M. Silva
"Limits to the Dynamic Range of Low-Power Continuous-Time Integrators"
IEEE Transactions on Circuits and Systems-1: Fundamental Theory and Applications, Vol. 48, No.7, July 2001
[15] J.P. Moreira & C.J.M. Verhoeven
"Fundamental Limits to the Dynamic Range of Integrated continuous-Time Integrators"
Proceedings of the 1998 IEEE ISCAS '98. Vol. 1, 31 May-3 June 1998.
[16] B. Razavi
"Design of Analog CMOS Integrated Circuits"
McGraw-Hill Higher Educations, 2001
[17] Ka Nang Leung & Philip K. T. Mok
" Analysis of Multistage Amplifier–Frequency Compensation"
IEEE Transactions on Circuits and Systems—I: Fundamental Theory and Applications, Vol. 48, No. 9, September 2001

10 Appendices

10.1 Butterworth parameters

N	a_1	a_2	a_3	a_4	a_5
2	$\sqrt{2}$				
3	2	2			
4	$2\sqrt{2}\cos\left(\frac{\pi}{8}\right)$	$\sqrt{2}+2$	$2\sqrt{2}\cos\left(\frac{\pi}{8}\right)$		
5	$\sqrt{5}+1$	$\sqrt{5}+3$	$\sqrt{5}+3$	$\sqrt{5}+1$	
6	$\sqrt{2}+\sqrt{6}$	$4+2\sqrt{3}$	$3\sqrt{2}+2\sqrt{6}$	$4+2\sqrt{3}$	$\sqrt{2}+\sqrt{6}$

10.2 Butterworth calculations

10.2.1 1st order

$$H_{NTF}(s)=\frac{s}{s+\omega_c} \qquad Zeros_H=[\ ]$$

$$H(s)=\frac{\omega_c}{s} \qquad Poles_H=0$$

$$G_{PWM}=\omega_c(=\omega_{UG})$$

10.2.2 2nd order:

$$H_{NTF}(s)=\frac{s^2}{s^2+\sqrt{2}\omega_c s+{\omega_c}^2} \qquad Zeros_H=-\frac{\omega_c}{\sqrt{2}}$$

$$H(s)=\frac{\sqrt{2}\omega_c s+{\omega_c}^2}{s^2} \qquad Poles_H=[0\ 0]$$

$$G_{PWM}=\sqrt{2}\omega_c$$

10.2.3 3rd order:

$$H_{NTF}(s)=\frac{s^3}{s^3+2\omega_c s^2+2{\omega_c}^2 s+{\omega_c}^3} \qquad Zeros_H=\left[\left(-\frac{1}{2}+\frac{1}{2}i\right)\omega_c\ \left(-\frac{1}{2}-\frac{1}{2}i\right)\omega_c\right]$$

$$H(s)=\frac{2\omega_c s^2+2{\omega_c}^2 s+{\omega_c}^3}{s^3} \qquad Poles_H=[0\ 0\ 0]$$

$$G_{PWM}=2\omega_c$$

10.3 Chebyshev polynomials & Stop-band ripple

10.3.1 Chebyshev polynomials

$$C_0(x) = 1$$
$$C_1(x) = x \qquad \text{(10-1)}$$
$$C_{n+1}(x) = 2xC_n(x) - C_{n-1}(x)$$

10.3.2 Stop-band ripple

$$R_s = \frac{1}{20\log_{10}\sqrt{1+\varepsilon^2}}\ (\text{dB}) \Leftrightarrow \quad \varepsilon = \frac{1}{\sqrt{10^{\frac{R_s}{10}}-1}} \qquad \text{(10-2)}$$

10.4 Chebyshev calculations

(based on [7])
Inverse Chebyshev functions are in 2 different versions depending on the order.
For even functions:

$$H(s) = \frac{\prod_m \left(s^2 + A_{2m}\right)}{\prod_m \left(s^2 + B_{1m}s + B_{2m}\right)} \qquad \text{(10-3)}$$
$$m = 1, 2 \ldots \left[n/2\right] - 1 \quad (n \text{ even})$$

and for odd functions:

$$H(s) = \frac{s\prod_m \left(s^2 + A_{2m}\right)}{\left(s+\sigma_R\right)\prod_m \left(s^2 + B_{1m}s + B_{2m}\right)} \qquad \text{(10-4)}$$
$$m = 1, 2 \ldots \left[\left(n-1\right)/2\right] - 1 \quad (n \text{ odd})$$

to calculate the parameters of the functions:
First D is calculated from ε. This will be the form of the ellipse on which the poles will lay.

$$D = \frac{\sinh^{-1}\left(\frac{1}{\varepsilon}\right)}{n} \qquad \text{(10-5)}$$

The pole locations are found by D and the angle ϕ_m. ϕ_m is again depended on the order of the filter:

$$\phi_m = \frac{\pi\left(2m+1\right)}{2n}, m = 0, 1 \ldots, \left(n/2\right) - 1 \ (n \text{ even})$$
$$\phi_m = \frac{\pi\left(2m+1\right)}{2n}, m = 0, 1 \ldots, \left[\left(n-1\right)/2\right] - 1 \ (n \text{ odd}) \qquad \text{(10-6)}$$

Next the real and imaginary components of the poles are found by:

$$\sigma_m = -\sinh\left(D\right)\cdot\sin\left(\phi_m\right)$$
$$\omega_m = \cosh\left(D\right)\cdot\cos\left(\phi_m\right) \qquad \text{(10-7)}$$

if the filter order is odd, a real pole will be located in the left half plane according to:

$$\sigma_R = -\sinh(D) \cdot \omega_s \qquad \textbf{(10-8)}$$

In [7] these poles will be inverted. But because a high-pass version is calculated this is not necessary, because a high-pass filter has all poles and zeros inverted.
Last to do is to calculate parameters used in (10-3) and (10-4) as follow:

$$B_{1m} = -2\sigma_m \omega_s$$

$$B_{2m} = (\sigma_m^2 + \omega_m^2)\omega_s^2 \qquad \textbf{(10-9)}$$

$$A_{2m} = \frac{\omega_s^2}{\left(\sec(\phi_m)\right)^2}$$

10.5 Chebyshev Parameters

N	*Rs* for f_{car} = 350 kHz. $\omega_s = 44100\pi$ rad/sec	*Rs* for f_{car} = 700 kHz. $\omega_s = 44100\pi$ rad/sec
2	28.4741	40.2270
3	37.1559	54.4450
4	43.0897	65.6189
5	47.3240	74.6075

10.6 Matlab/Simulink Simulation parameters

Simulation time step: $T_s = 88.58 \text{ ns} \left(= \frac{1}{f_s} = \frac{1}{BW_{audio} \cdot 512} = \frac{1}{22050 \cdot 512} \right)$

Input signal:

- sine wave
- $f_{sig} = 2.16$ kHz
- amplitude = 0.5
- number of cycles with startup cycle (cyc) = 42

Carrier frequency:

- triangular wave
- amplitude $= \int_0^{\frac{1}{4 f_{car}}} \frac{G_{PWM}}{f_{car}} dt = \frac{G_{PWM}}{(2 f_{car})^2}$

Comparator:

- output $= \begin{cases} 1 & (\text{input} \geq 0) \\ -1 & (\text{input} < 0) \end{cases}$

Output filter:

- 4^{th} order butterworth low pass
- cutoff frequency = 100 kHz

Voltage supply error:

- sine wave
- $f_{vdde} = 458.6$ Hz $\left(= \text{FFT resolution} \cdot 9 = \frac{f_{sig}}{cyc} \cdot 9 \right)$
- amplitude = 0.1 (10% of comparator output)

Global white noise:

- gaussian
- bandwidth = $\frac{f_s}{16}$
- amplitude = 0.1 (10% of comparator output)

FFT:

- FFT constant: $fftc = \frac{cyc}{f_{sig}} \cdot f_s$
- FFT resolution $\Delta f = \frac{f_{sig}}{cyc} Hz / bin$
- Windowing: Hanning

10.7 Matlab/Simulink Simulation results

10.7.1 No noise sources

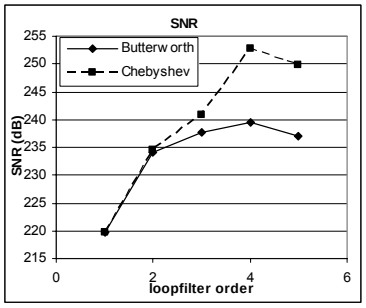

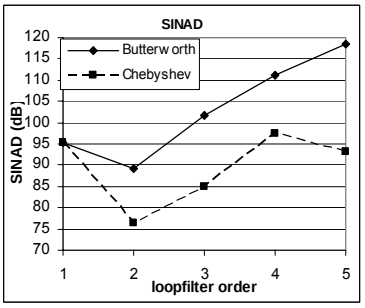

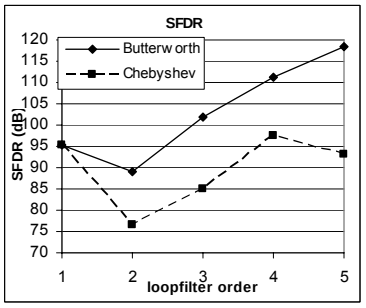

10.7.2 Supply Voltage error only

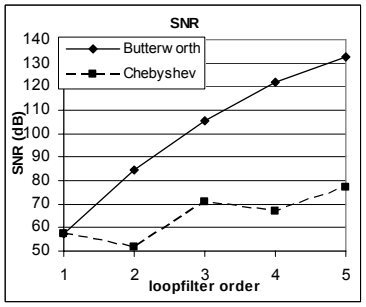

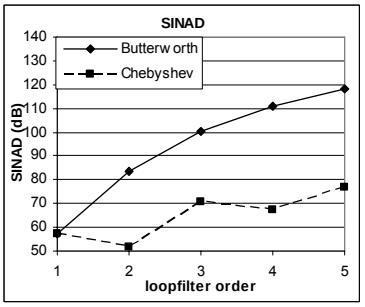

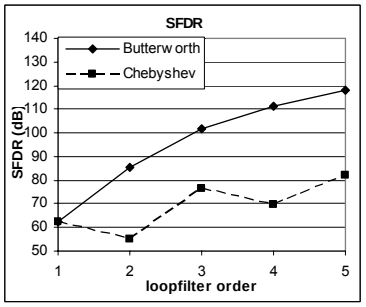

10.7.3 Carrier placement, no noise sources with 50% modulation depth and Butterworth type NTF

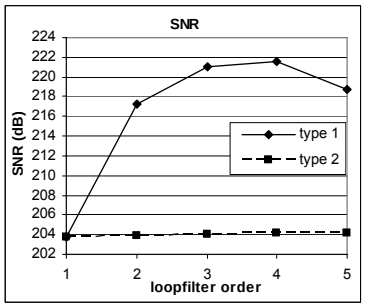

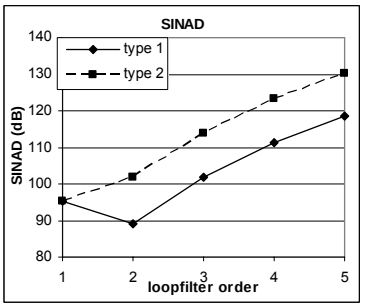

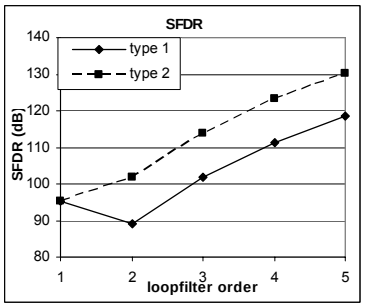

10.7.4 Carrier placement, Jitter noise only with 50% modulation depth and Butterworth type NTF

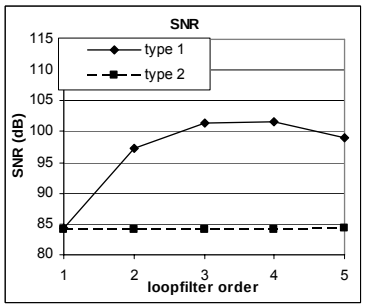

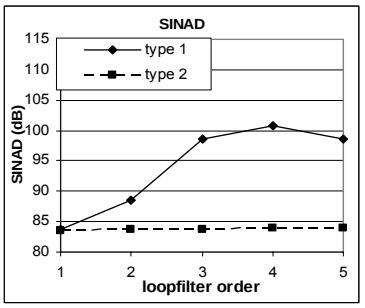

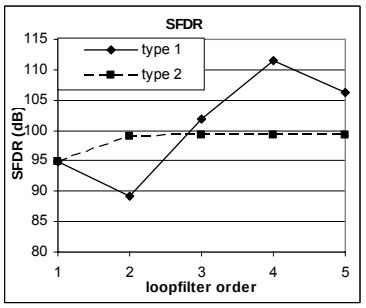

10.7.5 Output stage noise only with 50% modulation depth

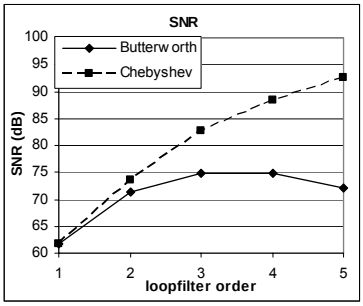

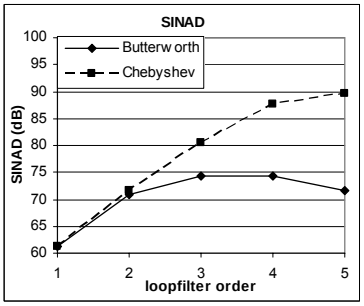

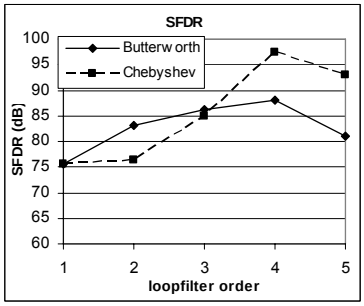

10.8 Jitter noise calculations

In this appendix the noise due to the jitter of the oscillator is calculated.

First of all an oscillator is used which has a -114 dB/Hz component on 10 kHz from its carrier frequency of 350 kHz. And noise spectrum is considered to have a -20 dB/dec slope from it carrier frequency (Figure 56).

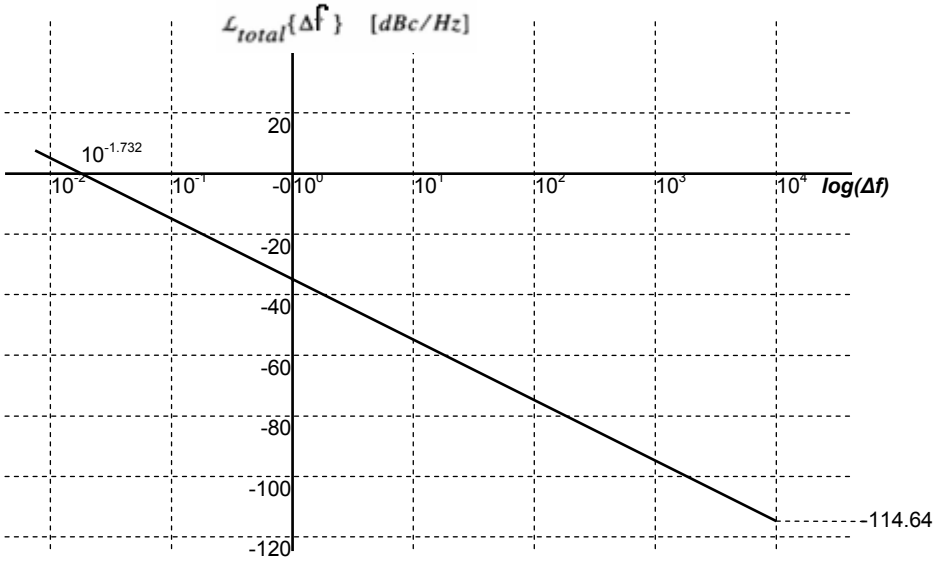

Figure 56: Jitter noise spectrum of an oscillator around it carrier frequency

Because the carrier is high frequency its noise at low frequency can be considered to have a flat spectrum as sketched in Figure 57.

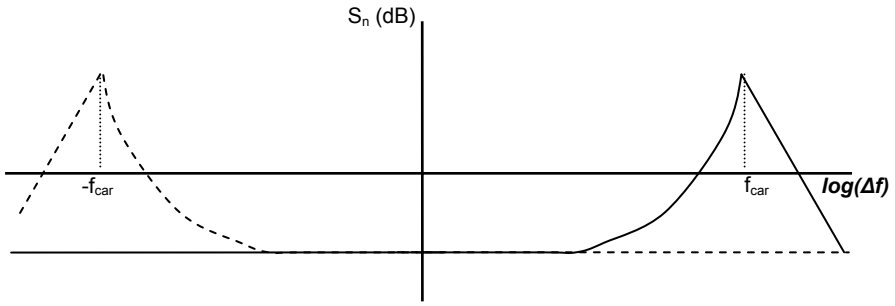

Figure 57: Sketch of Jitter noise spectrum of an oscillator.

With a carrier of 350 kHz with -114 dB/Hz at 10 kHz from its carrier frequency will have about -145 dB/Hz noise power at DC and thus for low frequencies. The total noise in the audio bandwidth will there for be (-145 dB + 10*log(20000) =) -102 dB for single side. Due the noise power from the negative side (see Figure 57) the noise power in the audio bandwidth will be doubled and thus -99 dB.
This is now only for a sine-wave oscillator. The actual oscillator is a block wave. Due to the higher harmonics another 3 dB should be added, which makes the final noise power of the oscillator -96 dB in the audio bandwidth.

In the simulations in §4.6 the oscillator signal has a 4 times bigger amplitude (=12 dB in power) as the filtered output signal. Due to this the SNR should be 84 dB

10.9 Open loop calculations

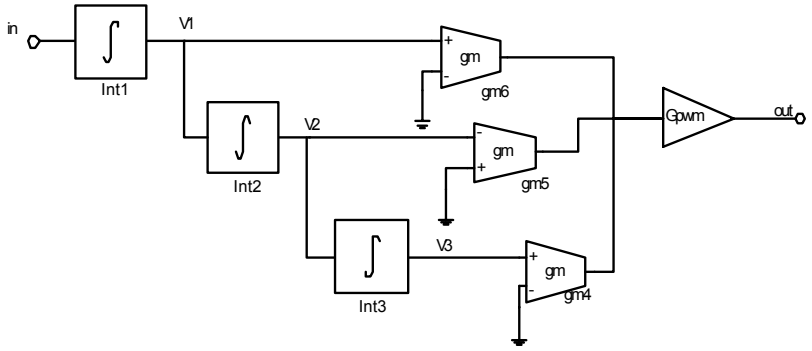

Figure 58: schematic for the loop-filter's open loop calculations

In these calculations the integrators have the simplified transfer function (6.15), which is as follow:

$$H_{int}(s) = \frac{-1}{sR_xC_x} \qquad \textbf{(10-10)}$$

The transconductors are simple V/I converters

$$I_{out\_VI}(s) = gm \cdot V_{in\_VI} \qquad \textbf{(10-11)}$$

With this data the open loop transfer function is calculated:

$$\left.\begin{aligned} V_1 &= \frac{-V_{in}}{sR_1C_1} \\ V_2 &= \frac{-V_1}{sR_2C_2} = \frac{V_{in}}{s^2R_1R_2C_1C_2} \\ V_2 &= \frac{-V_2}{sR_3C_3} = \frac{-V_{in}}{s^2R_1R_2R_3C_1C_2C_3} \\ V_{out} &= G_{pwm}\left(gm_7V_1 + gm_6V_2 + gm_5V_3\right) \end{aligned}\right\} V_{out} = \frac{-G_{PWM}\left(s^2R_2R_3C_2C_3gm_7 + sR_3C_3gm_6 + gm_5\right)V_{in}}{s^3R_1R_2R_3C_1C_2C_3}$$

(10-12)

$$H_{open-loop}(s) = \frac{V_{out}}{V_{in}} = \frac{-G_{PWM}\left(s^2R_2R_3C_2C_3gm_7 + sR_3C_3gm_6 + gm_5\right)}{s^3R_1R_2R_3C_1C_2C_3} \qquad \textbf{(10-13)}$$

10.10 Miller integrator calculations

10.10.1 Normal miller integrator

This appendix shows the calculations of the transfer function of a miller integrator. The calculations are done on the basis of a small signal model (Figure 59)

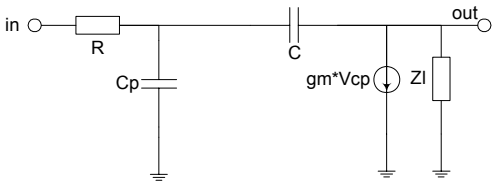

Figure 59: Miller intergrator small signal model

From this small signal model 8 equations can be formed and 8 unknown values have to be solved:

$$\begin{aligned}
&1: I_R = I_{C_p} + I_C \\
&2: I_C = gm \cdot V_{C_p} + I_{Z_l} \\
&3: V_{in} = V_R + V_{C_p} \\
&4: V_{C_p} = V_C + V_{out} \\
&5: V_R = R \cdot I_R \\
&6: V_{out} = Z_l \cdot I_Z \\
&7: V_C = \frac{I_C}{sC} \\
&8: V_{C_p} = \frac{I_{C_p}}{sC_p}
\end{aligned}
\left\{
\begin{aligned}
&I_C = gm \cdot V_{C_p} + I_{Z_l} \\
&V_{C_p} = V_{in} - V_R \\
&V_R = V_{in} - V_C - V_{out} \\
&I_R = \frac{V_{in} - V_C - V_{out}}{R} \\
&I_{C_p} = (V_C + V_{out}) sC_p \\
&V_C = \frac{gm \cdot V_{out} + I_{Z_l}}{-sC + gm} \\
&I_Z = \frac{V_{out}}{Z_l} \\
&V_{out} = \frac{Z_l (sC - gm) V_{in}}{s^2 RCZ_l C_p + s\left(CR(gmZ_l + 1) + Z_l C + RC_p\right) + 1}
\end{aligned}
\right.$$

(10-14)

Now the transfer function is:

$$H(s) = \frac{Z_l (sC - gm)}{s^2 RCZ_l C_p + s\left(CR(gmZ_l + 1) + Z_l C + RC_p\right) + 1} \qquad \textbf{(10-15)}$$

With the same 8 equations used in (10-14) the input impedance could be calculated and will result in:

$$Z_{in}(s) = \frac{s^2 RCZ_l C_p + s\left(CR(gmZ_l + 1) + Z_l C + RC_p\right) + 1}{s^2 CZ_l C_p + s(C(gmZ_l + 1) + C_p)} \qquad \textbf{(10-16)}$$

When the parasitic capacitance is considered very small ($\underline{C_p} \approx 0$) the input impedance results in:

$$Z_{in}(s) = \left(R + \frac{Z_l}{gmZ_l + 1} \right) + \frac{1}{sC\left(gmZ_l + 1\right)} \quad \textbf{(10-17)}$$

If $gm \cdot Z_l >> 1$:

$$Z_{in}(s) = \left(R + \frac{1}{gm} \right) + \frac{1}{sC\left(gmZ_l\right)} \quad \textbf{(10-18)}$$

10.10.2 Zero cancellation modified miller integrator

This appendix shows the calculations of the transfer function of the modified miller integrator. The calculations are done on the basis of a small signal model (Figure 60)

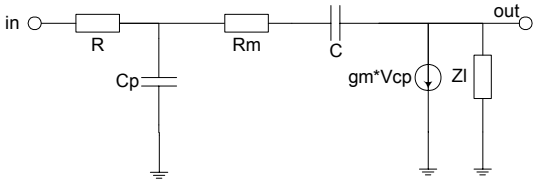

Figure 60: Miller intergrator with zero cancellation small signal model

From this small signal model 10 equations can be formed and 10 unknown values have to be solved:

$$\begin{aligned}
&1: I_R = I_{C_p} + I_{R_m} \\
&2: I_{R_m} = I_C \\
&3: I_C = gm \cdot V_{C_p} + I_{Z_l} \\
&4: V_{in} = V_R + V_{C_p} \\
&5: V_{C_p} = V_{R_m} + V_C + V_{out} \\
&6: V_R = R \cdot I_R \\
&7: V_{R_m} = R_m \cdot I_{R_m} \\
&8: V_{out} = Z_l \cdot I_Z \\
&9: V_C = \frac{I_C}{sC} \\
&10: V_{C_p} = \frac{I_{C_p}}{sC_p}
\end{aligned}
\left\{
\begin{aligned}
&I_{R_m} = I_C \\
&I_C = gm \cdot V_{C_p} + I_{Z_l} \\
&V_{C_p} = V_{in} - V_R \\
&V_R = V_{in} - V_{R_m} - V_C - V_{out} \\
&I_R = \frac{V_{in} - V_{R_m} - V_C - V_{out}}{R} \\
&I_{C_p} = \left(V_{R_m} + V_C + V_{out}\right) sC_p \\
&V_{R_m} = \frac{\left(gm \cdot V_C + gm \cdot V_{out} + I_{Z_l}\right) R_m}{1 - gmR_m} \\
&V_C = \frac{gm \cdot V_{out} + I_{Z_l}}{sC\left(1 - gmR_m\right) - gm} \\
&I_Z = \frac{V_{out}}{Z_l} \\
&V_{out} = \frac{Z_l \left(sC\left(1 - gmR_m\right) - gm\right) V_{in}}{s^2 RCC_p \left(Z_l + R_m\right) + s\left(CR\left(gmZ_l + 1\right) + Z_l C + R_m C + RC_p\right) + 1}
\end{aligned}
\right.$$

(10-19)

Now the transfer function is:

$$H(s) = \frac{Z_l \left(sC\left(1 - gmR_m\right) - gm\right)}{s^2 CC_p R\left(Z_l + R_m\right) + s\left(CR\left(gmZ_l + 1\right) + Z_l C + R_m C + RC_p\right) + 1} \quad \textbf{(10-20)}$$

With the same 10 equations used in (10-19) the input impedance could be calculated and will result in:

$$Z_{in}(s) = \frac{s^2 CC_p R(Z_l + R_m) + s\left(CR\left(gmZ_l + 1\right) + Z_l + R_m + RC_p\right) + 1}{s^2 CC_p (Z_l + R_m) + s\left(C\left(gmZ_l + 1\right) + C_p\right)} \qquad \textbf{(10-21)}$$

When the parasitic capacitance is considered very small ($\underline{C_p} \approx 0$) the input impedance results in:

$$Z_{in}(s) = \frac{sC\left(R\left(gmZ_l + 1\right) + Z_l + R_m\right) + 1}{sC\left(gmZ_l + 1\right)} \qquad \textbf{(10-22)}$$

If $gm \cdot Z_l >> 1$:

$$Z_{in}(s) = \left(R + \frac{Z_l + R_m}{gmZ_l}\right) + \frac{1}{sC\left(gmZ_l\right)} \qquad \textbf{(10-23)}$$

10.11 Noise calculations of an integrator

In this paragraph the input referred noise voltage is calculated of an integrator. Figure 61 shows the model used in these calculations.

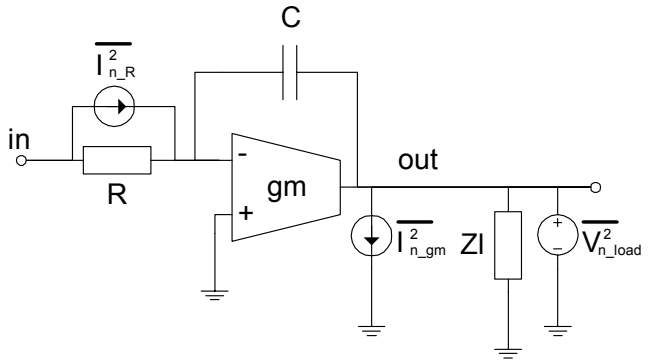

Figure 61: Noise in an integrator

And also the following equations:

$$\overline{I_{n\_R}^2} = \frac{4kT}{R} \qquad \textbf{(10-24)}$$

$$\overline{I_{n\_gm}^2} = 4kT\gamma gm \qquad \textbf{(10-25)}$$

$$S_Y(f) = S_X(f)\left|H(f)\right|^2 \qquad \textbf{(10-26)}$$

For every calculation one uses superposition. Meaning, only one source is active. All other sources are left out and the input is tied to ground.

10.11.1 Resistor noise

The easiest calculation is that of the resistor. Here Ohm's law is applied to calculate the transfer function:

$$H_R(s) = \frac{V_{in}}{I_R} = R \qquad \textbf{(10-27)}$$

Using (10-24), (10-26) and (10-27) the input referred noise voltage becomes:

$$\overline{V_{n\_R\_in}^2} = 4kTR \qquad \textbf{(10-28)}$$

10.11.2 Gm noise

A little more difficult is the noise calculation for the gm noise. First the transfer function has to be calculated from the noise current source at the output of the transconductor to a voltage at the input. For these calculations the same model and equations of paragraph 10.10.1 are used.
Using those equations the transfer function is:

$$H_{gm}(s) = \frac{V_{in}}{I_{gm}} = \frac{1 + sRC_p}{gm} \overset{RCp<<1}{\Longrightarrow} H(s)_{gm} = \frac{1}{gm} \qquad \textbf{(10-29)}$$

Using (10-25), (10-26) and (10-29) the input referred noise voltage becomes:

$$\overline{V_{n\_gm\_in}^2} = \frac{4kT\gamma}{gm} \qquad \textbf{(10-30)}$$

10.11.3 Noise from the load

The transfer function to calculate the input referred voltages noise is already calculated in paragraph 10.10.1. One just uses the transfer function of the integrator. From this report it is already known, if *gm* is high enough and C_p is small enough the transfer function is:

$$H(s) = \frac{V_{out}}{V_{in}} = \frac{1}{sRC} \Longrightarrow H(s)_{in} = \frac{V_{in}}{V_{out}} = sRC \Longrightarrow H(j\omega)_{in} = j\omega RC \quad \textbf{(10-31)}$$

Using (10-26) and (10-31) the input referred noise voltage becomes:

$$\overline{V_{n\_out\_in}^2} = (\omega RC)^2 \overline{V_{n\_load}^2} \quad \textbf{(10-32)}$$

10.11.4 Total input referred noise voltage

All the input referred noise voltage sources calculated by superposition in the previous paragraphs are power signal. Because of this all sources can be added together to determine the total input referred noise voltage. Adding equation (10-28), (10-30) and (10-32) one gets a total input referred noise voltage of:

$$\overline{V_{n\_in}^2} = 4kT\left(R + \frac{\gamma}{gm}\right) + (\omega RC)^2 \overline{V_{n\_load}^2} \quad \textbf{(10-33)}$$

10.12 Cadence Simulation Model

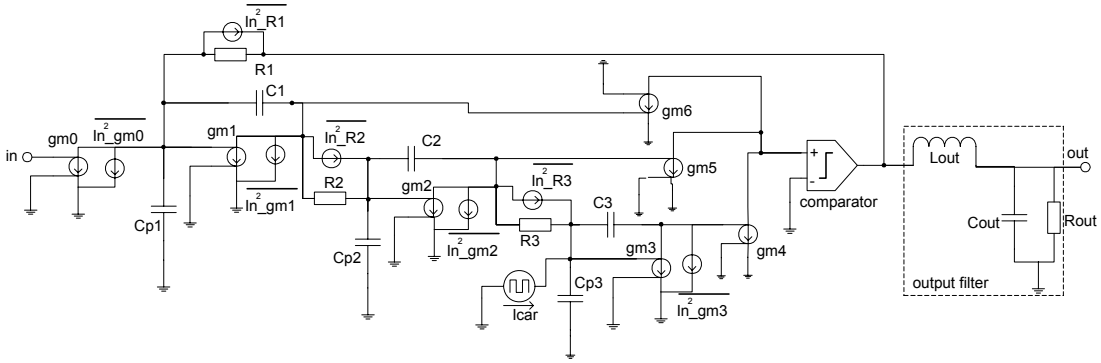

Figure 62: Cadence simulation model of total system

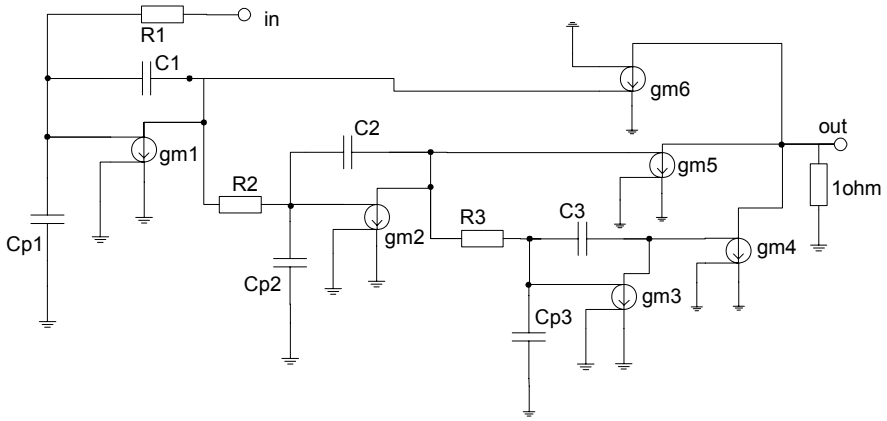

Figure 63: Cadence simulation model for open loop transfer function